U.S. Department
of Transportation

**National Highway
Traffic Safety
Administration**

DOT HS 807 868
Final Report

August 1992

Evaluation of NHTSA Light Vehicle Handling Simulations

Technical Report Documentation Page

1. Report No.	2. Government Accession No.	3. Recipient's Catalog No.
DOT HS 807 868		

4. Title and Subtitle	5. Report Date
Evaluation of NHTSA Light Vehicle Handling Simulations	August 1992
	6. Performing Organization Code: NRD-22
7. Author(s): Jeffrey P. Chrstos and Gary J. Heydinger	8. Performing Organization Report No.: VRTC-87-0086
9. Performing Organization Name and Address: National Highway Traffic Safety Administration, Vehicle Research and Test Center, P.O. Box 37, East Liberty, Ohio 43319	10. Work Unit No. (TRAIS)
	11. Contract or Grant No.
12. Sponsoring Agency Name and Address: National Highway Traffic Safety Administration, 400 Seventh Street, S.W., Washington, D.C. 20590	13. Type of Report and Period Covered: Final, 5/91 to 2/92
	14. Sponsoring Agency Code

15. Supplementary Notes

The discussion and conclusions in this paper represent the opinions of the authors and not necessarily those of the NHTSA or the Transportation Research Center Inc. The work reported in this report was executed under contract to the NHTSA, US DOT.

16. Abstract

This report contains evaluations of four light vehicle stability and control simulations developed for the NHTSA: FOROL developed by Dynamic Research Inc., the "Intermediate Maneuver Induced Rollover Simulation" (IMIRS) and the "Advanced Dynamic Vehicle Simulation" (ADVS), both developed by the University of Missouri, and "Vehicle Dynamics Analysis, Non-Linear" (VDANL) developed by System Technology, Inc.

The focus of these evaluations is each simulation's ability to accurately predict light vehicle responses during flat road handling and crash avoidance maneuvers. Each simulation is first described on an analytical basis. The overall modeling approach is described along with detailed descriptions of the modeling of the vehicle sub-systems. For each simulation, any areas found to be inadequately modeled are reported.

The ability of each simulation to predict flat road vehicle responses is evaluated by comparing the simulation predictions to experimentally measured vehicle responses. These comparisons are done in both the time and frequency domains.

The intent of this report is only to evaluate the capabilities of each simulation in its current form, and recommend a direction for future work in this area. It is not the intent of these evaluations to determine if the developers of the simulations met the requirements of their contracts.

17. Key Words	18. Distribution Statement
Simulation Vehicle Dynamics Handling Evaluation	Document is available to the public from the National Technical Information Service, Springfield, VA 22161

19.Security Classif.(of this report)	20.Security Classif.(of this page)	21.No. of Pages	22.Price
Unclassified	Unclassified		

Table of Contents

List of Figures

List of Figures

List of Tables

Department of Transportation
National Highway Traffic Safety Administration

TECHNICAL SUMMARY

Report Title:	
Evaluation of NHTSA Light Vehicle Handling Simulations	
Report Author(s):	Date:
Jeffrey P. Chrstos and Gary J. Heydinger	
Transportation Research Center, Inc.	Feb. 1992

Over the years, the NHTSA has funded the development of several vehicle dynamics simulations as a part of research projects in the area of light vehicle stability and control and rollover. Because these development efforts were performed independently of each other, there has been some amount of duplication of effort or "reinventing of the wheel" occurring in the simulation development. This is not necessarily undesirable; combining the best parts of the various approaches to such a complex problem can lead to a better solution. The next logical step in this effort is to take stock of what has been done and to select the best features of each approach and to integrate these into a single simulation. It is also important to identify shortcomings, if any, where more simulation development work is necessary.

This report contains evaluations of four light vehicle stability and control simulations developed for the NHTSA: FOROL developed by Dynamic Research Inc., the "Intermediate Maneuver Induced Rollover Simulation" (IMIRS) and the "Advanced Dynamic Vehicle Simulation" (ADVS), both developed by the University of Missouri, and the most recent version of "Vehicle Dynamics Analysis, Non-Linear" (VDANL) developed by System Technology, Inc. The report contains an analytical review that describes and evaluates the modeling techniques and capabilities of each simulation. Each simulation's ability to predict low to moderate g flat road vehicle responses has been examined by comparing simulation predictions to experimentally measured vehicle responses.

The FOROL simulation models light vehicles in open-loop, flat ground handling maneuvers up to vehicle rollover. FOROL is an 18 degree-of-freedom lumped parameter model using composite parameters to describe the suspension system and an empirical tire model. The significant non-linearities present in the vehicle and tire systems are included in the model. Open-loop handwheel angle and brake pedal force are the maneuver control inputs allowed. Speed control is accomplished by either a fixed drive torque at the rear wheels or a speed governor allowing constant speed operation. The vehicle parameters required by FOROL are fairly standard and can be measured in the laboratory at the VRTC. Calspan tire parameters are used in the quasi-static tire model. The effort required to generate the simulation input data deck is typical of the other simulations at the VRTC.

The IMIRS simulation models light vehicles in open-loop, flat ground handling maneuvers up to vehicle rollover. IMIRS contains a 3 degree of freedom handling model coupled to a 5 degree of freedom rollover model. An empirical, steady state tire model using Calspan curve fit parameters is used. The significant non-linearities present in the vehicle and tire systems are included in the

model. Open-loop roadwheel angle and longitudinal acceleration are the maneuver control inputs allowed.

The analytical review revealed that IMIRS contains a fixed roll axis vehicle model comprised of a simple kinematic suspension model with no suspension compliances included. All wheel kinematics associated with vehicle bounce are neglected. No steering system is modeled, therefore neglecting the affects of steering system compliance and freeplay. The braking model is limited to a user specified longitudinal acceleration profile with no vehicle longitudinal dynamics modeled.

The ADVS simulation models light vehicles in open-loop, handling maneuvers up to and including vehicle rollover. ADVS contains a 14 degree of freedom vehicle handling/rollover model. An empirical, steady state tire model based principally on Calspan curve fit parameters is used. The significant non-linearities present in the vehicle and tire systems are included in the model. Open-loop roadwheel angle and longitudinal acceleration are the maneuver control inputs allowed.

The analytical review revealed that the ADVS model is a complex Lagrangian formulation of the dynamic equations describing vehicle motions. An equivalent swing axle suspension model is used for independent suspension systems. For solid axle type suspensions, a fixed roll axis model is used. Only road wheel camber change is included in the kinematic suspension model with no axle roll steer effects included. No modeling of suspension system compliance is included. No steering system is modeled, therefore neglecting the affects of steering system compliance and freeplay. The braking model is limited to a user specified longitudinal acceleration profile with no vehicle longitudinal dynamics modeled.

The VDANL simulation model was evaluated for light vehicles in open-loop flat ground handling maneuvers. VDANL also allows modeling closed-loop vehicle response and sloped roadways. The VDANL simulation is a 17 degree of freedom vehicle model that allows simulating vehicle response up to and including vehicle rollover. An empirical, steady state tire model using Calspan curve fit parameters is used, with lateral tire force dynamics included. The significant non-linearities present in the vehicle and tire systems are included in the model. Open-loop hand wheel angle, throttle position or desired speed, and brake pedal force are the maneuver control inputs allowed.

The analytical review revealed that VDANL contains a 6-degree-of-freedom model of the vehicle sprung mass coupled to the unsprung masses. The vehicle suspension systems are described using fairly complete models for wheel kinematics and compliances. For independent suspensions, the classic fixed roll axis model has been abandoned, in favor of functions describing the kinematic relationships of the tire contact patch relative to the sprung mass. A fixed roll axis model is used, however, for solid axle suspension systems.

This evaluation has found VDANL to be the most highly developed and tested vehicle handling simulation developed for NHTSA. Its ability to predict vehicle directional responses was found to be better than the other simulations evaluated (previously, an earlier version of VDANL was found to be superior to the "Improved Dynamic Simulation, Fully Non-Linear" (IDSFC) developed by the University of Michigan for the NHTSA). Of the simulations evaluated, VDANL most correctly characterized vehicle transient behavior.

1.0 Introduction

Over the years, the NHTSA has funded the development of several vehicle dynamics simulations as a part of research projects in the area of light vehicle stability and control and rollover. Because these development efforts were performed independently of each other, there has been some amount of duplication of effort or "reinventing of the wheel" occurring in the simulation development. This is not necessarily undesirable; combining the best parts of the various approaches to such a complex problem can lead to a better solution. The next logical step in this effort is to take stock of what has been done and to select the best features of each approach and to integrate these into a single simulation. It is also important to identify shortcomings, if any, where more simulation development work is necessary.

During 1986 to 1989, VRTC extensively evaluated two simulations developed for NHTSA [1], the "Improved Digital Simulation, Fully Comprehensive" (IDSFC) and "Vehicle Dynamics Analysis, Non-Linear" (VDANL). VDANL was identified as having advantages both in terms of its ability to predict vehicle responses, and in the ease of measurement of its parameters. This report contains evaluations of four additional light vehicle stability and control simulations: FOROL developed by Dynamic Research Inc. [2], the "Intermediate Maneuver Induced Rollover Simulation" (IMIRS) [3] and the "Advanced Dynamic Vehicle Simulation" (ADVS) [4], both developed by the University of Missouri, and the most recent version of VDANL [5] developed by System Technology, Inc.

The focus of these evaluations is each simulation's ability to accurately predict light vehicle responses during flat road handling and crash avoidance maneuvers. However, the ability of the simulations to predict rollover is not investigated. Each simulation is first described on an analytical basis. The overall modeling approach is described along with detailed descriptions of the modeling of the vehicle sub-systems. For each simulation, any errors or areas found to be inadequately modeled are reported.

The vehicle and tire parameters required to run the simulations are described along with the test methods required to measure them. Two of the simulations described the test methods recommended to measure some or all of their parameters. In these cases, the test methods are also evaluated. For all of the simulations, the requirements for parameter measurements are compared to the current measurement capability at the VRTC.

Each simulation's ability to predict flat road vehicle responses is evaluated by comparing the simulation predictions to experimentally measured vehicle responses. These comparisons are done in both the time and frequency domains.

Where the simulations have capabilities beyond flat road maneuvering, such as curb impacts, soft soil interaction, rough road, etc., the models are described. However, for these maneuvers, the VRTC has no experimental data that the simulation predictions can be compared against. Therefore, the models are described, but with no experimental verification.

The evaluation of each of the four simulations is a self contained document and can be read independently of the others. It should be noted that the intent of these evaluations is not to determine if the developers of the simulations met the requirements of their contracts. No reviews of the original task orders outlining the requirements or scope of the simulations were made by the authors. The intent of this report is only to evaluate the capabilities of each simulation in its current form, and recommend a direction for future work in this area.

The conclusion of this report ties together the four evaluations. The simulations' capabilities are compared. Recommendations about future NHTSA simulation usage and development are also made.

2.0 Introduction: FOROL

In August of 1988, the National Highway Traffic Safety Administration contracted Dynamic Research, Inc. (DRI) to perform a study of the dynamic response properties of modified suspension pickup trucks and utility vehicles. The contract, titled "Rollover, Braking, and Dynamic Stability - Modified Suspension Vehicles", was completed in June 1990. The final report, No. DOT HS 807 (662, 663, 664), containing 3 volumes was completed in August 1990.

The purpose of DRI's study was to study the steady state and dynamic responses of pickup trucks and utility vehicles with extensively modified (raised) suspension systems and oversized tires. Three vehicles were tested: a 1985 Toyota 1/2 ton pickup, a 1986 Chevrolet K-20 3/4 ton pickup, and a 1986 Chevrolet S-10 Blazer. Each vehicle was tested in three configurations: original equipment, raised suspension (approx. 3 inches) with OE tires, and raised suspension with oversized tires.

The vehicles were tested in 5 maneuvers: straight line braking, trapezoidal steering, braking in a turn, steady state turning, and fixed frequency sinusoidal steering. These maneuvers were carried up to the limit of vehicle performance. An automatic vehicle controller was developed and used for all tests. The raw field test data is contained in Volume III of the DRI report. For each maneuver, forward speed, handwheel angle, roll angle, lateral acceleration, yaw rate, and sideslip angle are given. For maneuvers involving braking, front and rear brake line pressures, pitch angle, pedal force, and longitudinal acceleration are also given.

A non-linear, lumped parameter vehicle dynamics simulation, called FOROL, was developed as part of this contract. FOROL contains 18 degrees-of-freedom and allows open-loop command inputs of handwheel angle and brake pedal force. Either fixed speed or fixed drive wheel torque are allowed. A few example simulation runs are included in Volume I of the DRI report.

Volume II of the DRI report contains the simulation model derivation, source code, and parameter measurement procedures. The source code, executable program, and vehicle and tire parameter files were also provided by DRI. The simulation has been implemented on both an Apollo workstation and IBM compatible personal computers.

Volume II of the DRI report contains the following overview of FOROL:

"The vehicle is assumed to consist of 5 bodies - the sprung mass and 4 wheels. The unsprung masses are neglected, except that the spin and yaw effects of the wheel masses are accounted for parametrically.

The vehicle is assumed to be symmetric about the x-z plane.

There are a total of 18 degrees of freedom. These include 6 for the sprung mass, 4 for wheel spin, 4 for deflection of the springs between the sprung mass and the wheels, and 4 for the wheels' steering compliance. Sprung mass angular rotations may be large, however, execution is halted should the roll angle exceed 75 degrees. Large steer angles are also considered.

The suspension is considered to consist of 4 collinear spring and damper pairs located between the sprung mass and each of the wheels. The springs and dampers are considered to be cantilevered at their respective upper cups, and therefore do not rotate with respect to the vehicle center of gravity. Also the springs and dampers are parallel to the vehicle x-z plane.

The springs have an approximately linear force/deflection relationship with compression and extension bump stops. The dampers have a bilinear (for compression and extension) force/velocity relationship. The static roll center for each axle lies at the height of the springs upper cups.

For geometric and kinematic purposes, the wheels are assumed to be uniform circular discs, inertially symmetric about a plane which is normal to the spin axis and bisects the tire and having a single compressible radial spring and damper in the plane of the tire. Actual wheel and tire static flexibility and distortion are included, however, in terms of the forces and moments produced by the tire. The rolling radius of the tire is assumed to vary with normal load (i.e., tire compression is included).

The tire forces and moments are provided for in detail, using an empirical nonlinear modified McHenry model. The resulting tire forces and moments are assumed to act at and about a contact point defined as the intersection of the horizontal plane and a line which lies in the wheel plane, and is normal to and passes through the tire spin axis (offsets are implicit in the tire data, as noted above).

The roadway is assumed to be flat and level. The tires can come off the roadway, but the wheels are not allowed to spin backwards.

Brake torques can be provided to each wheel through brake pedal force time history inputs, subject to brake system ratios. The brake system model consists of a brake pedal, master cylinder, booster, proportioning valve, and wheel cylinders. The rear wheels can also have a driving torque; alternately, the rear wheel speeds can be governed to maintain the vehicle at a commanded forward velocity.

Steering can be input by means of a steering wheel angle time history input or by a sinusoidal input of given amplitude and frequency. Compliance steer is included as a function of tire circumferential force, side force, and aligning moment. No initial caster, camber, or toe angles are considered."

2.1 Governing Equations

2.1.1 Rigid Body Dynamics and Simulation Degrees of Freedom

The equations developed for the FOROL simulation are formulated based on a lumped-parameter system model. Five lumped masses (inertias) are included in the vehicle model. These include a single mass representation for the vehicle body and moment of inertias for each of the four wheels.

The only mass modeled (the inertias at each wheel are only for rotation about their Y and Z axis) in the simulation is the sprung mass of the vehicle. Figure 1, Figure 2, and Figure 3 (Taken from the DRI report - Reference 2) show the position of the sprung mass from a right side, front, and top view, respectively. These figures also show most of the vehicle geometric parameters (lengths and angles), the locations where springs and dampers are included in the models, and the basic vehicle coordinate systems used in the simulation.

Based on the DRI documentation, it is unclear as to where the sprung mass position is modeled to reside in the simulation model. At one point in the discussion of the axis systems used in the simulation, the vehicle body fixed coordinate system is said to be "fixed at the mass center of the unperturbed vehicle", while later in the report the origin of the body fixed coordinate system is said to be "fixed at the mass center of the frame assembly". The first description suggests that the sprung mass is modeled

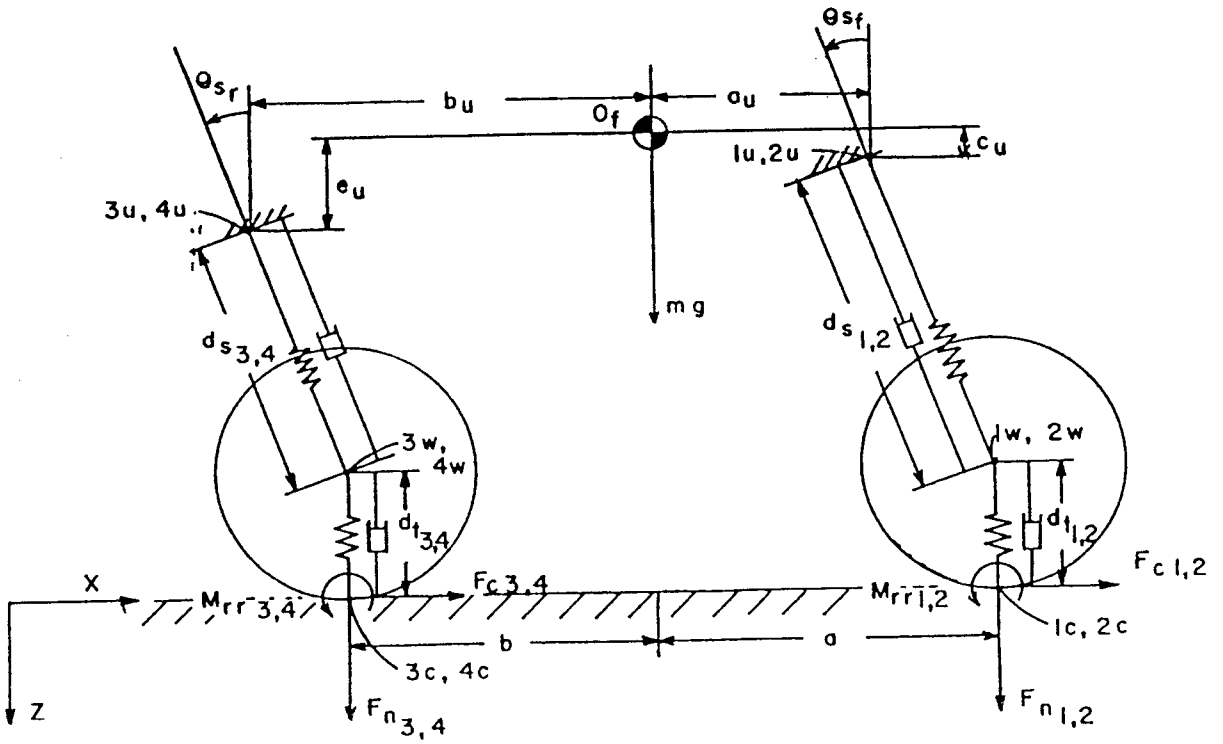

Figure 1 - FOROL Simulation Vehicle Geometry, Right Side View

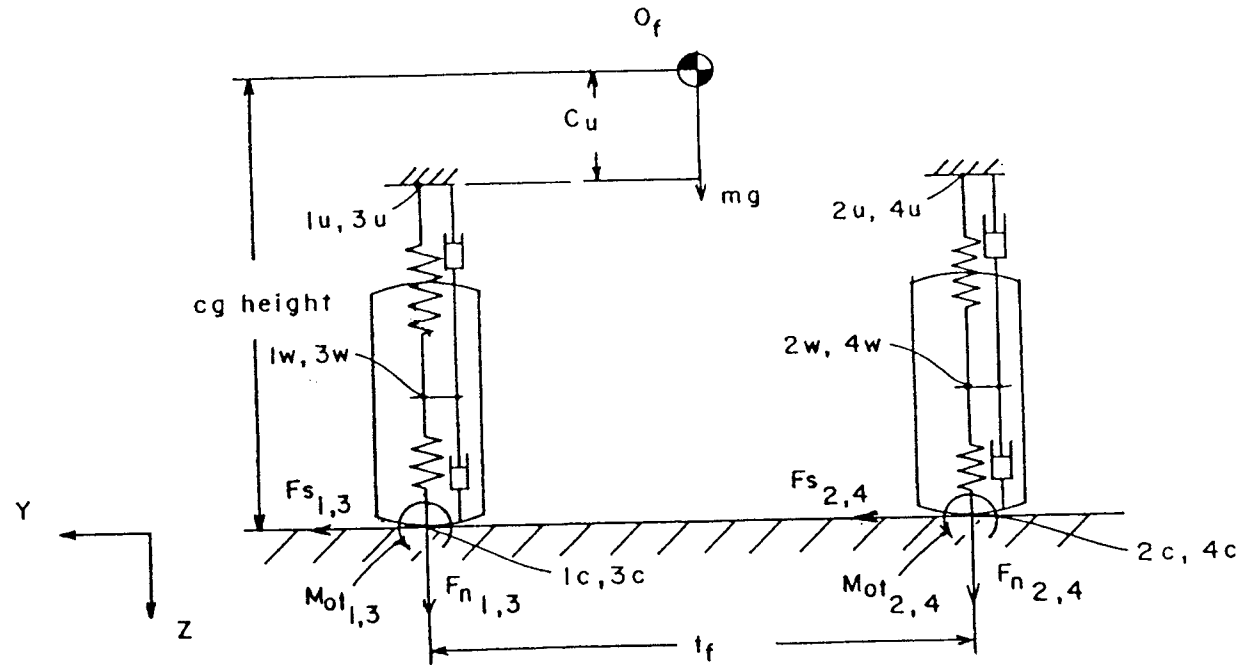

Figure 2 - FOROL Simulation Vehicle Geometry, Front View

to reside at the vehicle center of gravity, while the latter description suggests that the sprung mass is modeled at the sprung mass center of gravity. In the discussion of parameter determination, no mention

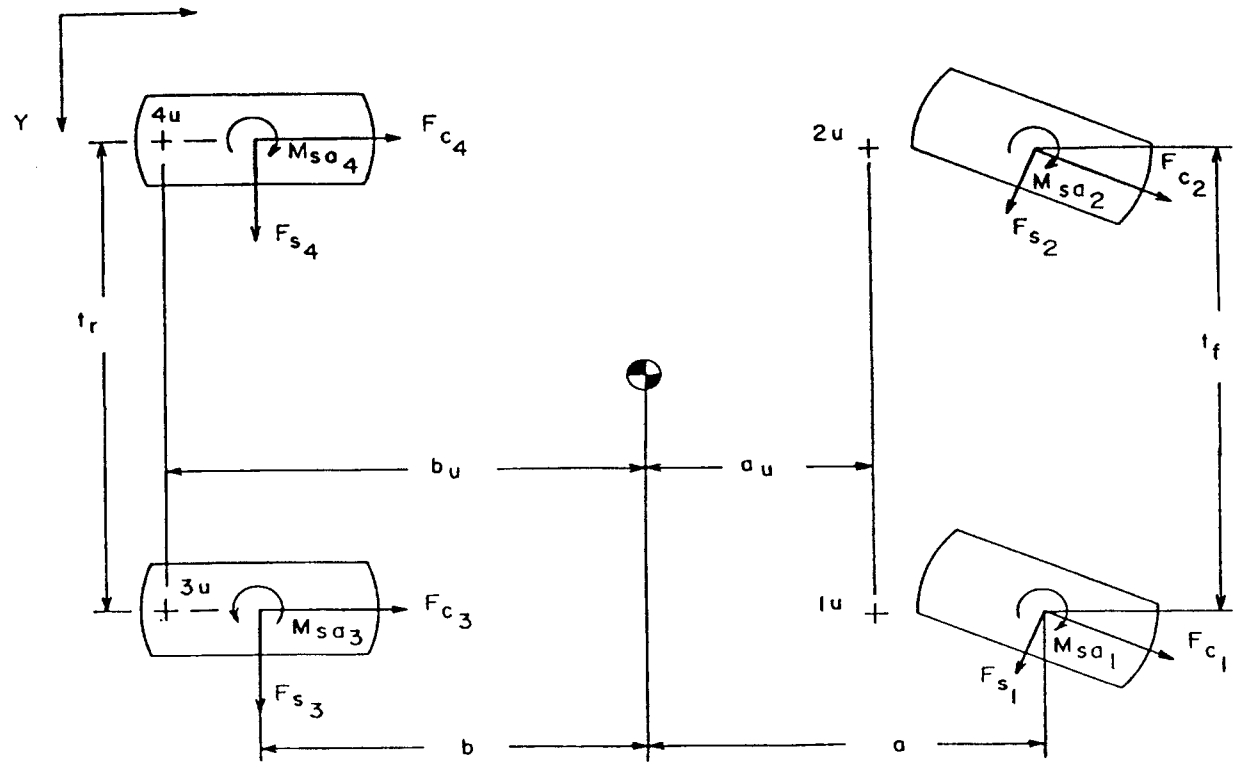

Figure 3 - FOROL Simulation Vehicle Geometry, Top View

is made concerning the determination of the sprung mass center of gravity position. It is unclear what the simulation is actually using for the origin of the body fixed coordinate system, which is the position where the sprung mass resides in the model.

The equations of motion for the vehicle are written with respect to the frame fixed axis system. All three translations and three rotations, for a total of six simulation degrees of freedom, are allowed. No simplifying assumptions are made concerning the motions of the moving coordinate systems, and the complete, nonlinear three dimensional equations of motion are developed based on Newton and Euler formulations. External forces and moments acting on the inertial system are included in the equations of motion using appropriate axis system transformations. That is, the forces and moments acting on the sprung mass (tire forces and moments in this model) are transformed into the body fixed coordinate system so that the derivatives of the linear and angular acceleration vectors defining the sprung mass motion can be determined.

The derivatives of the linear and angular acceleration are numerically integrated to provide the linear and angular velocity and position vectors for the vehicle sprung mass. For this type of simulation, this is the usual technique for determining rigid body motions.

As stated in Reference [6], "The effects of the relative motion of the unsprung masses on the vehicle inertia tensor are neglected". This simply means that no unsprung masses are explicitly modeled in this simulation. The unsprung mass rotational inertia effects are not included in the pitch and roll dynamics. For the pitch and roll dynamics, neglecting the effects of the unsprung masses most likely does not have a large effect on simulation results. The unsprung mass rotational inertia is included in the yaw dynamics as the measurement of total yaw inertia is used in the equations.

Neglecting the unsprung masses is a more critical issue when the lateral and longitudinal dynamics are considered. For passenger cars and other light vehicles, the unsprung masses make up a considerable portion of the total vehicle mass. Based on past work at the VRTC, for the types of pickup trucks used in DRI research, the unsprung masses contribute approximately 15% to total vehicle mass. Neglecting this mass will affect the lateral and longitudinal dynamic predictions of the simulation.

Suspension systems typically introduce jacking forces and motions. Suspension jacking is not included in the FOROL model. Also, in general, suspension roll stiffness and roll damping can not be accurately modeled by including only the vertical, translational stiffness and damping characteristics of the suspension springs and shock absorbers. Additional suspension roll stiffness and damping exists because of the design and components of the suspension; for example, anti-roll bars and suspension bushings. The FOROL model includes no auxiliary roll stiffness or damping.

As stated earlier, each wheel is modeled to have some "mass" associated with it. These masses are only included in the model as wheel spin moment of inertias and wheel yaw moment of inertias. The actual masses of the wheels, as with the rest of the unsprung mass, are not explicitly included in the simulation models. Suitable axis systems are prescribed to each wheel, as are transformation matrices relating the wheel coordinate systems to the vehicle body fixed and ground fixed coordinate systems.

The wheel spin moment of inertias are used in the wheel spin equations of motion. These equations, which introduce four degrees of freedom to the simulation, are typical of this type of simulation. The wheel yaw moment of inertias are used in a differential equation to describe wheel steering compliance for each wheel. (See Section 2.1.3 - Steering System Model for comments). These equations also introduce four degrees of freedom to the simulation model.

The FOROL simulation has 18 degrees of freedom. As mentioned, there are six sprung mass degrees of freedom, four wheel spin degrees of freedom, and four wheel steering degrees of freedom. The

remaining four degrees of freedom are for the suspension deflections between the wheels and sprung mass in a direction parallel with the vehicle x-z plane. These suspension deflection degrees of freedom arise from the fact that the FOROL model includes springs and dampers between the sprung mass and the wheel centers, and between the wheel centers and the road.

2.1.2 Suspension Model

Kinematics:

The suspension description in FOROL is a fairly simple fixed roll axis composite model. The sprung mass is suspended by four collinear spring and damper pairs located above each wheel. The spring/dampers are assumed parallel to the vehicle x-z plane and can be angled relative to the z-axis. The roll axis is assumed to act through the upper spring cups of the front and rear suspension. No differentiation between solid and independent suspension systems is made in the model.

Since the unsprung masses are neglected, the vertical force acting on each tire is the force reaction of the spring/damper pair. The model contains no additional roll stiffness parameters and assumes all roll stiffness is generated solely by the spring/dampers. In an actual vehicle, roll stiffness is a composite effect of both the spring/dampers and in many vehicles, an additional anti-roll bar. Even neglecting the effects of anti-roll bars, in FOROL, the spring/dampers are assumed to act at the vehicle track width. In all vehicle suspensions, the spring/dampers are inboard of the wheels and their contribution to roll stiffness will be less than predicted by FOROL. It would be possible to artificially set the spring/damper values to give the correct composite roll stiffness, however, this would make any pitch or bounce mode predictions incorrect. The front to rear distribution of the vehicle roll stiffness has first order affects on vehicle steady state and transient responses.

The spring force is modeled using a 9^{th} order function of spring deflection that is fit to the spring/bump stop force-deflection curve measured at the roadwheel. This allows modeling the spring and the bump stop with a single equation, with the bump stop and the rebound stop having equal stiffnesses.

The suspension dampers are modeled as linear functions of suspension velocity with separate compression and extension damping coefficients. These coefficients are measured on a shock tester with the shocks removed from the vehicle. Because the springs and shocks are modeled as collinear and acting above each wheel, the vehicle deflection to shock deflection ratio in the simulation is set based on the

spring geometry. In actual vehicles, the shocks and springs are often not collinear and have different motion gain ratios relative to the sprung mass. To get the damping values correct for suspension bounce or pitch motions, the damping coefficients would need to be scaled based on the differences between the simulation and the actual vehicle motion gain ratios (no mention of this was found in the report). In addition, as in the discussion of roll stiffness above, by assuming that the shocks act as the vehicle track width, roll damping due to the shocks will be higher than in the actual vehicle.

FOROL does not model roadwheel camber change during vehicle bounce or roll motions. The roadwheel camber angles are computed by a coordinate transformation from the sprung mass reference system to the wheel coordinate system. This basically sets the wheel camber angles equal to the sprung mass roll angle, with small corrections made to pitch and yaw angles. This was confirmed with test runs of FOROL.EXE. The wheel camber angles are computed for each axle and the left and right side wheel camber angles are assumed to be equal.

For the vehicles used in this study, all suspensions except the S-10 front suspension, were solid axles. For these suspensions, camber change due to bounce or roll will be negligible during handling maneuvers. For most independent suspension systems, wheel camber angle due to roll will be less than the sprung mass roll angle. The FOROL suspension model is unable to deal with these differences. The suspension model resembles a pure trailing arm or sliding pillar type of model (neither are in common use today).

The FOROL suspension model models roadwheel steer due to sprung mass bounce or roll motions through the use of "cantilevered axial springs". Each end of the axle will move longitudinally during its bounce motion as a function of the spring angle. This approach can account for the roll steer in unsteered axles. However, for steered axles, the steering linkage can add additional roll steer. Research by the authors has shown that roll steer (roadwheel steer due to body roll) can have a significant affect on vehicle steady state and transient responses. Measurements at the VRTC have shown roll steer coefficients (measured in degrees of steer per degree of body roll) as high as 0.25 (deg/deg).

Compliance:

FOROL models suspension compliance as only affecting the road wheel steer angles. Linear coefficients are used to give road wheel steer angle due to lateral force, longitudinal force, and aligning moment. The implementation of the compliance is given in the next section on the steering system

model. The modeling appears to be correct and the inclusion of steer compliance due to longitudinal force is a useful addition.

FOROL does not model any camber compliance due to lateral force. It should be noted, however, that no sensitivity analysis of vehicle response to camber compliance has been performed to date by the authors and this is an area of future research.

2.1.3 Steering System Model

The steering system model uses handwheel angle as its control input option. This control input can be a user specified 6 point file or an internally generated fixed frequency sinusoid. The model consists of a single handwheel to front roadwheel gain, linear coefficients for steer compliance due to lateral and longitudinal forces and aligning moments at the tire contact patch. Two additional parameters are the tire/wheel assembly mass moment of inertia about its z-axis and a front compliance axis damping coefficient. FOROL has no provision for rear wheel steering, Ackerman steering effects, or speed sensitive power assisted steering boost.

The equation used to compute the roadwheel steer angle (front and rear) due to steering system compliance is given by Equation (1). This equation gives the angular acceleration of the wheel due to compliance. Integrating twice gives the steer angle due to compliance. For the front axle, this steer angle is then added to the steer angle due to handwheel rotation (handwheel angle divided by steering system gain) to give the roadwheel steer angle relative to the sprung mass.

$$\ddot{\delta}_{c_l} = \frac{1}{I_{ZZ_W}} \left(-K_{M_{sa}} \delta_{c_l} - C_{M_{sa}} \dot{\delta}_{c_l} + M_{sa} + F_c \Delta_y + F_s \Delta_x \right) \tag{1}$$

where:

δ_{c_l}:	*Compliance Steer*
I_{ZZ_W}:	*Tire/Wheel Inertia about its Z-Axis*
$K_{M_{sa}}$:	*Aligning Moment Compliance Coefficient*
$C_{M_{sa}}$:	*Damping Coefficient*
M_{sa}:	*Aligning Moment*
F_c:	*Circumferential Tire Force*
F_s:	*Tire Side Force*
Δ_y:	*Effective Moment Arm - Circumferential Force*
Δ_x:	*Effective Moment Arm - Side Force*

Using the parameters in the report for the three vehicles in the OE configuration, the steering system natural frequencies are above 15 hertz, the damping ratios were estimated by DRI to be 1.0 (critically damped). With the large tires of the MOD2 configurations, the natural frequencies dropped to approximately 6 hertz with damping ratios less than 0.5. These frequencies are above the range of the vehicle ride and handling frequencies.

Through simulation runs, it was found that predicted yaw rate was insensitive to the steering system inertia and damping parameters (values too low will cause numerical instability). Simulation runs also confirmed that the steering system compliance modeling acts correctly, however the accuracy of the model could not be tested.

Equation (1) assumes a single spring steering model with no interaction between the roadwheels. Research has shown that power steering effects on steering system compliance cannot be accounted for properly using a single spring model [1]. Power steering systems modify the effective steering column compliance as measured at the roadwheels. However, the compliance present in the steering system linkage between the steering box or rack and the roadwheels is unaffected by power steering systems.

An additional limitation with the steering model in FOROL is that steering system freeplay is not included. Some light vehicles, especially pickup trucks and utility vehicles, can have a large amount of steering system freeplay (up to ± 8 degrees at the handwheel). Research has shown that freeplay can have a large influence on vehicle steady state and transient behavior [1]. It is unknown how introducing a large non-linearity such as freeplay would affect the numerical stability of the steering model in FOROL.

2.1.4 Braking Model

The brake system consists of a brake pedal force input, a pedal force to line pressure gain, a fixed proportioning valve brake point and gain, a vacuum booster limit and gain, and front and rear pressure to torque gains. There is no left-right asymmetry. No antilock brake option is provided.

This brake system model is adequate for non-antilock vehicles with fixed proportioning valves. Load sensing brake proportioning valves are common in light trucks, and the number of vehicles equipped with antilock brakes is increasing rapidly. These options should be included in any simulation used for studying limit vehicle performance.

2.1.5 Drivetrain Model

FOROL has no drivetrain model. Two options are available for controlling forward speed. For constant speed operation, a speed governor is used to supply torque to the drive wheels to maintain constant speed. For tests involving longitudinal acceleration, a fixed torque may be input to the drive wheels. FOROL is only set up to simulate rear wheel drive vehicles.

Running FOROL using the speed governor option, it was found that for high handwheel angles (greater than approximately 100 degrees), the drive torque was insufficient to maintain the initial forward speed. The simulation limits the maximum drive torque to 250 foot pounds. This makes comparison of high g steady state response with experimental data very difficult. The required modifications to the simulation software to allow more drive torque are easily implemented.

Future NHTSA simulations will require complete drivetrain models. This will include front, rear, and four wheel drive options. For the NADS, this is an area where extensive modeling work will be required. Future IVHS research may also require simulations with extensive drivetrain models.

2.1.6 Tire Model

Quasi-Static:

The FOROL simulation uses a modified McHenry tire model to represent the quasi-static characteristics of the tires. Variations of this tire model, which assume that forces and moments act at a point contact within the tire/road contact area, are widely used in vehicle dynamic simulation tire models. The coordinate system used in the FOROL tire model is also widely used. This tire model represents the nonlinear characteristics for all of the most important tire relationships; for example, longitudinal force versus slip, side force versus slip angle, etc. Inputs to the tire model include normal load, slip angle, camber angle, and longitudinal slip. Tire model outputs include lateral and longitudinal force and aligning and overturning moment.

The model includes combined braking/driving effects with simultaneous steering effects using a modified friction ellipse. This requires that the vector sum of the lateral tire force and longitudinal tire force remains on or within an ellipse whose axes are defined by maximum side force and maximum circumferential force values. The use of friction ellipse concept is fairly widespread.

Longitudinal force, as a function of longitudinal slip, is determined from empirical equations based on the curve fits of Calspan data. This force is limited by the surface coefficient of friction and the friction ellipse. In the FOROL tire model, tire side force is composed of forces arising from the slip angle and from the camber angle. Both slip angle and camber angle effects are determined from empirical equations based on Calspan data. Side force is also limited by the surface coefficient of friction and the friction ellipse. As is common for empirical tire models of this type, some of the coefficients used in the empirical equations for longitudinal and side force are functions of tire normal force. This accounts for the tire normal load changes which occur during the maneuver.

Empirical relationships relating the tire aligning moment and overturning moment to slip angle and camber angle are used in the tire model. The tire aligning moment and overturning moment models require parametric data from tire tests at two normal load conditions. The actual moments are computed by interpolating using the actual normal load which occurs during the simulation run. Calspan coefficients are used to define the aligning moment and overturning moment relationships with slip angle and camber angle. As is the case with the tire side force, the contributions from slip angle and camber angle are summed to get the total aligning moment and overturning moment.

In all, the tire model requires 39 parameters based on Calspan measurements. Although the details of the FOROL tire model may differ somewhat from tire models used previously at the VRTC, it is for the most part quite similar to other McHenry-based tire models used at the VRTC. Based on the authors experience, this tire model formulation appears to be adequate for modeling the tire quasi-static forces and moments. A detailed evaluation of the tire model would require comparison with experimental results. This is beyond the scope of this study. However, a more detailed evaluation of existing tire models is forthcoming at the VRTC. Certain attributes of the FOROL tire model are unique and may warrant inclusion in an improved tire model.

Dynamic:

FOROL contains no tire dynamics. All tire forces are generated instantaneously based on the empirical quasi-static tire model. As shown previously by the authors [1, 7], this will limit FOROL's ability to predict transient vehicle responses. Research by the authors has demonstrated that the side force lag present in tires reduces effective vehicle yaw rate damping.

2.1.7 Driver Model

FOROL contains no driver model. Control inputs to the vehicle are provided by handwheel angle and brake line pressure script files. These files are limited to a 6 point time versus angle or force description of the control input. There is also an option to have the simulation generate a fixed frequency, fixed amplitude sinusoidal handwheel angle input.

In the course of past simulation evaluation and metric computation programs, the authors have found it to be important to provide the simulation with realistic driver generated control inputs [1, 7] . When comparing simulation predictions to field test data, simulations are "driven" with measured handwheel and brake pressure data from the field tests. A 6 point input file is sufficient to accurately characterize the control inputs for only simple maneuvers such as pseudo-step inputs and trapezoidal lane change maneuvers. FOROL could easily be modified to allow more data points in the input file. This would allow any type of steering input to be studied.

FOROL, with no driver model, cannot simulate any closed-loop maneuvers. This does not present a problem at present. However, future research for NADS and IVHS may need a driver model.

2.1.8 Aerodynamic Model

No vehicle aerodynamics are modeled by FOROL. This does not present a problem for the NHTSA's current crash avoidance research.

2.1.9 Solution Method

For the FOROL simulation, two numerical integration algorithms are available. One is a first-order Adams-Bashford fixed step-size integration routine and the other is a variable step-size Runge-Kutta routine. The first-order Adams-Bashford integrator is a very simple numerical integrator. The first-order Adams-Bashford integrator is sufficient for vehicle handling simulations as long as no braking maneuvers are simulated. The FOROL documentation examples use an integration step size of 0.001 seconds. This step size provides reasonable results and the run times are acceptable. Using a 25 Mhz IBM Model 80 386 personal computer with a math co-processor, and a step size of 0.001 seconds, a 5 second simulation run requires about 1 minute and 20 seconds of computer run time. Using smaller integrator step sizes

increases the simulation run time, while larger step sizes reduce integrator accuracy and may result in numerical stability problems.

Using a step size of 0.001 seconds, the first-order Adams-Bashford integrator becomes unstable for braking maneuvers. Integrating the wheel spin equations is a problem from a numerical integration stability perspective. Methods have been devised to cope with the highly nonlinear longitudinal tire force characteristics which arise during the simulation of braking maneuvers. These methods involve using perturbation analysis to describe the wheel spin moment equations in a more numerically solvable form. FOROL does not utilize any perturbation analysis to solve the wheel spin equations.

Although no mention is made in the report, it is assumed that the variable step-size Runge-Kutta integration routine was made available in the FOROL simulation to deal with the highly nonlinear conditions/equations which occur while simulating braking maneuvers. This integrator is considerably more sophisticated than the first-order Adams-Bashford fixed step-size integrator. The Runge-Kutta integrator does adequately solve the wheel spin equations even during braking. However, computer run time is sacrificed using the variable step-size Runge-Kutta integrator. With the Runge-Kutta routine, a 5 second simulation run requires about 9 minutes and 20 seconds of computer run time. If simulation run time is not a concern, then using this integrator provides an acceptable procedure to solve the simulation equations, even during braking simulations.

2.1.10 Miscellaneous

The FOROL simulation provides a routine to determine simulation initial conditions (trim position). This routine finds the initial pitch angle, CG height, and tire loads by an iterative process. For runs made using the parameter decks provided by DRI, no problems were encountered concerning the computation of initial conditions.

2.2 Parameter Measurement

The vehicle and tire parameters required to run FOROL and the methods DRI used to measure them are contained in Appendix C of the DRI report. This section will describe the parameters, review the test methods used to obtain them, and assess the effort required for the VRTC to measure/obtain them.

2.2.1 Required Parameters

The parameters for FOROL can be broken in four main categories: geometric, inertial, suspension/steering, and tire.

Geometric:

The geometric parameters required by FOROL are listed in Table I. These are all descriptive parameters that characterize the physical dimensions of the vehicle. The parameters locating the height of the upper spring cup, BU and EU, are used to define the roll axis position and are not necessarily the physical location of the springs in the vehicle.

Table I - Geometric Parameters

Name	Units	Description
TF	ft	Front Track width: measured from center line of tires
TR	ft	Rear Track width: measured from center line of tires
AU	ft	Longitudinal distance from CG to top of front spring cup
CU	ft	Vertical distance from CG to top of front spring cup
BU	ft	Longitudinal distance from CG to top of rear spring cup
EU	ft	Vertical distance from CG to top of rear spring cup
THETASF	rad	Front spring angle about Y-axis
THETASR	rad	Rear spring angle about Y-axis
RW	ft	Undeflected tire radius

Inertial:

The inertial parameters required by FOROL are listed in Table II. These parameters describe the sprung mass and wheel inertial properties (center of gravity position and mass moment of inertia).

In the FOROL description of the vehicle, only the vehicle sprung mass is used (see section on Rigid Body Dynamics) with no description of the unsprung masses. The pitch and roll mass moments of inertia are for the sprung mass only, while the yaw inertia and yaw/roll product of inertia are for the total vehicle. The single center of gravity position used in the simulation is for the total vehicle.

Table II - Inertial Parameters

Name	Units	Description
A	ft	Longitudinal distance from total CG to front axle
B	ft	Longitudinal distance from total CG to rear axle
MS	sl	Sprung mass
IXXS	$sl \cdot ft^2$	Sprung mass roll moment of inertia
IYYS	$sl \cdot ft^2$	Sprung mass pitch moment of inertia
IZZ	$sl \cdot ft^2$	Total vehicle yaw moment of inertia
IXZ	$sl \cdot ft^2$	Total vehicle yaw/roll product moment of inertia
IYYW	$sl \cdot ft^2$	Wheel spin moment of inertia
IZZW	$sl \cdot ft^2$	Wheel yaw (about steer axis) moment of inertia
Z	ft	Total vehicle center of gravity height

Suspension/Steering:

The parameters for the FOROL suspension model, shown in Table III, are curve fit parameters from suspension bounce and steer test data. Steering system parameters are given by an overall system gain along with compliance terms. The brake system is described by parameters for a proportioning valve, wheel pressure/torque gains and a vacuum booster. A discussion of the modeling for all these systems is given above.

Tire:

The tire model in FOROL is a modified McHenry model. This model uses curve fit parameters, listed in Table IV, from quasi-static tire force and moment data. A non-linear tire vertical stiffness equation and linear vertical tire damping are also included.

2.2.2 Test Methods

The following is a review of the test methods used by DRI to measure/obtain the parameters for the FOROL. Appendix C of the DRI report contains descriptions of the parameter measurement procedures.

Geometric:

DRI states that "*...mass and geometry measurements, were simple to measure, requiring no special procedures.*" The geometric parameters contained in Table I are assumed to have been measured using a steel tape. This should be sufficient for geometric parameters of this kind if the measurements are made with care.

Table III - Suspension Parameters

Name	Units	Description
FDS1F	lb	Front spring force at deflection DS1F
DS1F	ft	Reference front spring deflection
DS2F	ft	Front bump stop deflection
ASF	$(lb/ft)^9$	Ninth order front bump stop spring coefficient
BSF	lb/ft	Linear front spring coefficient
FDS1R	lb	Rear spring force at deflection DS1F
DS1FR	ft	Reference rear spring deflection
DS2R	ft	Rear bump stop deflection
ASR	$(lb/ft)^9$	Ninth order rear bump stop spring coefficient
BSR	lb/ft	Linear rear spring coefficient
CS1F	lb·sec/ft	Front spring extension damping coefficient
CS2F	lb·sec/ft	Front spring compression damping coefficient
CS1R	lb·sec/ft	Rear spring extension damping coefficient
CS2R	lb·sec/ft	Rear spring compression damping coefficient
KMSAF	ft·lb/rad	Coefficient for front steer compliance due to aligning moment
KFCF	lb/rad	Coefficient for front steer compliance due to circumferential force
KFSF	lb/rad	Coefficient for front steer compliance due to side force
CMSAF	ft·lb·sec/rad	Front steer compliance damping coefficient
KMSAR	ft·lb/rad	Coefficient for rear steer compliance due to aligning moment
KFCR	lb/rad	Coefficient for rear steer compliance due to circumferential force
KFSR	lb/rad	Coefficient for rear steer compliance due to side force
CMSAR	ft·lb·sec/rad	Rear steer compliance damping coefficient
SWRATIO	rad/rad	Ratio of steering wheel angle to front wheel angle
GAIN1	psi/lb	Ratio of brake master cylinder pressure to pedal force
PVBREAK	psi	Proportioning valve brake pressure
PVGAIN	psi/psi	Proportioning valve input/output pressure ratio above PVBREAK
GAIN2F	ft·lb/psi	Ratio of front brake torque to line pressure
GAIN2R	ft·lb/psi	Ratio of rear brake torque to line pressure
BLIMIT	lb	Pedal force at which booster limits
BGAIN	lb/lb	Ratio of booster force out to force in

In the description of the simulation model, the height of the spring cups (CU and EU) are said to define the roll axis position. Therefore, these measurements are not to the physical position of the spring cups. However, no measurement technique is presented for measuring the roll axis or roll center positions. During the review of the rigid body dynamics, no inclusion of a roll axis was found.

Inertial:

The description of the inertial parameter techniques by DRI contains no information about the type or accuracy of any of the instruments used. Therefore, only general comments about the procedures are possible.

The longitudinal center of gravity position (A and B) require only vehicle corner weights and a steel tape to measure wheelbase. The accuracy of the scales used will determine the accuracy of these

Table IV - Tire Parameters

Name	Units	Description
DT1	ft	Tire sidewall height at static load
AT	$(lb/ft)^9$	Ninth order tire rim bottoming spring coefficient
BT	lb/ft	Linear tire spring coefficient
CT	lb·sec/ft	Linear tire damping coefficient
FRMAX	lb	Radial force when tire is compressed to the rim
RPEAK	—	Ratio of circumferential friction coefficient to normalized maximum side force coefficient
SPEAK	—	Slip ratio at peak circumferential force
AFSAL	—	Normalized front force due to slip angle coefficient
BFSAL	—	Normalized front force due to slip angle coefficient
AMUS	$1/lb^2$	Coefficients for maximum side force coefficient
BMUS	1/lb	Coefficients for maximum side force coefficient
CMUS	—	Coefficients for maximum side force coefficient
BFYAL	—	Cornering stiffness coefficient
BFYAMX	—	Coefficient for saturation side force due to slip angle
ABARSAT	rad	Side force saturation slip angle
BFYXMX	—	Coefficient for saturation side force due to camber angle
BFYXI	—	Coefficient for side force due to camber angle
XBARSAT	rad	Side force saturation camber angle
AFSXI	—	Normalized front force due to camber angle coefficient
BFSXI	—	Normalized front force due to camber angle coefficient
FN1	lb	Tire test lowest normal load
FN2	lb	Tire test highest normal load
BOTA11	ft·lb/rad	Linear coefficient for overturning moment due to slip angle for FN1
BOTA12	ft·lb/rad	Linear coefficient for overturning moment due to slip angle for FN1
BOTA21	ft·lb/rad	Linear coefficient for overturning moment due to slip angle for FN2
BOTA22	ft·lb/rad	Linear coefficient for overturning moment due to slip angle for FN2
AOT1	rad	Slip angle above which BOTA12 is used
AOT2	rad	Slip angle above which BOTA22 is used
AOTX1	$ft·lb/rad^2$	Coefficient for overturning moment due to camber angle for FN1
BOTX1	ft·lb/rad	Coefficient for overturning moment due to camber angle for FN1
AOTX2	ft·lb/rad	Coefficient for overturning moment due to camber angle for FN2
BOTX2	ft·lb/rad	Coefficient for overturning moment due to camber angle for FN2
AMSAA1	$ft·lb/rad^3$	Coefficient for aligning moment due to slip angle for FN1
BMSAA1	$ft·lb/rad^2$	Coefficient for aligning moment due to slip angle for FN1
CMSAA1	ft·lb/rad	Coefficient for aligning moment due to slip angle for FN1
AMSAA2	$ft·lb/rad^3$	Coefficient for aligning moment due to slip angle for FN2
BMSAA2	$ft·lb/rad^2$	Coefficient for aligning moment due to slip angle for FN2
CMSAA2	ft·lb/rad	Coefficient for aligning moment due to slip angle for FN2
AMSA1	rad	Aligning moment saturation slip angle for FN1
AMSA2	rad	Aligning moment saturation slip angle for FN2
MSASAT1	ft·lb	Aligning moment due to slip angle saturation for FN1
MSASAT2	ft·lb	Aligning moment due to slip angle saturation for FN2
BMSAX1	ft·lb/rad	Coefficient for aligning moment due to camber angle for FN1
BMSAX2	ft·lb/rad	Coefficient for aligning moment due to camber angle for FN2

measurements. Scales with 1 percent accuracy will give longitudinal center of gravity position to within approximately 0.5 inches. It is not thought that simulation predictions are extremely sensitive to these measurements and standard shop equipment will suffice in most cases.

The procedure to measure total vehicle center of gravity height is similar to the procedure used by Systems Technology, Inc. A detailed error analysis of this procedure is contained in [8]. This analysis showed that center of gravity height was very sensitive to scale accuracy. Using scales with a rated accuracy of ± 1 percent, 2s (2 standard deviations) error bounds ranging from ± 0.44 to ± 1.3 inches were computed.

In addition to scale accuracy, it was found that longitudinal suspension compliance, if not accounted for or eliminated, will cause systematic, vehicle dependent measurement errors up to +0.35 inches. There is no mention of any accounting for this in the DRI procedure.

Total vehicle mass moment of inertias are measured using the "horizontal axis pendulum method". The entire vehicle is suspended by two parallel cables from the shop ceiling and allowed to oscillate about the axis of interest. No information is given about the specific method of attaching the cables to the vehicle. Therefore, no estimates can be made about the accuracy of this method. If it is possible to have the vehicle oscillate solely about the pivot axis at the shop ceiling, this method may work well. However, any other rotation by the vehicle will make this a complex pendulum and add errors to the measurements. DRI states that it is preferable to have the support lines as short as possible. This can be verified using simple calculations. Using support lines of 5 feet, the roll inertia to be measured is approximately equal to the vehicle pendulum (mass of the vehicle times the cable length squared). With support lines much longer than this, the vehicle roll inertia will only be a small fraction of the total system inertia measured using this method and therefore be very difficult to measure accurately.

An additional source of error in this type of measurement is determining the cable length accurately. The length needed is from the pivot axis to the vehicle center of gravity. Cable length is a squared term in the simple pendulum equation used and therefore inertia measurements are very sensitive to this length. Any error in the center of gravity height measurements will affect the inertia measurements. A 1 inch error in cable length will give a 5 to 10 percent error in roll moment of inertia, depending on the size of the vehicle.

For the pitch and roll inertias, only the sprung mass values are used by FOROL. The measurements made measure the total vehicle inertias and the contributions of the unsprung masses need to be removed. The DRI report says this is done mathematically, though no details are given. To do this accurately, the unsprung masses need to be removed, weighed, and their individual inertias measured.

The wheel spin and yaw moment of inertias are reported to be measured using a torsional pendulum. No information, however, is given about the test device used. These measurements can be performed with a simple trifilar pendulum, and if done with care can be quite accurate.

Suspension/Steering:

The suspension linear spring rates are measured by mounting a string potentiometer vertically between the vehicle frame and axle near the centerline of the vehicle. The sprung mass is then loaded, and the tire loads and the suspension deflection are recorded. A straight line fit of the data then gives the spring rate. The suspension bump stop stiffness is estimated. The model also requires the front and rear spring force at the spring "reference or center" position.

The viscous damping parameters are given by compression and extension damping coefficients for the front and rear shocks. These measurements were made by an outside shop with a shock dyno.

Suspension steer compliances due to forces in the ground plane are measured by applying forces in the ground plane and measuring the resulting steer angles. Compliance due to aligning moment is measured by applying a moment to the wheel about its z-axis and measuring the resulting steer angles.

The braking system parameters were measured using a pedal force transducer, and front and rear brake line pressure transducers. Single axle straight line braking stops were used to measure wheel torque to line pressure ratios. These are standard procedures.

Steering ratio was measured by measuring roadwheel angle using radius plates while the handwheel was rotated. If done with care, this method can be fairly accurate.

Tire:

Tire vertical stiffness was measured for a non-rolling tire by applying vertical loads and measuring the tire deflection with a string pot. This measurement technique appears to be good. Tire damping is measured by bouncing the tire in a fixture and measuring the decay of amplitude of the oscillations.

Tire force and moment parameters were measured using plots from the Calspan TIRF machine. Examples of the data reduction, performed by hand, are given in Appendix D of the DRI report.

2.2.3 Compatibility with VRTC

Equipment currently available at the VRTC can measure most of the parameters needed for the FOROL simulation. The following are the parameters that can not be measured at the VRTC.

Tire vertical damping ratio. A fixture similar to that described by DRI would need to be constructed. This would not be a large task, and would provide useful data for any simulation used.

Product moment of inertia. The Inertial Parameter Measurement Device (IPMD) used at the VRTC for inertial measurements was not designed to measure the product moment of inertia. The IPMD can not be modified for this measurement, and a new machine would need to be designed and constructed. It is not thought that the product of inertia has a significant influence on vehicle directional control and therefore need not be measured (this is a very difficult measurement to make).

Shock absorber damping coefficients. A shock dyno is not available at the VRTC. However, shocks can be sent out to be measured. This is a time consuming and expensive process. If measuring shock absorber characteristics becomes necessary at the VRTC, then better methods of obtaining shock data will need to be investigated.

Tire force and moment data. The VRTC does not have a tire test machine. All tire testing needs to be done by outside labs. There are no plans at the present time to get this capability at the VRTC.

2.3 Road Profile

FOROL assumes an infinite, flat road surface with a constant coefficient of friction. No interaction with roadside obstacles can be simulated. It is not stated if the surface friction can be changed for different simulation runs. The parameters RPEAK may be able to be changed to simulate low or high friction surfaces. However, the effect on the tire model is unknown.

2.4 Comparison with Experimental Data

DRI provided hard copies of all the experimental runs in Appendix E of their report. It was thought that this would provide a good benchmark to compare with the simulation predictions. However, review of the experimental data showed there were discrepancies between the lateral acceleration and yaw rate

measurements. Upon review of their experimental data, DRI revealed that a calibration error (reported values were thirty five percent low) was found in all of the yaw rate measurements. Because of this, all comparisons of simulation predictions to experimental data in this report were restricted to lateral and longitudinal acceleration.

2.4.1 Steady State

Ramp steer maneuvers were run to compare the steady state simulation predictions with the experimental data. Runs were made at VRTC for the Toyota and the K20 pickups, utilized in the DRI research program, in their original equipment configurations. Vehicle speed and handwheel angle measurements were taken from the experimental data and input into the simulation. Lateral acceleration was used for the comparisons. In all cases, the simulation predictions were significantly higher than the experimental data. The results are shown in Table V. Lateral acceleration predictions ranged from 30 to 95 percent higher than the experimental data.

Table V - Steady State Lateral Acceleration Comparisons

			experiment / simulation
Vehicle	Speed (mph)	Steer Angle (deg)	A_y (g's)
Toyota	55	30	0.17 / 0.27
Toyota	55	50	0.28 / 0.43
Toyota	55	70	0.33 / 0.55
K-20	55	50	0.22 / 0.43
K-20	55	70	0.39 / 0.55
K-20	55	100	0.50 / 0.67

Simulated straight line braking maneuvers were run to compare the simulated braking predictions with the experimental data. The results for the Toyota are shown in Table VI. It can be seen that the A_x predictions are fairly close, but the front to rear brake line pressure distribution is biased toward the rear in the simulation data. This is thought to be a simulation input parameter problem and not a fundamental problem with the simulation.

Table VI - Steady State Longitudinal Comparisons

Vehicle	Pedal Force (lbs)	experiment / simulation A_x (g's)	Front Pressure (psi)	Rear Pressure (psi)
Toyota	10	0.17 / 0.15	300 / 220	250 / 220
Toyota	20	0.28 / 0.29	555 / 443	360 / 440
Toyota	33	0.47 / 0.47	1000 / 732	555 / 681
Toyota	45	0.67 / 0.64	1472 / 998	777 / 891

2.4.2 Dynamic

Past research at VRTC has shown frequency response techniques to be quite useful for evaluating dynamic/transient simulation predictions [9, 10]. By generating vehicle output (eg. lateral acceleration) frequency response to handwheel angle inputs, much can be learned about the characteristics and validity of a simulation model.

Lateral acceleration frequency responses to handwheel angle inputs have been generated from FOROL simulation runs and from the experimental data in the DRI report. Figure 4 shows the simulated and experimental lateral acceleration frequency response magnitude curves for the Toyota Pickup at 55 mph in its standard configuration, and Figure 5 shows the corresponding phase angle curves. These frequency response curves have been generated by measuring the amplitude ratio and phase shift of the lateral acceleration response relative to the handwheel angle input at discrete sinusoidal frequencies.

Research at VRTC has shown that, for the purposes of evaluating a simulation, frequency response comparisons with experimental results can be performed in the vehicle's linear operating range. The experimental and simulated sinusoidal steering inputs used to generate the frequency response curves resulted in lateral acceleration levels which are believed to be in the linear regime for the vehicle. For the simulation runs used to generate the frequency response curves, frequencies of 0.1, 0.2, 0.5, 1.0, 2.0, and 5.0 hertz, and handwheel angle amplitudes of ± 45 degrees were used. Experimental data was available at 0.1, 0.33, 0.5, and 1.0 hertz with a variety of handwheel angle amplitudes.

Figure 4 shows that at low frequency levels the experimental lateral acceleration magnitude is considerably less than the simulated lateral acceleration. This is in agreement with the steady state results

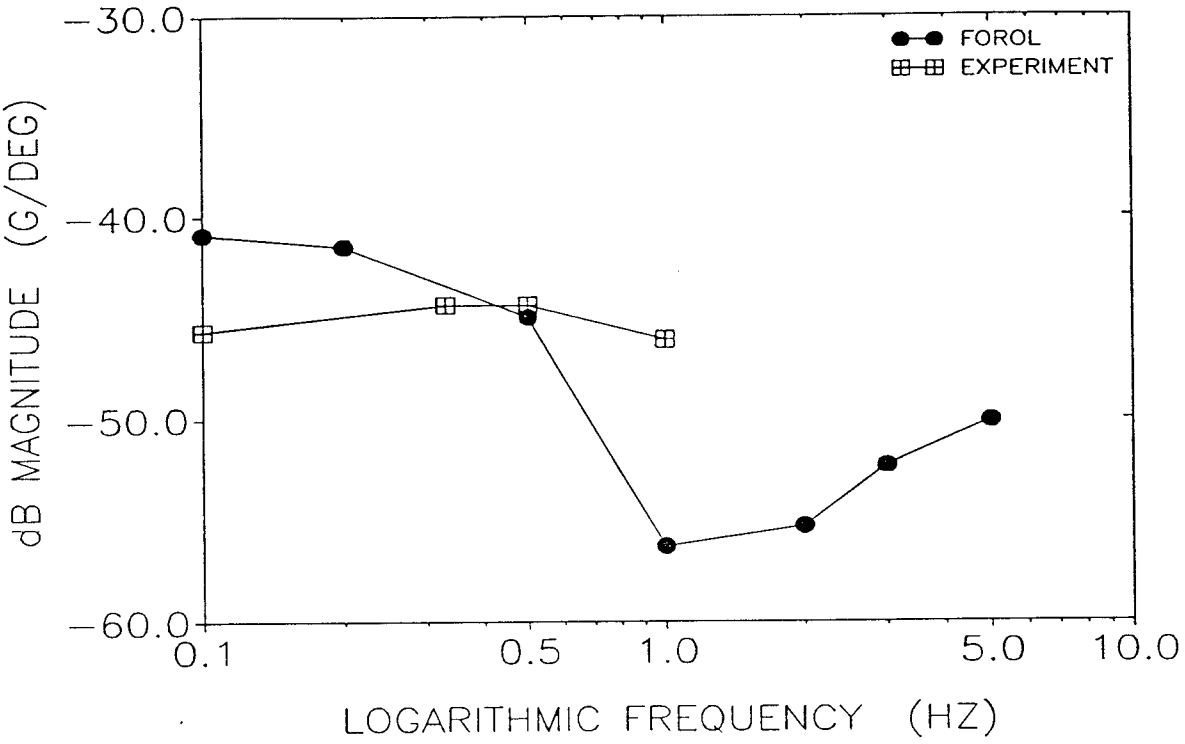

Figure 4 - Lateral Acceleration Frequency Response Magnitude 55 mph Toyota Pickup

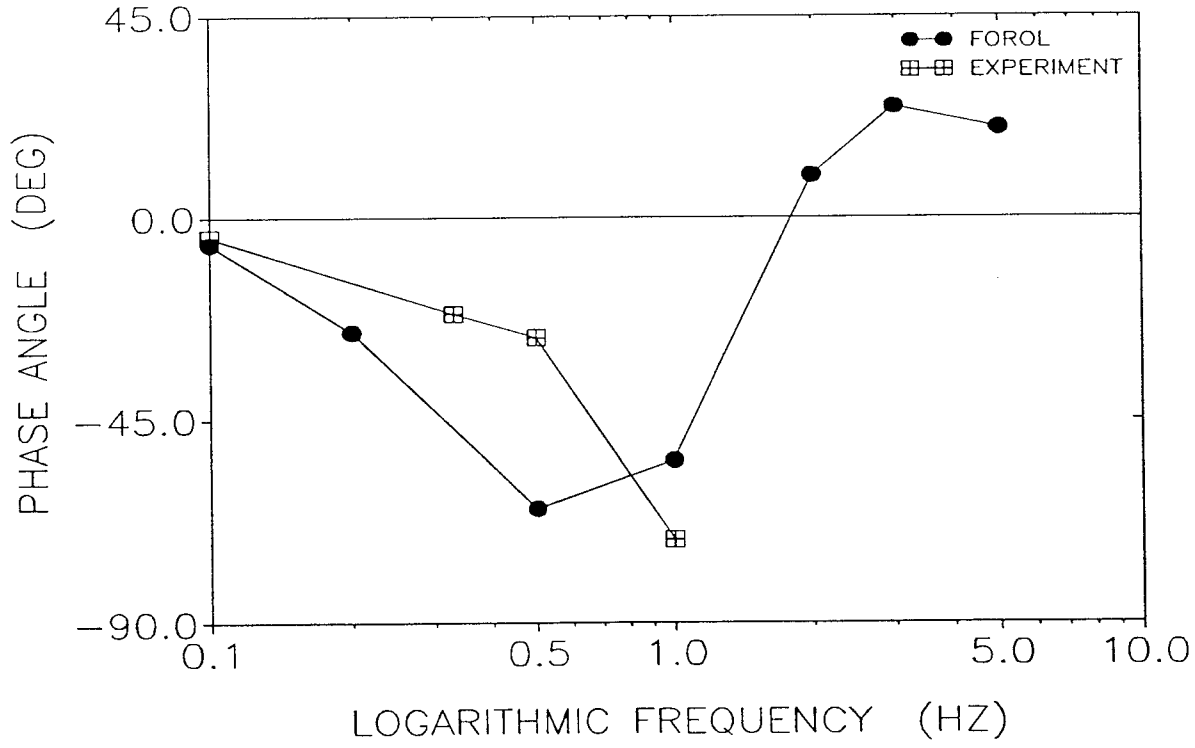

Figure 5 - Lateral Acceleration Frequency Response Phase Angle 55 mph Toyota Pickup

provided in Table V. The reasons for the low frequency discrepancies are the same as for the steady state discrepancies.

The experimental lateral acceleration magnitude is relatively flat up to one hertz, the highest frequency for which data was available, while the simulated magnitude has its valley at near one hertz. The shape of the simulated magnitude curve is typical for lateral acceleration frequency response. However, based on the limited experimental data, and lack of agreement with the data available, it is difficult to judge the quality of the simulation's ability to predict frequency and transient responses.

As shown on Figure 5, the lateral acceleration frequency response phase angles show disagreement between the experimental and simulated results. Again, the shape of the simulated phase angle curve is typical for lateral acceleration phase angle. The experimental curve tends toward a minimum value at a higher frequency than the simulated curve. This fact, along with the shape of the experimental curve on Figure 4, indicate that the lateral acceleration magnitude valley for the experimental vehicle likely occurs at some frequency above one hertz. Unfortunately, available experimental data does not extend to high enough frequencies to confirm this.

These discrepancies in the lateral acceleration frequency response curves indicate model deficiencies and/or experimental problems. Based on past work at VRTC, the fact that the FOROL simulation does not include tire dynamics may account for some of the discrepancy seen between the simulated and experimental magnitude and phase angle curves [7].

3.0 Introduction: IMIRS

In September of 1988, the National Highway Traffic Safety Administration contracted Dr. Andrzej G. Nalecz of the University of Missouri-Columbia to develop the Intermediate Maneuver Induced Rollover Simulation (IMIRS). The main project goals were to investigate light vehicle rollover behavior, develop a rollover predictor function based on energy analysis, and perform time domain sensitivity analysis for light vehicles in both rollover and non-rollover maneuvers. The final report, DOT-HS-807-672, and the IMIRS were delivered in February 1991.

The report contains an IMIRS user's manual along with the derivation of the IMIRS model equations and results of the time domain sensitivity analysis using IMIRS along with the University of Missouri-Columbia developed general purpose sensitivity algorithms. IMIRS was developed as a PC based vehicle handling and rollover model. For the sensitivity analysis, a Fortran version was developed to run on a VAX computer. This evaluation will focus on the PC based model that was delivered to the NHTSA. The evaluation will not include the sensitivity analysis portion of the contract.

The following is a short description of the IMIRS simulation from the final report.

> *"The Intermediate Maneuver Induced Rollover Simulation (IMIRS) represents a package of computer programs which can be used to investigate the handling and stability properties of a wide range of passenger vehicles, light trucks, and utility vehicles. The package is capable of accurately predicting vehicle directional response (the forward, lateral and yawing degrees of freedom), as well as vehicle rolling motion (the roll angles of sprung and unsprung masses as well as the relative translation between sprung and unsprung masses) . The tire model utilized in the IMIRS is based on the non-dimensional approach and is capable of operating over a very wide regime of operating conditions (i.e. slip angle, normal load, and slip ratio.) This model uses tire data which is currently available for a wide variety of different tires. Eight different kinematic configurations of front suspension systems can be employed in conjunction with any one of 19 different rear independent and dependent suspension systems. The user may investigate vehicle response using a variety of different steering and braking input signals including (but not limited to) step, ramp and sinusoidal inputs. These inputs may be stored for subsequent simulation runs.*

The IMIRS represents an enhanced version of the Lateral Weight Transfer Simulation (LWTS) developed by Dr. A.G. Nalecz in 1986 (NHTSA-U.S. DOT Contract No. DTNH22-86-P-07326). The following additions and improvements have been made in this newer version:

* *The ability to simulate vehicle skidding motion after the tire limits of adhesion have been reached.*

* *The ability to simulate maneuver induced vehicle rollover.*

* *Separate roll degrees of freedom for sprung and unsprung masses.*

* *A more sophisticated braking model which uses slip ratio to determine braking force.*

* *The use of additional Calspan tire data to determine tire aligning moment, camber thrust, sliding friction, and the slip ratio at peak braking as functions of tire normal and side load.*

* *The additional choice of step, ramp, sinusoidal, or arbitrary steering inputs. These inputs can be stored and recalled for later runs.*

* *The additional choice of step, ramp or arbitrary braking/thrust inputs which can be stored and recalled for later runs.*

* *The addition of simple aerodynamics to compute the affects of airflow on vehicle yaw.*

* *Complete graphics support for CGA, EGA, and VGA graphics cards, partial support for Hercules graphics cards.*

The entire software package is menu driven (using menus identical to those employed in the LWTS) and requires a minimum of computer expertise on the part of the user. The

user need only be familiar with rudimentary vehicle dynamics terminology in order to effectively use the software."

The IMIRS simulation was delivered with both source and executable code. Two sample vehicle data decks were also included.

3.1 Governing Equations

3.1.1 Rigid Body Dynamics and Simulation Degrees of Freedom

The IMIRS simulation uses two coupled dynamic models to simulate vehicle response. One model represents the handling mode of vehicle operation. Figure 6, (taken from the IMIRS documentation - Reference 3) shows the IMIRS handling model, which has three degrees of freedom. The other model represents the roll characteristics of the vehicle using five degrees of freedom. Figure 7 shows the IMIRS roll model.

The three degrees of freedom in the IMIRS handling model are longitudinal velocity, lateral, and yaw rate. Figure 6 shows the handling model coordinate system. These are typical degrees of freedom for three degree of freedom handling models. The equations developed for the handling model consider one mass, equal to the mass of the entire vehicle and one moment of inertia, the total vehicle yaw moment of inertia. Lateral, longitudinal, and yaw motions are confined to a plane parallel to the road plane. The differential equations describing this handling model are well established and, accordingly, no derivation of them is provided.

The derivatives of the linear and angular accelerations are numerically integrated to provide the linear and angular velocity and position vectors for the vehicle. For this type of simulation, this is the usual technique for determining rigid body motions.

This simple model does neglect some secondary dynamics associated with the handling characteristics of the vehicle. For instance, the lateral inertial forces generated by the dynamic roll motions of the sprung mass are not included in the model. Some of these secondary effects are included in simulation models at VRTC, and although their contributions to total vehicle response are not well established, they are thought to be fairly small.

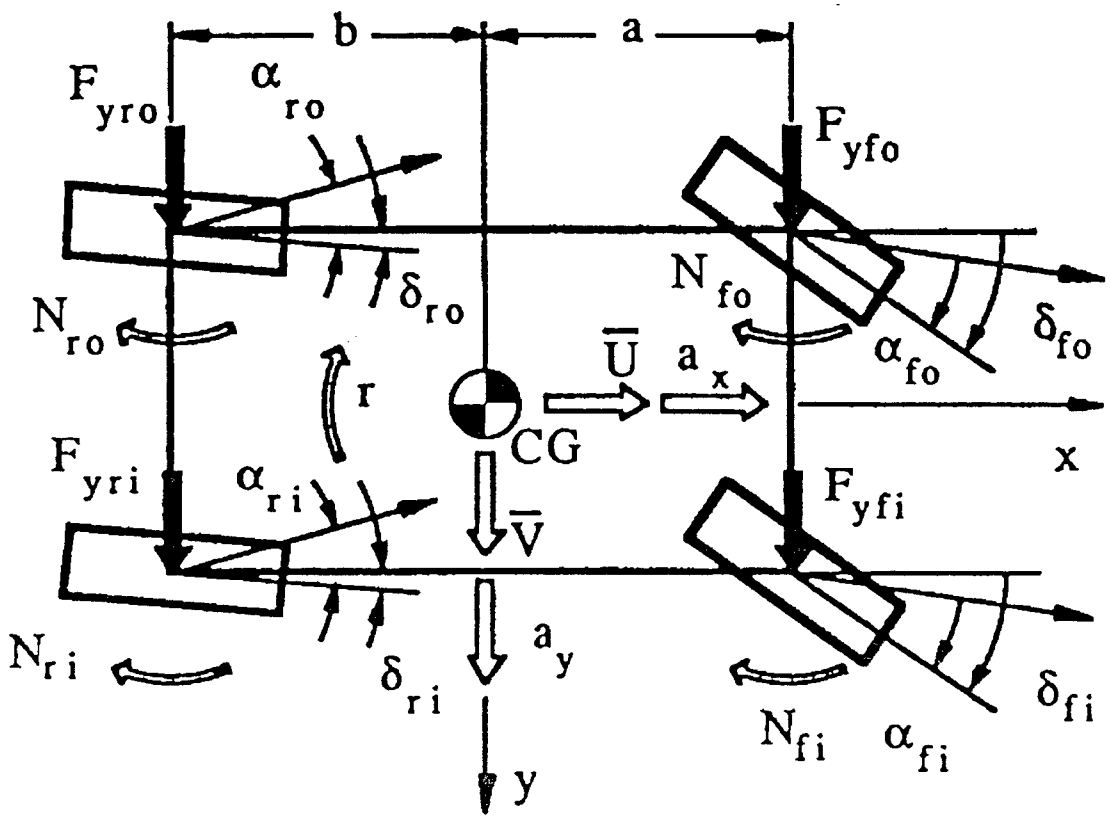

Figure 6 - IMIRS Handling Model

The five degrees of freedom included in the IMIRS roll model are roll motion of the unsprung mass, roll motion of the sprung mass relative to the unsprung mass, lateral and vertical motion of the unsprung mass, and heave motion between the sprung and unsprung masses. As indicated in Figure 7, the roll model is a planar model based on the roll center concept. The equations of motion of the roll model have been derived using a Lagrangian formulation.

The Lagrangian formulation involves specifying the kinetic and potential energy terms associated with each of the generalized coordinates, which are the displacements associated with each of the individual degrees of freedom (Figure 7). Appropriate partial derivatives of these terms with respect to generalized coordinates and velocities are required. This formulation technique also involves specifying energy dissipation terms, and their associated partial derivatives with respect to the generalized velocities. Lastly, the external generalized forces need to be specified.

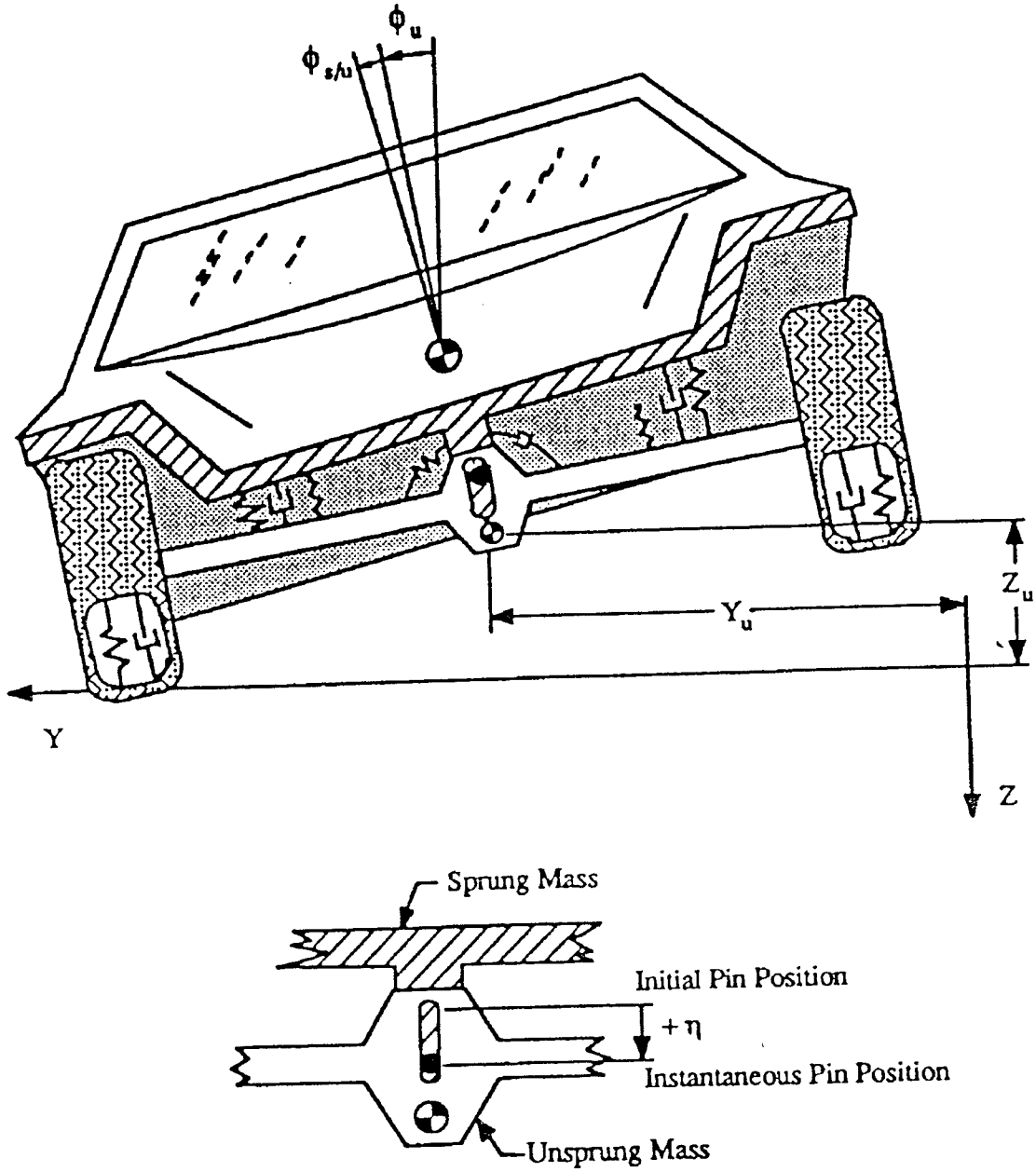

Figure 7 - IMIRS Rollover Model

The planar roll model includes the sprung mass and a single unsprung mass, as well as sprung mass moment of inertia and a single value for unsprung mass moment of inertia. Suspension loads from springs (including bump stop forces), dampers (shock absorbers), and auxiliary roll stiffness and damping are included in the Lagrangian formulation. Similarly, tire vertical forces from tire stiffness and damping are included in the roll model.

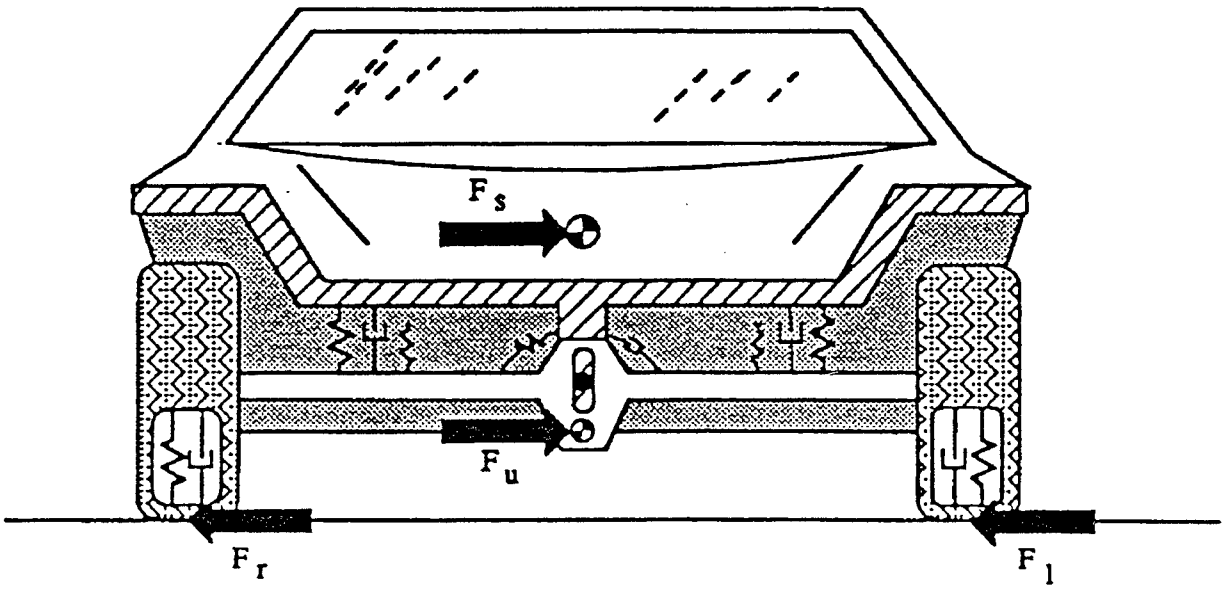

Figure 8 - External Forces to Planar Roll Model

The Lagrangian formulation of the roll model equations results in five coupled second-order differential equations. These equations are quite comprehensive for the given roll model. That is, no simplifying assumptions are made concerning the development or final form of the equations. This is somewhat opposite to the handling model equations, wherein only primary factors were included.

The five equations which comprise the roll model can be solved for the generalized accelerations and written in matrix form. The form of these equations is shown below.

$$\{ \ddot{q} \} = [M]^{-1}\{ f \} \tag{2}$$

where

$\{ \ddot{q} \}$ = *Generalized AccelerationVector*
$[M]^{-1}$ = *Inverse of the "Mass" Matrix*
$\{ f \}$ = *Generalized Forces*

Inverting the matrix [M] at each time step, since it is time dependent, allows for the solution of the coupled acceleration terms. The accelerations are numerically integrated to determine the generalized velocities and displacements. This routine of inverting a matrix in order to numerically solve a system of coupled differential equations is a standard simulation method, and is well suited to this type of model.

The vehicle roll model is coupled to the vehicle handling model through the external forces acting on the vehicle. These forces include the lateral reaction forces generated by the tires and the inertial forces acting on the vehicle masses, as illustrated in Figure 8.

The IMIRS simulation includes no degree of freedom for vehicle pitch dynamics. This is thought to be not critical for handling simulations, but may influence simulation predictions at near rollover conditions. No steering system is included in the simulation model, as are no wheel spin degrees of freedom.

In summary, the IMIRS simulation has eight degrees of freedom. As mentioned, there are three handling model degrees of freedom, yaw rate, lateral velocity, and longitudinal velocity, and five roll model degrees of freedom, roll motion of the unsprung mass, roll motion of the sprung mass relative to the unsprung mass, lateral and vertical motion of the unsprung mass, and heave motion between the sprung and unsprung masses

3.1.2 Suspension Model

Kinematics:

The IMIRS suspension model is based on the classical fixed roll axis approach. This roll axis is computed analytically by suspension system pre-processing programs. These programs have been written for 8 front suspension and 19 rear suspension configurations. They require the XYZ coordinates of the suspension system locating link pivot points. From this data, the roll center height is computed for use in the simulation. No other suspension kinematic information is computed by the pre-processors. As stated in Section 3.1.1, the IMIRS contains coupled handling and rollover models. The kinematics associated with the handling model will be discussed first, followed by the rollover model.

The extent of the road wheel kinematics described in the IMIRS documentation are the front wheel camber change and rear wheel steer due to the roll angle between the sprung and unsprung masses. Neither front axle roll steer or rear axle camber change due to roll are modeled. Past studies [1] have shown both of these suspension characteristics to influence vehicle directional response.

Examination of the source code revealed that the front axle camber angle change parameter is applied to both the front and rear axles. Due to differences in front and rear suspension system design, this

parameter will not be equal front to rear in most vehicles. This is most likely a coding problem and can be easily fixed.

The rear axle roll steer parameter contained in the data deck is not implemented in the simulation. This was confirmed with simulation runs where the roll steer parameter was changed with no effect on the simulation output. This is most likely a coding problem and can easily be fixed. Research [1] has shown that front and rear axle roll steer can have a significant influence on vehicle steady state and transient response.

The simulation parameters called "front/rear suspension auxiliary roll stiffness" are the total front and rear roll stiffness due to the composite contributions of the suspension springs and anti-roll bars. IMIRS uses these parameters to determine the front to rear roll stiffness distribution for the axle load transfer calculations in the handling model. In the rollover model, these parameters are combined to form the total vehicle roll stiffness and are used in the roll moment computations.

The data deck has a parameter for the combined front and rear suspension auxiliary roll damping. This parameter is used in the rollover model in the roll moment equations, however, it is not used in the handling model. The simulation therefore does not account for the individual axle roll damping in the load transfer computations. Roll damping does affect load transfer during transient maneuvers and therefore affects vehicle directional control. This could be implemented as a lateral load transfer due to roll velocity.

The modeling of the springs consists of linear rate springs with a prescribed static length and rate. These springs act between the unsprung and sprung masses at a specified spring track. Bump stops are described by an undeformed length and linear stiffness and act in the same line as the springs. Linear dampers are also modeled to act along this same line.

The rollover tire model contains vertical stiffness and damping. By computing tire deflection, the unsprung mass roll angle and center of gravity height relative to the ground can be computed.

Compliance:

No suspension system compliances are modeled by IMIRS. Past research [11, 12, 13] has demonstrated the importance of suspension system steer and camber compliances to forces and moments

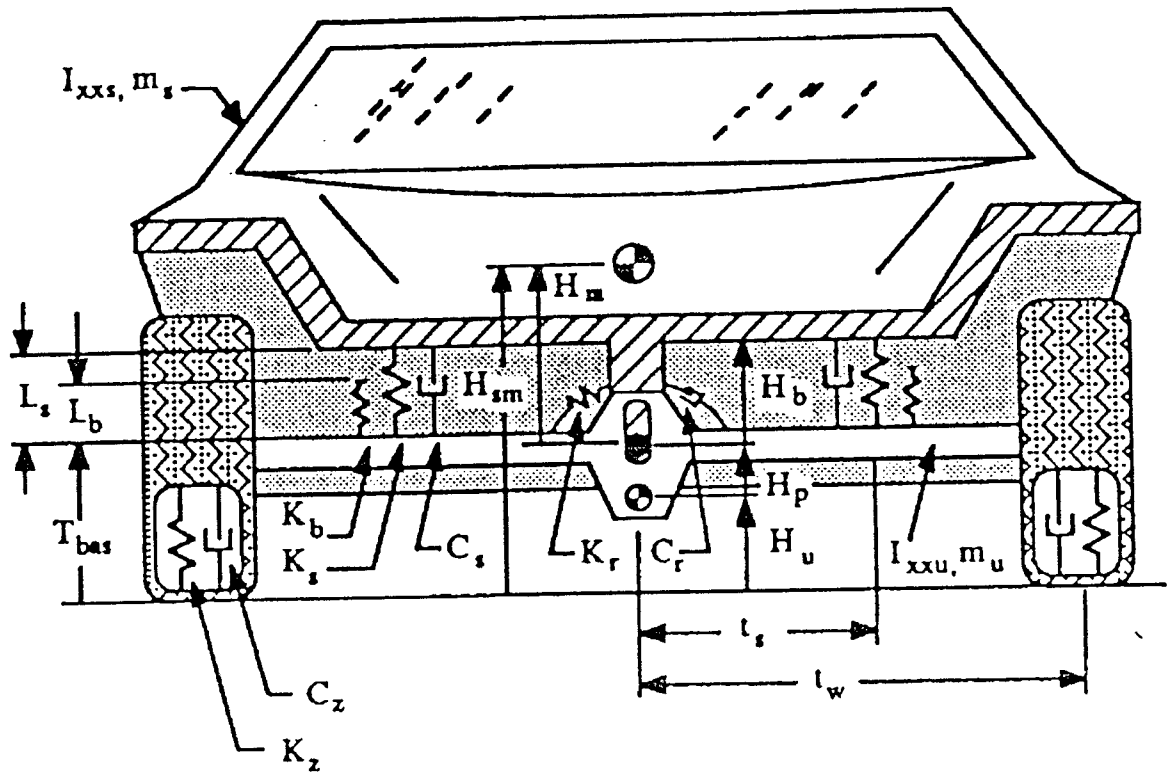

Figure 9 - IMIRS Rollover Model Showing Suspension Components and Dimensions

generated at the tire contact patch.

3.1.3 Steering System Model

The IMIRS does not model the vehicle steering system. Instead, steer angles are applied directly to the front wheels. The model thus ignores the effects of the steering system on vehicle response. The model also assumes that both front wheels steer equal amounts, therefore, ignoring any Ackerman steering affects.

Past research [1, 14] has shown steering system steer compliance due to tire aligning moments to have first order affects on vehicle steady state and transient response. Neglecting the steering system characteristics, and applying a steer angle to the front road wheels is not incorrect, and can be used to isolate the vehicle response from the influences of the steering system. However, the documentation makes no mention of this. Users of the simulation need to be aware of this limitation and not misinterpret the simulation predictions.

3.1.4 Braking Model

IMIRS uses a simple, fixed proportioning, fixed break point braking model. The front to rear brake force distribution,Q, is computed from:

$$Q = Q_0 + Q_1 \cdot (A_x - 0.3) \tag{3}$$

where Q_0 is the front to rear brake force distribution below 0.3 g's, and Q_1 is the rate of increase of front to rear brake force distribution above 0.3 g's.

This model assumes that the break point of the proportioning valve occurs at 0.3 g's, which may not be a valid assumption for many vehicles. The advantage of this brake model is it requires only 2 parameters. However, adding a variable break point would make the model better able to characterize the brake systems of the vehicle fleet with little added complexity.

The control input for the brake model is desired longitudinal acceleration. Therefore, IMIRS cannot be used to predict longitudinal acceleration from brake pedal force or brake line pressure inputs. This makes IMIRS unsuitable for studies using driver or driver model control force inputs.

This brake system model has no antilock brake option. Since the number of vehicles equipped with antilock brakes is increasing rapidly, it would be useful if this option was included for use in studying limit vehicle performance. In addition, load sensing brake proportioning valves are common and could be modeled.

3.1.5 Drivetrain Model

The IMIRS simulation does not contain a drivetrain model. Longitudinal acceleration (positive or negative) can be requested by the user using the brake input menu. The model allows a fixed percentage of the drive torque to be directed to the front axle, therefore allowing front, rear, or four wheel drive. No constant speed governor is provided.

When running pure cornering maneuvers, vehicle speed decreases due to tire friction. It is often desirable to simulate constant speed maneuvers such as a constant speed J-turn. Only through a trial and error approach could a longitudinal acceleration input to cancel the effects of the tire friction be

determined. To complicate matters, the longitudinal acceleration required for constant speed operation will be maneuver dependent.

Future NHTSA simulations will require complete drivetrain models. This will include front, rear, and four wheel drive options. For the NADS, this is an area where extensive modeling work will be required. Future IVHS research may also require simulations with extensive drivetrain models.

3.1.6 Tire Model

Quasi-Static:

The IMIRS simulation uses the Calspan (McHenry) tire model to represent the quasi-static characteristics of the tires. Variations of this tire model, which assume that forces and moments act at a point contact within the tire/road contact area, are widely used in vehicle dynamic simulation tire models. The coordinate system used in the IMIRS tire model is the standard SAE recommended coordinate system. This tire model represents the nonlinear characteristics for all of the most important tire relationships; for example, side force versus slip angle, longitudinal force versus slip, etc. Inputs to the tire model include normal load, slip angle, camber angle, and longitudinal slip (computed from desired braking or thrust acceleration). Tire model outputs include lateral and longitudinal force and aligning moment. Overturning moment is not included in the tire model.

The IMIRS simulation has no wheel spin dynamic equations to compute slip ratios. Instead, slip ratios are determined from the braking or driving forces, which are determined from the specified braking or driving accelerations. If the requested braking force is greater than the maximum braking force which the tire can generate, then the slip ratio is set to 1 (wheel locked). Similarly, if the requested driving force is greater than the maximum driving force which the tire can generate, then the slip ratio is set to -1 (wheel spin). For conditions between wheel spin and wheel lock, the slip ratio is determined using a golden section search (an iterative technique to numerically determine the independent variable (slip ratio) when the dependent variable (F_y, F_z, etc.) are known) to find the slip ratio which corresponds to the braking friction coefficient. This method appears to work well, and eliminates the need for dealing with the highly nonlinear wheel spin equations.

For steering only runs, the IMIRS slip ratio is set to zero. For braking or driving runs, the IMIRS simulation runs slower than the steering only runs since more computations are required to determine the slip ratios. More will be said about run times in a later section.

The model includes combined braking/driving (slip ratio) effects with simultaneous slip angle effects using a friction ellipse. This requires that the vector sum of the lateral tire force and longitudinal tire force remains on or within an ellipse whose axes are defined by maximum side force and maximum circumferential force values. The use of friction ellipse concept is fairly widespread among simulation tire models.

Longitudinal force, as a function of longitudinal slip, is determined from empirical equations based on curve fits of Calspan data. This force is limited by the surface coefficient of friction and the friction ellipse. In the IMIRS tire model, tire side force is composed of forces arising from the slip angle and from the camber angle. Both slip angle and camber angle effects are determined from empirical equations based on Calspan data. Side force is also limited by the surface coefficient of friction and the friction ellipse. Empirical relationships relating the tire aligning moment to normal force, side force, and camber angle are used in the tire model.

As is common for empirical tire models of this type, some of the coefficients used in the empirical equations for longitudinal and side force are functions of tire normal force. This is accounted for in the tire model, as the tire normal load changes which occur during the maneuver are included in the tire model computations.

In all, the tire model requires 23 parameters based on Calspan measurements. The IMIRS tire model is quite similar to tire models used previously at the VRTC. Based on the authors experience, this tire model formulation appears to be adequate for modeling the tire quasi-static forces and moments. A detailed evaluation of the tire model would require comparison with experimental results. This is beyond the scope of this study. However, a more detailed evaluation of existing tire models is forthcoming at the VRTC. Current plans are to include this (Calspan/McHenry) tire model in the proposed study. One attribute of the IMIRS tire model which is unique is the method used to determine slip ratio. This element of the IMIRS tire model warrants additional study as part of the future research project.

Dynamic:

IMIRS contains no tire dynamics. All tire forces are generated instantaneously based on the empirical quasi-static tire model. As has been shown by previous research [1, 7], this will limit IMIRS's ability to predict transient vehicle responses. Research has demonstrated that the side force lag present in tires reduces the effective vehicle yaw rate damping.

3.1.7 Driver Model

IMIRS contains no driver model. Control inputs to the vehicle are provided by handwheel angle and longitudinal acceleration script files or generated internally for step, ramp, or fixed frequency sinusoidal inputs. The script files are limited to a 22 point time versus angle or force description of the control input.

In the course of past simulation evaluation and metric computation programs, the authors have found it to be important to provide the simulation with realistic driver generated control inputs [1, 7] . When comparing simulation predictions to field test data, simulations are "driven" with measured handwheel and brake pressure data from the field tests. A 22 point input file is only sufficient to accurately characterize the control inputs for simple maneuvers such as pseudo-step inputs and trapezoidal lane change maneuvers. Modifying IMIRS to allow more points to describe steering inputs would be an easy task.

IMIRS, with no driver model, cannot simulate any closed-loop maneuvers. This does not present a problem at present. However, future research for NADS and IVHS may need a driver model.

3.1.8 Aerodynamic Model

IMIRS uses a simple aerodynamic model to estimate the influence of aerodynamic forces on the vehicle side force and yaw moment. No wind velocity or direction is modeled and the aerodynamic forces are assumed to act on the vehicle in the direction of its sideslip angle. The magnitude of the forces are dependent on the square of the total vehicle velocity, the sideslip angle, and the yaw rate. The equations used to compute the aerodynamic forces are:

$$\alpha = \tan^{-1} \frac{V}{U} \tag{4}$$

$$M_{Z_a} = \frac{1}{2} (V^2 + U^2) \rho_{air} S_a H_a C_n \alpha - C_{nd} r \quad (5)$$

$$F_{Y_a} = -\frac{1}{2} (V^2 + U^2) \rho_{air} S_a C_y \alpha \quad (6)$$

where: U and V, are the vehicle longitudinal and lateral velocities, ρ_{air}, is the density of air, S_a, is the projected frontal area of the vehicle, H_a, is the characteristic height of the vehicle, C_n, is the aerodynamic yaw moment coefficient, α, is the vehicle sideslip angle, C_{nd}, is the aerodynamic yaw damping coefficient, r, is the vehicle yaw rate, and C_y, is the aerodynamic side force coefficient.

The aerodynamic side force Equation (6) and the first term in the aerodynamic yawing moment Equation (5) model the effects of sideslip angle and are of the standard form used in automotive studies [15]. The second term of Equation (5), however, is not a "standard type" of aerodynamic parameter. It attempts to model the effect of vehicle yaw rate on the vehicle yawing moment. C_{nd}, the aerodynamic yaw damping coefficient, is multiplied by the vehicle's yaw rate. Typically, aerodynamic parameters are functions of the square of velocity, not linear functions of velocity. No references or derivations of this term are given in the report.

3.1.9 Solution Method

For the IMIRS simulation, the numerical integration algorithm used is a fourth order Runge-Kutta integrator. This is a common integrator for use in this type of simulation. This integrator is also used successfully for IMIRS braking simulation runs, since no wheel spin equations are present in the simulation.

For the handling model, the acceleration terms are solved explicitly. As mentioned above, the acceleration terms for the roll model are determined via the matrix inversion and multiplication. All velocity and displacement terms are then computed using the fourth order Runge-Kutta algorithm.

The IMIRS documentation suggests using an integration step size of 0.01 seconds. This step size provides reasonable results and the run times are acceptable. Using a 25 Mhz IBM Model 80 386 personal computer with a math co-processor, and a step size of 0.01 seconds, a 5 second, steering input only, simulation run requires about 2 minutes and 5 seconds of computer run time. A 5 second braking

run requires about 2 minutes and 45 seconds of computer run time. The increased run time for the braking run is because more computations are required to determine tire slip ratio. Using smaller integrator step sizes increases the simulation run time, while larger step sizes reduce integrator accuracy and may result in numerical stability problems.

3.1.10 Miscellaneous

The IMIRS simulation assumes zero initial conditions for all velocities and displacements which are required to start the initial numerical integrations. This is a fairly typical practice, and no problems were encountered concerning simulation start up.

The IMIRS incorporates a dynamic rollover predictor function called Rollover prevention Energy Reserve (RPER). The RPER criteria, based on energy principles, is computed to estimate rollover potential for a vehicle.

3.2 Parameter Measurement

The vehicle and tire parameters required to run IMIRS are listed in the Nalecz report. However, little description of the parameters is given and there are no references to the required measurement equipment or techniques. This section will describe the parameters, review the test methods needed to obtain them, and assess the effort required for the VRTC to measure/obtain them.

3.2.1 Required Parameters

The vehicle and tire parameters required by IMIRS, shown in Table VII, are taken from the Nalecz report. They will be discussed in five categories: geometric, inertial, suspension/steering, aerodynamic, and tire.

Geometric:

The geometric parameters required by IMIRS are: wheelbase, front/rear track width, and spring track width. These parameters are used to characterize the physical dimensions of the vehicle.

Table VII - Parameters required by IMIRS

VEHICLE MASS	1014.0000 [kg]
VEHICLE SPRUNG MASS	778.1000 [kg]
DISTANCE FROM SPRUNG MASS C.G. TO FRONT AXLE	1.3000 [m]
DISTANCE FROM SPRUNG MASS C.G. TO ROLL AXIS	0.6034 [m]
HEIGHT OF SPRUNG MASS C.G.	0.6930 [m]
YAW MOMENT OF INERTIA	1175.5000 [kg*m^2]
ROLL MOMENT OF INERTIA OF SPRUNG MASS	240.2600 [kg*m^2]
ROLL MOMENT OF INERTIA OF UNSPRUNG MASS	71.8300 [kg*m^2]
AUXILIARY ROLL DAMPING OF FRONT AND REAR SUSPENSIONS	0.0000 [Nm-s/rad]
WHEELBASE	2.0320 [m]
FRONT TRACK WIDTH	1.3081 [m]
REAR TRACK WIDTH	1.3081 [m]
UNSPRUNG MASS OF FRONT SUSPENSION	117.4800 [kg]
UNSPRUNG MASS OF REAR SUSPENSION	117.4800 [kg]
UNSPRUNG MASS C.G. HEIGHT OF FRONT SUSPENSION	0.3302 [m]
UNSPRUNG MASS C.G. HEIGHT OF REAR SUSPENSION	0.3302 [m]
FRONT SUSPENSION AUXILIARY ROLL STIFFNESS	3443.7300 [Nm/rad]
REAR SUSPENSION AUXILIARY ROLL STIFFNESS	5277.3301 [Nm/rad]
FRONT PROPORTION OF TOTAL VEHICLE ROLL STIFFNESS	0.5600 [-]
VERTICAL STIFFNESS OF TIRES	113140.0000 [N/m]
VERTICAL DAMPING COEFFICIENT OF TIRE	980.0000 [N-s/m]
RATE OF CHANGE OF FRONT TIRE INCLINATION	-0.0400
RATE OF CHANGE OF REAR AXLE STEER	0.0000
FRACTION OF BRAKING TORQUE APPLIED TO FRONT WHEELS	0.8000
HEAVY BRAKING PROPORTIONALITY FACTOR FOR FRONT WHEELS	0.0500
1 - FWD 2 - RWD 3 - 4WD	3
FRACTION OF DRIVING TORQUE APPLIED TO FRONT (4WD)	0.6000

**********TIRE DATA**********

TIRE SKID NUMBER 70.00		
A0 = -668.4600	A1 = 26.5400	A2 = 2146.6101
A3 = 1.2740000	A4 = 2225.0701	
B1 = -6.7450E-04	B3 = 1.3070	B4 = 2.9530E-07
P0 = 1.2073	P1 = -5.8430E-04	P2 = 3.9770E-07
S0 = 1.17379999	S1 = -8.4580E-04	S2 = 3.9450E-07
R0 = -0.23771000	R1 = 8.5360E-05	
K1 = -2.0610E-04	K2 = -1.7680E-04	K3 = 0.0740
CTN = 6.000000	CA1 = 30.000000	CR1 = 0.300000

**********SUSPENSION PARAMETERS**********

SUSPENSION SPRING TRACK WIDTH	0.9320 [m]
STATIC SUSPENSION SPRING LENGTH	0.1016 [m]
UNDEFORMED BUMP STOP LENGTH	0.0709 [m]
HEIGHT OF LOWER SUSPENSION SPRING MOUNT ABOVE GROUND	0.2032 [m]
COMBINED FRONT AND REAR SUSPENSION SPRING STIFFNESSES	84850.00 [N/m]
COMBINED FRONT AND REAR BUMP STOP STIFFNESSES	464030.0 [N/m]
COMBINED FRONT AND REAR SUSPENSION DAMPING COEFF.	3000.0000 [N-s/m]

**********AERODYNAMIC PARAMETERS**********

VEHICLE FRONTAL AREA	2.0000 [m^2]
CHARACTERISTIC HEIGHT OF VEHICLE	1.5000 [m]
AERODYNAMIC SIDEFORCE COEFFICIENT	0.3000 [-]
AERODYNAMIC ALIGNING MOMENT COEFFICIENT	0.2000 [-]
AERODYNAMIC YAW DAMPING COEFFICIENT	100.0000 [N-m-s]

Inertial:

The inertial parameters required by IMIRS describe the sprung and unsprung mass inertial properties (center of gravity positions and mass moment of inertias).

The roll mass moment of inertia is required for the sprung and unsprung masses separately, while the yaw inertia is for the total vehicle. Both the longitudinal and vertical positions of the sprung and unsprung mass center of gravities are required.

Suspension:

The required suspension parameters can be separated into 2 categories: geometric and stiffness/damping. The geometric parameters are used by the simulation pre-processor solely to compute roll center height and will be described first.

Table VIII is a list of the 27 different suspension types allowed by IMIRS. For each suspension type, the coordinates and all suspension pivot points, in the YZ plane, are required. Figure 10 shows the input screen and parameters required for a Hotchkiss type solid axle, while Figure 11 shows the same information for a Wishbone type independent suspension. Two additional geometric parameters are used to specify the wheel camber change and rear axle steer angle due to body roll.

The stiffness parameters are used to define the suspension roll stiffness for both the handling and rollover models. These include the front and rear suspension roll stiffnesses, front axle percent of total roll stiffness, the total vehicle spring stiffness, bump stop stiffness, and suspension damping in bounce and roll.

Braking:

The brake system is defined using one parameter for the fraction of the braking force applied to the front axle below 0.3 g's and one parameter for the percent reduction in front axle brake force per g above 0.3 g's.

Table VIII - Suspension Types Available in IMIRS

ILLUSTRATIONS OF SUSPENSION SYSTEMS

Front

Upper and lower control arms (Converging towards car center)
Upper and lower control arms (Converging away from car center)
Parallel upper and lower control arms
Macpherson strut
Trailing Link
Twin I-beam
Sliding pillar
Live Hotchkiss drive

Rear Independent

Swing axle
Low pivot swing axle
Single transverse a-arms for FWD
Single trailing arm
Semi-trailing arm
Chapman strut
Semi-independent for FWD
Weissach axle
Upper and lower control arms (Converging towards car center)
Upper and lower control arms (Converging away from car center)

Rear Dependent

Hotchkiss drive
Torque tube with panhard rod
Three link with panhard rod
Four link with parallel lower links
Four link with non-parallel lower links
Beam twist axle with panhard rod FWD
Rear wheel drive with sideways location on the center of axle
De Dion Axle
Beam Axle with leaf springs and lateral locating device

Aerodynamic:

The aerodynamic forces acting on the vehicle are described by five parameters in the IMIRS model. They are the vehicle frontal area and characteristic height of the vehicle along with the aerodynamic sideforce, aligning moment, and yaw damping coefficients. These parameters are used to compute the aerodynamic influences on vehicle lateral force and yaw moment.

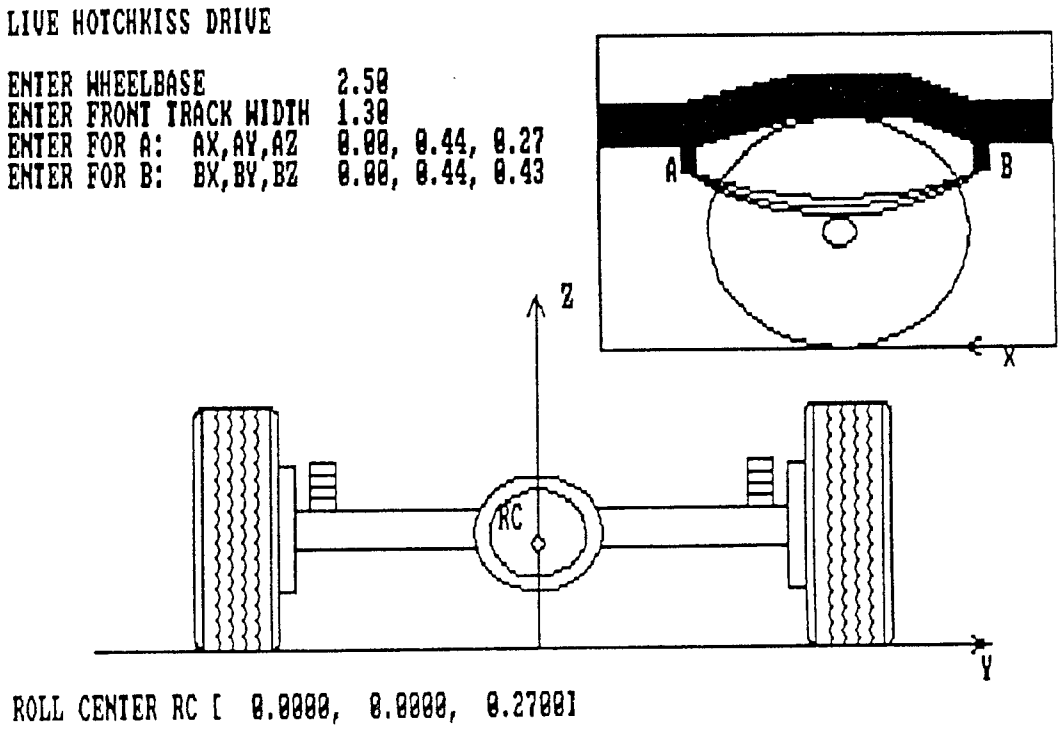

Figure 10 - Solid Axle Definition Screen

Tire:

The tire model is based on the standard Calspan model. Twenty two "Calspan" parameters, skid number, and tire vertical stiffness and damping are used to compute the tire forces and moments.

3.2.2 Test Methods

As stated previously, the Nalecz report gives no information regarding the measurement or definition of the parameters required for IMIRS. This increases the difficulty of using IMIRS. The parameters required for any simulation of this type and complexity have certain subtleties that are difficult to recognize without experience with the model. The authors of any model are in the best position to understand these subtleties from the start. During this evaluation, the exact "meaning" of some of the parameters could only be determined by close examination of the simulation source code. Many users, however, will not have this luxury.

3.2.3 Compatibility with Existing Measurement Equipment

Equipment currently available at the VRTC can measure most of the parameters needed for the IMIRS simulation. The following are the parameters that can not be measured at the VRTC.

Tire vertical damping ratio: A fixture similar to that described by DRI [2] would need to be constructed. This would not be a large task, and would provide useful data for any simulation used.

Shock absorber damping coefficients: A shock dyno is not available at the VRTC. However, shocks can be sent out to be measured. This is a time consuming and expensive process. If measuring shock absorber characteristics becomes necessary at the VRTC, then better methods of obtaining shock data will need to be investigated.

Tire force and moment data: The VRTC does not have a tire test machine. All tire testing needs to be done by outside labs. There are no plans at the present time to develop this capability at the VRTC.

Aerodynamic data: Frontal area and characteristic height could be estimated by measuring vehicle dimensions or using photographic techniques. However, the sideforce, aligning moment and yaw damping coefficients cannot be measured at the VRTC. No current research project requires simulating the aerodynamic influences on vehicle directional control. If the need arises, measurement techniques will need to be investigated.

3.3 Road Profile

IMIRS assumes an infinite, flat road surface with a constant coefficient of friction. No interaction with roadside obstacles can be simulated. The tire skid number may be changed to simulate low or high friction surfaces. Users should be cautioned that tire parameters will only be "accurate" for surface friction levels near that of the test surface. This limits the ability of any simulation that uses tire data from a single friction surface to simulate vehicle response over a large range of surface frictions (without additional tire data).

3.4 Comparison with Experimental Data

The IMIRS report contains a J-turn and a lane change maneuver for comparison of the simulation predictions to experimental data. The data decks used for the comparisons are not given. The report also states that the J-turn comparisons were done using a preliminary version of the IMIRS model.

In order to check the performance of the IMIRS model, a data deck for a Suzuki Samurai was generated using parameters measured by the VRTC (Table IX). The model was run and comparisons made to experimental data measured at the VRTC as part of an earlier simulation evaluation program. The comparisons were made in both the time and frequency domains.

Because IMIRS does not have a steering system (Section 3.1.3), direct comparisons with experimental data using a driver supplied control input (hand wheel angle) can not be made. At a given forward speed, if a road wheel steer angle is input to the simulation to match the lateral acceleration level of an experimental run, at steady state, the yaw rate, by definition will be correct because it is a function of forward speed and lateral acceleration ($r = A_Y / U$).

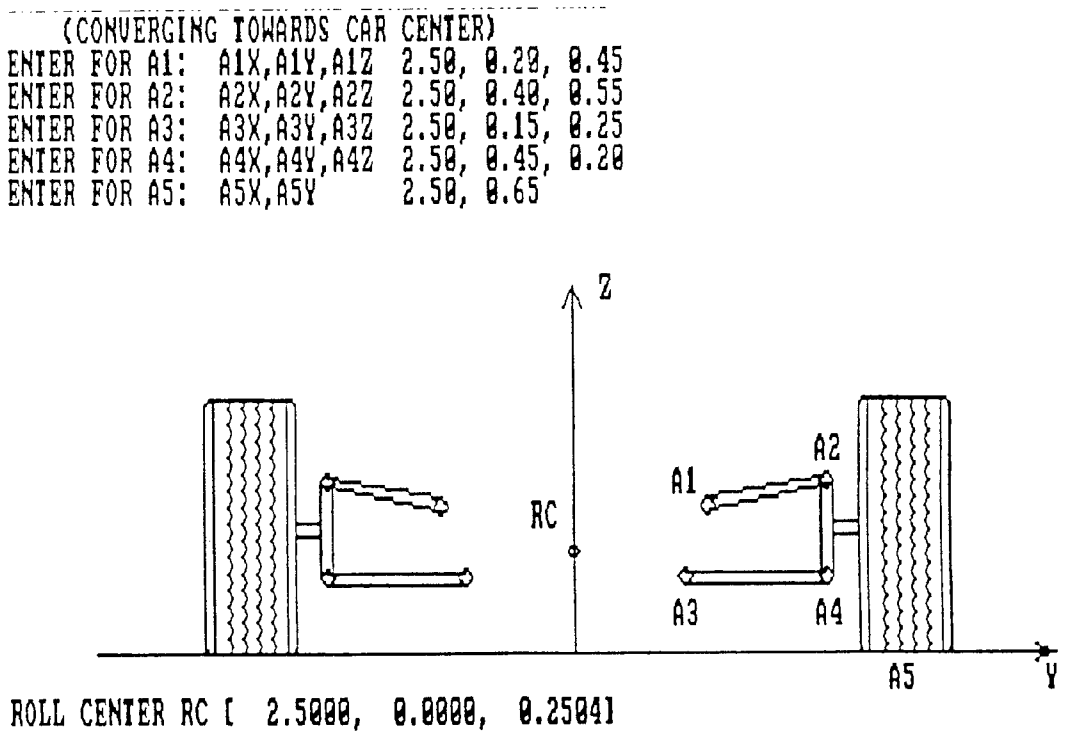

Figure 11 - Independent Suspension Definition Screen

Table IX - Suzuki Samurai Data Deck Generated by VRTC

```
VEHICLE WEIGHT ------------------------------------------  2484.0000 [lbf]
VEHICLE SPRUNG WEIGHT -----------------------------------  1967.0000 [lbf]
DISTANCE FROM SPRUNG WEIGHT C.G. TO FRONT AXLE ----------    42.3000 [in]
DISTANCE FROM SPRUNG WEIGHT C.G. TO ROLL AXIS -----------    16.5942 [in]
HEIGHT OF SPRUNG WEIGHT C.G. ----------------------------    27.1000 [in]
YAW MOMENT OF INERTIA -----------------------------------   898.0000 [lbf-s^2-ft]
ROLL MOMENT OF INERTIA OF SPRUNG MASS -------------------   167.4000 [lbf-s^2-ft]
ROLL MOMENT OF INERTIA OF UNSPRUNG MASS -----------------    53.0000 [lbf-s^2-ft]
AUXILIARY ROLL DAMPING OF FRONT AND REAR SUSPENSIONS ---     0.0000 [lbf-s-ft]
WHEELBASE -----------------------------------------------    80.0000 [in]
FRONT TRACK WIDTH ---------------------------------------    51.5000 [in]
REAR TRACK WIDTH ----------------------------------------    51.5000 [in]
UNSPRUNG WEIGHT OF FRONT SUSPENSION ---------------------   258.5000 [lbf]
UNSPRUNG WEIGHT OF REAR SUSPENSION ----------------------   258.5000 [lbf]
UNSPRUNG WEIGHT CG HEIGHT OF FRONT SUSPENSION -----------    12.7000 [in]
UNSPRUNG WEIGHT CG HEIGHT OF REAR SUSPENSION ------------    12.7000 [in]
FRONT SUSPENSION AUXILIARY ROLL STIFFNESS ---------------  6124.0000 [ft-lbf/rad]
REAR SUSPENSION AUXILIARY ROLL STIFFNESS ----------------  5011.0000 [ft-lbf/rad]
FRONT PROPORTION OF TOTAL VEHICLE ROLL STIFFNESS --------     0.550 [-]
VERTICAL STIFFNESS OF SINGLE TIRE -----------------------  1030.000 [lbf/in]
VERTICAL DAMPING COEFFICIENT OF SINGLE TIRE -------------    20.000 [lbf-s/in]
RATE OF CHANGE OF FRONT TIRE INCLINATION ----------------     0.0400
RATE OF CHANGE OF REAR AXLE STEER -----------------------     0.0000
FRACTION OF BRAKING TORQUE APPLIED TO FRONT WHEELS ------     0.6200
HEAVY BRAKING PROPORTIONALITY FACTOR FOR FRONT WHEELS --      0.2000
1 - FWD   2 - RWD   3 - 4WD -----------------------------     3
FRACTION OF DRIVING TORQUE APPLIED TO FRONT (4WD) -------     0.0000

**************************TIRE DATA*************************

TIRE SKID NUMBER     100.00
A0 =   -261.9100   A1 =     23.1100   A2 =   2675.9900
A3 =   1.1680000   A4 =   2295.6899
B1 = -9.4750E-04   B3 =      1.4690   B4 =  4.3160E-07
P0 =       1.2071  P1 = -4.1940E-04   P2 =  2.6720E-07
S0 =  1.21290004   S1 = -9.3470E-04   S2 =  4.4600E-07
R0 = -0.19200000   R1 =  4.0600E-05
K1 = -1.7280E-04   K2 =  1.5510E-04   K3 =       0.0690
CTN =   6.000000   CA1 =  30.000000   CR1 =   0.300000

************************SUSPENSION PARAMETERS************************

SUSPENSION SPRING TRACK WIDTH ---------------------------    32.7500 [in]
STATIC SUSPENSION SPRING LENGTH -------------------------     4.4000 [in]
UNDEFORMED BUMP STOP LENGTH -----------------------------     2.0000 [in]
HEIGHT OF LOWER SUSPENSION SPRING MOUNT ABOVE GROUND ---     12.0000 [in]
COMBINED FRONT AND REAR SUSPENSION SPRING STIFFNESSES --      453.00 [lbf/in]
COMBINED FRONT AND REAR BUMP STOP STIFFNESSES ----------      4000.0 [lbf/in]
COMBINED FRONT AND REAR SUSPENSION DAMPING COEFF. ------     16.7000 [lbf-s/in]

************************AERODYNAMIC PARAMETERS************************

VEHICLE FRONTAL AREA ------------------------------------    25.0000 [ft^2]
CHARACTERISTIC HEIGHT OF VEHICLE ------------------------     2.5000 [ft]
AERODYNAMIC SIDEFORCE COEFFICIENT ----------------------  0.0000000 [-]
AERODYNAMIC ALIGNING MOMENT COEFFICIENT -----------------  0.0000000 [-]
AERODYNAMIC YAW DAMPING COEFFICIENT ---------------------  0.0000000 [Lb-ft-s]
```

3.4.1 Steady State

A ramp steer maneuver was run to compare the time domain simulation predictions with the experimental data. The run was made at 50 mph with a nominal lateral acceleration levels of 0.4 g's. In order to match the simulated yaw rate with the experimentally measured yaw rate, a slowly increasing

steer maneuver (road wheel steer angle increased at 0.25 degrees per second with constant forward speed) and the road wheel angle required to give the experimentally measured yaw rate was determined.

Figure 12 shows the IMIRS predictions and the experimental yaw rate time domain response for the 50 mph, 0.4 g J-turn. As can be seen, the simulation transient response predictions are significantly more damped than the actual vehicle. For the J-turn maneuver used for comparison, the experimental data showed approximately 60 percent yaw rate peak overshoot. The IMIRS prediction, however, only showed 2.3 percent overshoot. This result is in contrast to the J-turn comparisons given in the IMIRS report. In that maneuver, the yaw rate predictions showed a very lightly damped response. Since both runs were simulating a Suzuki Samurai in a J-turn, it is assumed that changes have been made in the simulation since the time that the comparisons in the report were made.

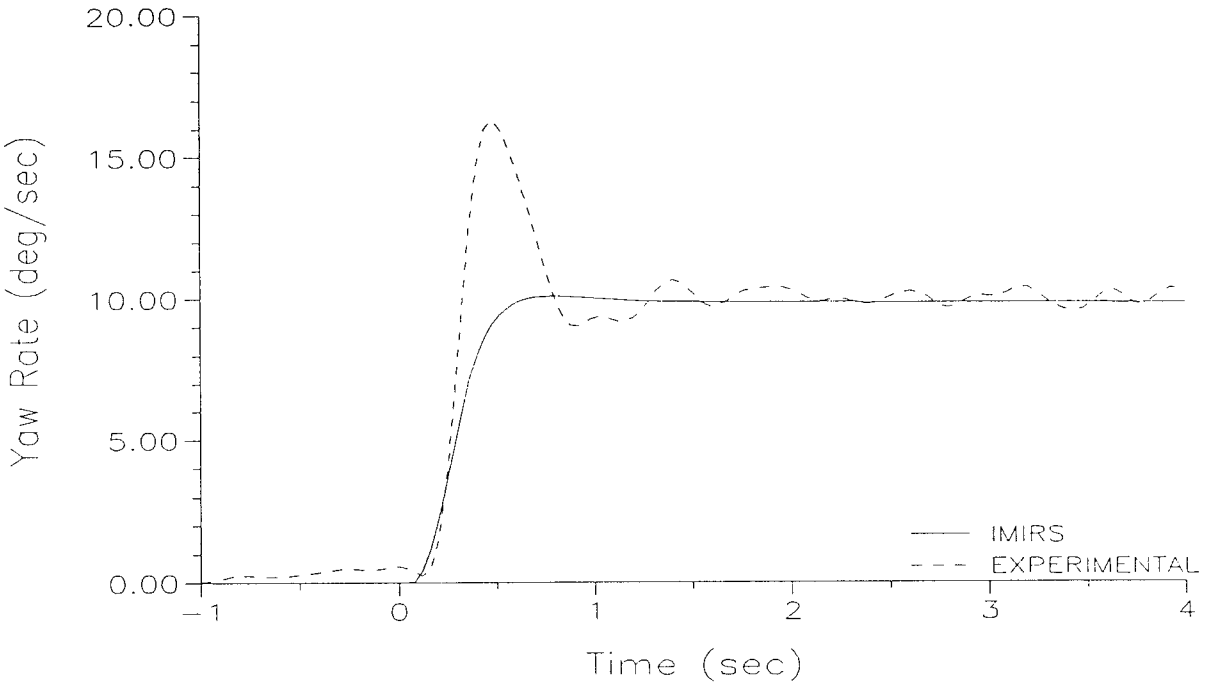

Figure 12 - Samurai Steady State Comparisons

3.4.2 Transient

Past research at VRTC has demonstrated that frequency response techniques are quite useful for evaluating dynamic/transient simulation predictions [9, 10]. By generating vehicle output (eg. yaw rate) frequency response to handwheel angle inputs, much can be learned about the characteristics and validity of a simulation model.

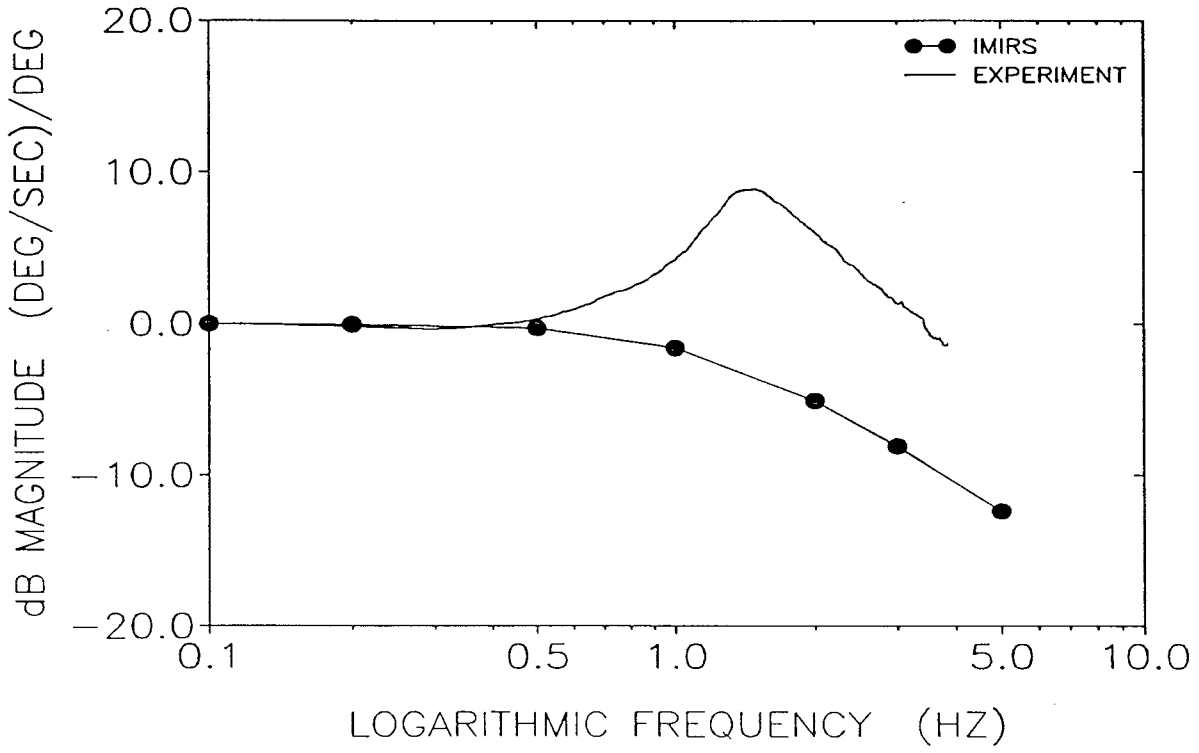

Figure 13 - Yaw Rate to Handwheel Angle Frequency Response Magnitude 50 mph Suzuki Samurai

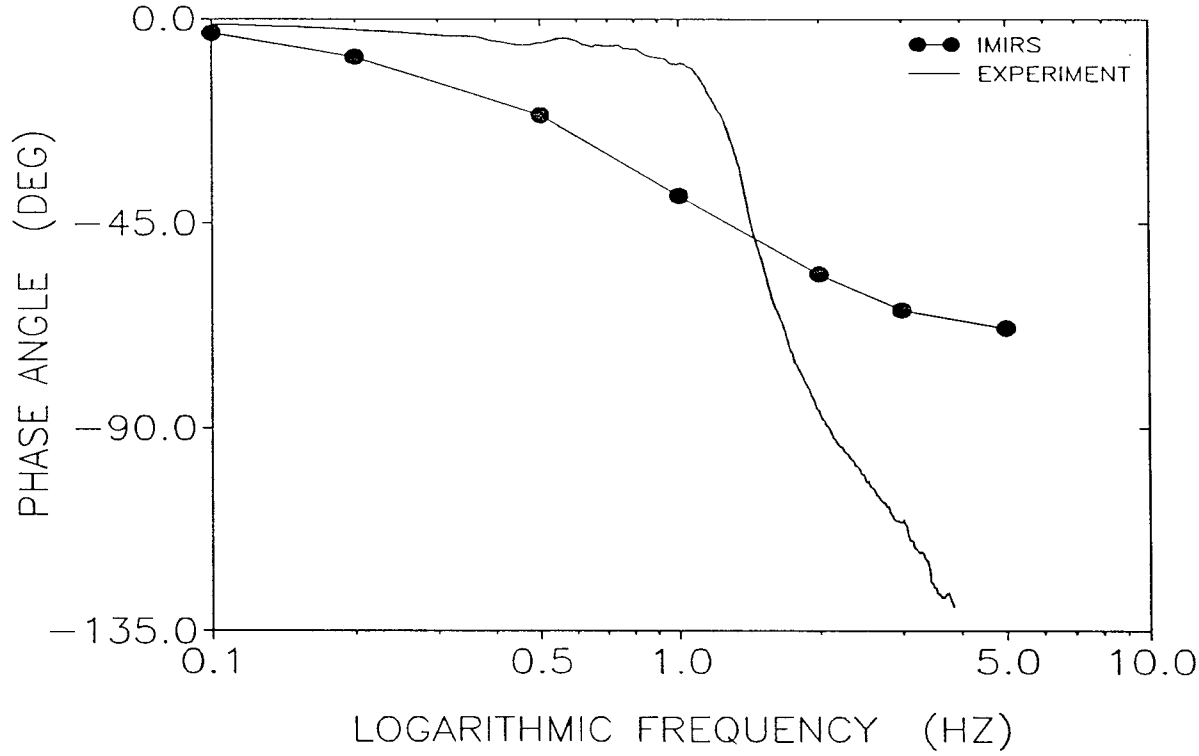

Figure 14 - Yaw Rate to Handwheel Angle Frequency Response Phase Angle 50 mph Suzuki Samurai

Yaw rate frequency responses to road wheel angle inputs have been generated from IMIRS simulation runs and to handwheel angle inputs from the experimental data from the VRTC for a Suzuki Samurai. Figure 13 shows the normalized simulated and experimental yaw rate frequency response magnitude curves for the Samurai at 50 mph, and Figure 14 shows the corresponding phase angle curves. These frequency response curves have been generated by measuring the amplitude ratio and phase shift of the yaw rate response relative to the handwheel angle input at discrete sinusoidal frequencies.

Research at VRTC has shown that, for the purposes of evaluating a simulation, frequency response comparisons with experimental results can be performed in the vehicle's linear operating range. The experimental and simulated sinusoidal steering inputs used to generate the frequency response curves resulted in lateral acceleration levels which are believed to be in the linear regime for the vehicle. For the simulation runs used to generate the frequency response curves, frequencies of 0.1, 0.2, 0.5, 1.0, 2.0, and 5.0 hertz, and road wheel angle amplitudes of ± 0.85 degrees were used. Experimental data was generated from a sinusoidal sweep steering maneuver with a handwheel angle amplitude of approximately ± 45 degrees.

The experimental yaw rate magnitude increases at the higher frequency range shown on Figure 13. Based on work done at VRTC and elsewhere, many vehicles exhibit this underdamped behavior, and have yaw rate resonance frequencies at approximately 1.0 hertz. The simulated frequency response magnitude does not exhibit this underdamped response. Research performed at VRTC has shown that front axle roll steer, which is not modeled by IMIRS, has a significant effect on the Samurai yaw rate damping [16]. In addition, research at the VRTC has shown that modeling tire dynamics in a simulation has a considerable influence on simulated yaw rate transient response. Tire side force lag dynamics have been shown to reduce simulated yaw rate damping [7]. The fact that the IMIRS simulation does not include tire dynamics accounts for some of the discrepancy seen between the shapes of simulated and experimental magnitude curves.

Typically, experimental yaw rate phase angle high frequency asymptotes are near or below -180 degrees. However, the simulated phase angle curve appears to be asymptotic to about -90 degrees. This apparent discrepancy also indicates model deficiencies, the main one most likely being lack of tire dynamics.

4.0 Introduction: ADVS

During the period of 1988 to 1991, The Department of Mechanical and Aerospace Engineering at the University of Missouri-Columbia, under the direction of Dr. Andrzej G. Nalecz, developed the Advanced Dynamic Vehicle Simulation (ADVS) for the National Highway Traffic Safety Administration (Contract No. DTNH22-87-D-27174). The final report (in draft form as of May 1991) contains 3 Volumes: Part I - User's Manual, Part II - Technical Report, and Part III - Applications [4, 17, 18].

The ADVS simulation was delivered with source code, object files, executable code, example data sets. The program is written in Fortran and runs on a VAX minicomputer. The following is a short description of the ADVS simulation taken from the User's Manual.

> *"The ADVANCED DYNAMIC VEHICLE SIMULATION (ADVS) is one the most sophisticated computer simulations developed for the VAX minicomputer to investigate the complex dynamic behavior of vehicles in a variety of maneuvers and under diverse environmental conditions. The ADVS was primarily developed for simulating the following typical vehicle rollover situations:*
>
> 1. *On-road, untripped vehicle rollover resulting from combined steering and braking, e.g. attempt by driver to avoid a collision due to sudden intrusion of another vehicle.*
>
> 2. *Off-road, vehicle rollover resulting from failure of vehicle to track roadway, e.g. failure of vehicle to negotiate a curve.*
>
> 3. *Off road, vehicle rollover resulting from loss of control during combined braking and steering maneuvers, e.g. locking or saturation of front and/or rear wheels causing vehicle to skid or spin out of control.*
>
> *In all cases, the ADVS vehicle model has the capability of simulating all phases of vehicle motion including vehicle motion preceding the initiation of rollover, actual rollover motion, subsequent inflight or airborne motion, vehicle-ground impact and post-impact motion. In cases involving off road rollover, the rollover tripping mechanism may include a rigid barrier (curb), sinkage of the wheels into soil or sod, and sloping embankments.*

Since the ADVS is capable of simulating vehicle motion preceding rollover, it can also be used to investigate the complex vehicle handling maneuvers which do not result in vehicle rollover. Thus a variety of vehicle sub-limit and limit maneuvers such as combined steering and braking, locking and/or saturating the wheels, vehicle skidding or spin out, etc., on a variety of terrain types and conditions can also be simulated.

The detailed description of the ADVS simulation model is presented in the ADVS Technical Report. However, shown below are some of the ADVS simulation features.

The ADVS features:

1. *A 14 degree-of-freedom nonlinear dynamic vehicle model which accounts for the spatial motion of the vehicle's sprung mass (6 degrees), the relative motions of the front and rear unsprung masses with respect to the sprung mass (4 degrees), and the rotations of all four wheels (4 degrees).*

2. *The support of any combination of suspension types. Front and rear suspension systems may either be dependent or independent.*

3. *The nonlinear kinematic and dynamic characteristics, and effects of the suspension systems (stiffness, damping, roll steer, roll camber, bump stops, anti-roll bars, etc.).*

4. *The suspension/wheel crash impact model which accounts for both elastic and plastic deformations.*

5. *The ability to add passengers and loads to the sprung mass.*

6. *The capability of simulating any rigid or deformable prismatic terrain surface of up to 19 different planes.*

7. *The vehicle-terrain impact model which accounts for all elastic and plastic deformations resulting from post-rollover vehicle contact with the terrain.*

8. *The motion of the deformed/undeformed vehicle after the contact with the terrain has occurred.*

9. *Some of the most complicated tire frictional, impact and soil models available. These models can deal with high camber, high slip angles, a full range of slip ratios, unlimited friction regime, overload conditions, impacts with curbs, interactions with soil surfaces, deformations in three dimensions, and the calculations of all the side forces, longitudinal forces, and aligning moments.*

10. *Flexible steering, braking or accelerating, and initial condition inputs."*

4.1 Governing Equations

4.1.1 Rigid Body Dynamics

The ADVS model uses three lumped masses to describe the mass of the vehicle. A sprung mass, a front unsprung mass, and a rear unsprung mass are included in the simulation model. Figure 15 shows the vehicle model with a dependent suspension (solid axle suspension), and Figure 16 shows the vehicle model with an independent suspension. These figures are taken from the ADVS documentation.

The sprung mass is modeled using all six degrees of freedom. That is, the lateral, longitudinal, and vertical degrees of freedom are included in the model, as are the yaw, roll, and pitch degrees of freedom. The equations of motion of the sprung mass have been derived using a Lagrangian formulation.

The Lagrangian formulation involves specifying the kinetic and potential energy terms associated with each of the generalized coordinates, which are the displacements associated with each of the six individual degrees of freedom. Appropriate partial derivatives of these terms with respect to generalized coordinates and with respect to the generalized velocities are required. This formulation technique also involves specifying energy dissipation terms, and their associated partial derivatives with respect to the generalized velocities. Lastly, the external generalized forces are specified.

The unsprung mass modeling also uses a Lagrangian formulation. For both dependent and independent suspension systems, two generalized coordinates indicate suspension motion relative to the sprung mass, and to describe the kinetic and potential energy for the Lagrangian formulation.

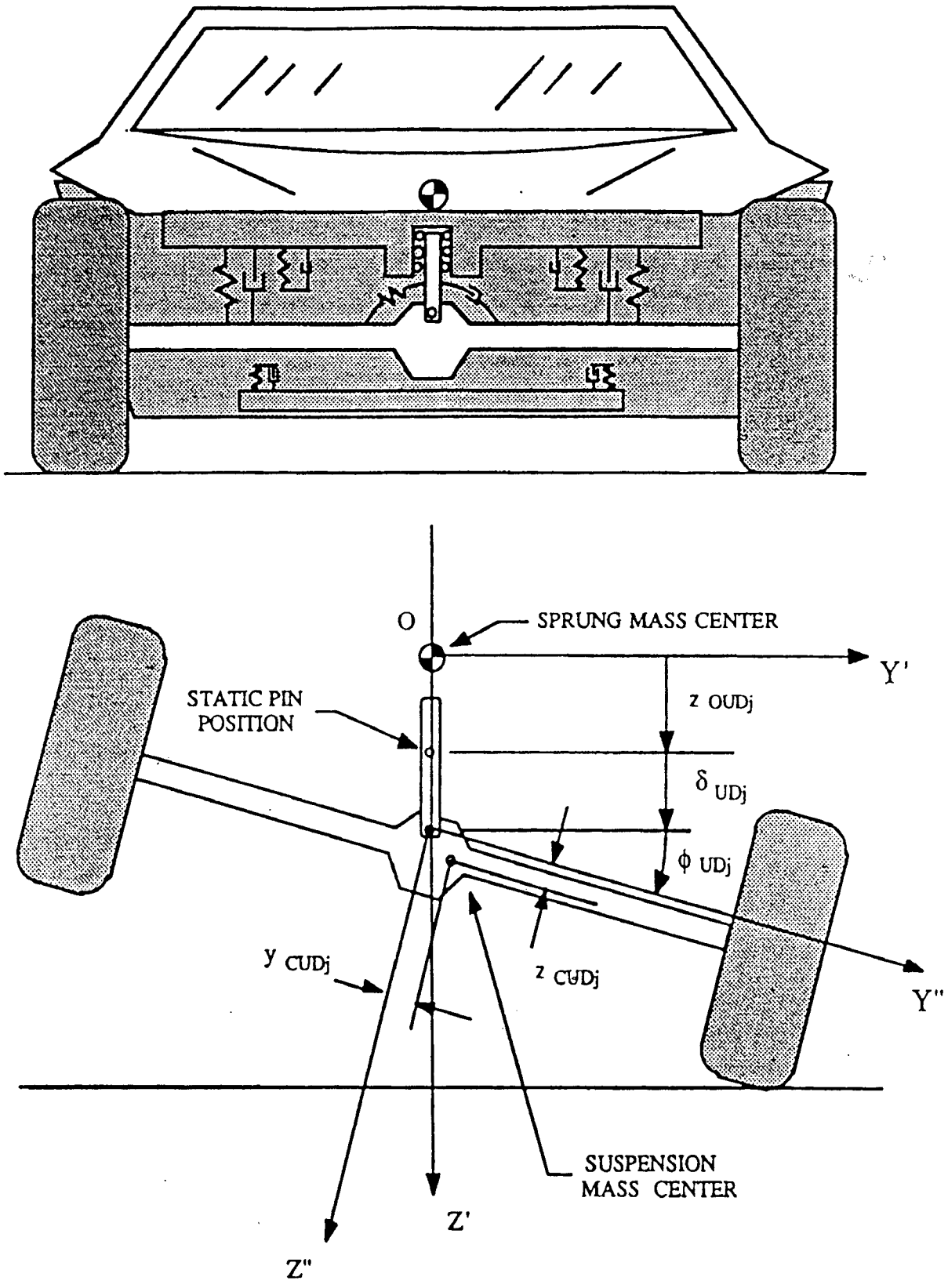

Figure 15 - ADVS Vehicle Model - Dependent Suspension Case

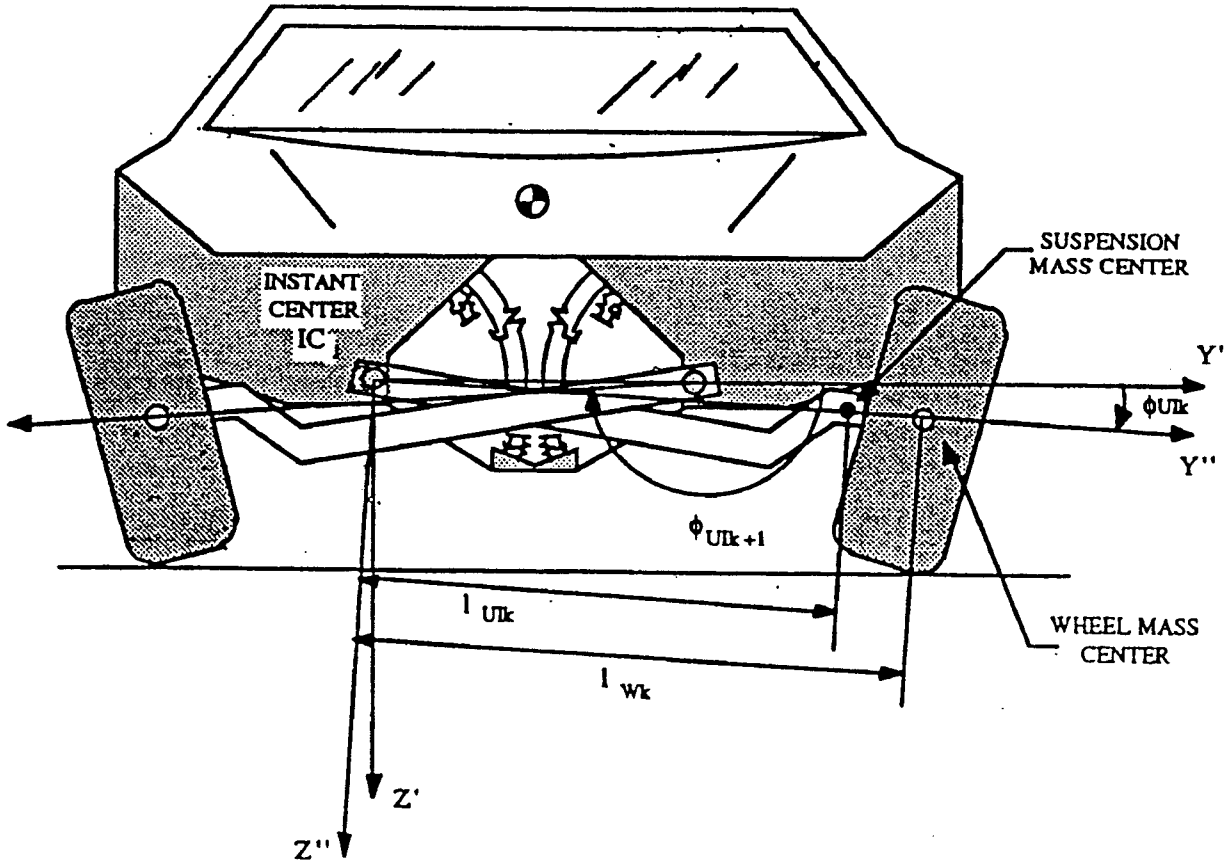

Figure 16 - ADVS Vehicle Model - Independent Suspension Case

For all dependent suspension systems, the ADVS model uses a rigid member, solid axle representation (Figure 15). For dependent suspension systems, the two generalized coordinates are the vertical displacement of the suspension roll center and the rotation angle of the solid axle of the equivalent suspension system.

For all independent suspension systems, ADVS models them using an equivalent swing axle suspension system representation (Figure 16). In the case of an independent suspension, the generalized coordinates are the rotation angles of the right-side and left-side swing axles of the equivalent suspension system.

Front and rear suspension forces are confined to act in planes parallel to the vehicle y-z plane. These planes pass through the front and rear axles. This is a common way to model suspension forces in simulations of this type. Modeling the front and rear suspension systems separately, as opposed to

lumping their effects together at the vehicle c.g., is an improvement over the University of Missouri's Intermediate Maneuver Induced Rollover Simulation (IMIRS) discussed in Chapter III.

A Lagrangian formulation is also used to describe the wheel spin equations. A generalized coordinate, wheel spin angle, is associated with each wheel, resulting in a total of four degrees of freedom. The rotational kinetic energy, inertia matrices, and coordinate transformations associated with each wheel are specified.

Three components of generalized forces are included in the ADVS Lagrangian formulation. These are conservative generalized forces resulting from potential energy, dissipative generalized forces resulting from viscous damping, and generalized forces arising from external forces, such as tire forces and aerodynamic forces.

The conservative generalized forces include affects from the gravitational potential energy of the sprung mass, unsprung masses, and wheel masses, and the storage potential energy of the linear and rotational suspension springs, linear and rotational bump stop stiffnesses, and auxiliary roll stiffness. The dissipative generalized forces include affects from the linear and rotational suspension viscous dampers (shock absorbers), the linear and rotational bump stop viscous damping, and auxiliary roll damping.

In total, the ADVS simulation has 14 degrees of freedom. As mentioned, there are six sprung mass degrees of freedom, four unsprung mass degrees of freedom, and four wheel spin degrees of freedom. Accordingly, there are 14 Lagrange equations, each written with respect to a generalized coordinate associated with the individual degrees of freedom. The ADVS model was developed without making any simplifying assumptions concerning the dynamic interaction of the vehicle subsystems, without small angle approximations, and without any perturbation linearization of the equations of motion describing system behavior. Using a Lagrangian approach for a model this complex, without any simplifying assumptions, results in a large number of equations necessary to describe the vehicle dynamics. The large number of equations is necessary to generate all of the terms in the Lagrange equations, particularly the kinetic and potential energies, and associated partial derivatives with respect to each of the generalized coordinates.

The 14 Lagrange equations, which comprise the vehicle and wheel spin models, can be solved for the generalized accelerations and written in matrix form. The form of these equations is shown below.

$$\{\ddot{q}\} = [M]^{-1}\{f\}$$

where

$\{\ddot{q}\}$ = *Generalized AccelerationVector*
$[M]^{-1}$ = *Inverse of the "Mass" Matrix*
$\{f\}$ = *Generalized Forces*

(7)

Inverting the "mass" matrix [M] at each time step, since it is time dependent, allows for the solution of the coupled acceleration terms. The accelerations are numerically integrated to determine the generalized velocities and displacements. This routine of inverting a matrix in order to numerically solve a system of coupled differential equations is a standard simulation method, and is well suited to this type of model.

For the ADVS simulation, the mass matrix has dimension 14x14. Unlike most vehicle dynamics simulations of this type, the ADVS model does not uncouple the wheel spin equations from the vehicle dynamics model. If the wheel spin equations were uncoupled from the vehicle dynamics, two separate systems of coupled equations would result; one with a 10x10 mass matrix and the other with a 4x4 mass matrix. This would allow for a reduction in simulation run time, as the total computational time of the matrix inversions would be reduced. Also, uncoupling the wheel spin equations allows for more efficient numerical integration techniques to be used for the simulation of handling dynamics. Only the wheel spin equations need be solved using a small time step, and then only during braking maneuvers.

4.1.2 Suspension Model

Kinematics

ADVS has two suspension models that can be used to model either independent or dependent (solid axle) suspension systems at each vehicle axle. For independent suspension systems, an equivalent swing axle model is used (Figure 17). Dependent suspension systems are represented using a beam axle model (Figure 18). The independent suspension model will be described first, followed by the dependent suspension model.

Independent suspension systems are modeled using an equivalent swing axle model. This equivalent swing axle is defined as having its pivot point at the instant center of rotation of the wheel, relative to the sprung mass, when the wheel is in its static position. Figure 17 shows this suspension in schematic form. The instant center of rotation of the suspension in the YZ plane can be found graphically using the Arnhold-Kennedy theorem. The swing axle pivot is assumed to remain fixed with respect to the

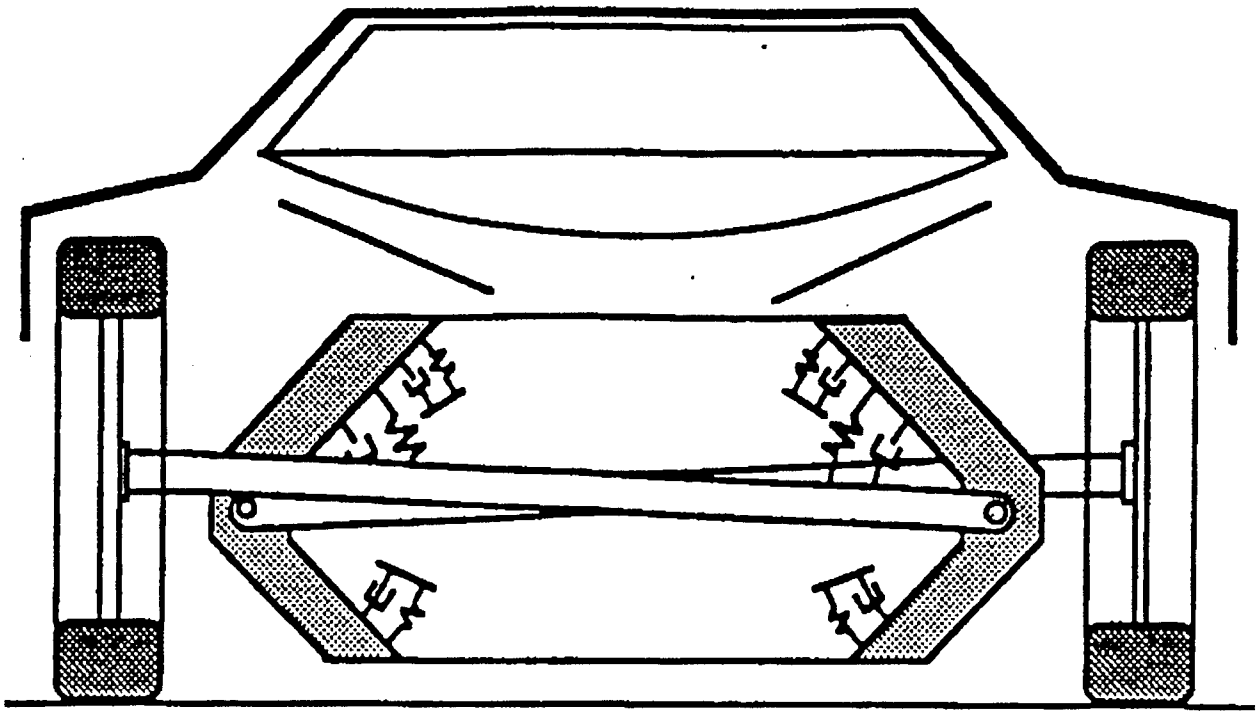

Figure 17 - ADVS Kinematic Suspension Model: Independent Suspension

sprung mass. This equivalent swing axle defines how the forces developed at the tire contact patch are fed into the sprung mass. This suspension representation is used in place of the classic fixed roll center model. It should be noted that at the vehicle's static position, the equivalent swing axle and the fixed roll center models are equivalent.

Independent suspension springs are modeled as torsional springs located at the swing axle pivot points. A second-order polynomial is used to represent the stiffness of the torsional spring as a function of angular displacement of the swing arm. A bilinear torsional damper (compression and rebound) is also located at the pivot point to provide viscous damping. Spring and damping rates measured at the roadwheels must be transformed to equivalent effective angular rates at the pivot axis.

An anti-roll bar is modeled as acting between the swing axle pivot points and has linear stiffness and viscous damping properties. The anti-roll bar generates a moment proportional to the difference in the swing axle angle angular displacements. A moment proportional to the difference in the swing axle angle angular velocities is also generated. As with the swing axle torsional springs and dampers, the anti-roll bar stiffness and damping must be transformed from the rates measured at the roadwheels to equivalent effective angular rates between the pivot axes.

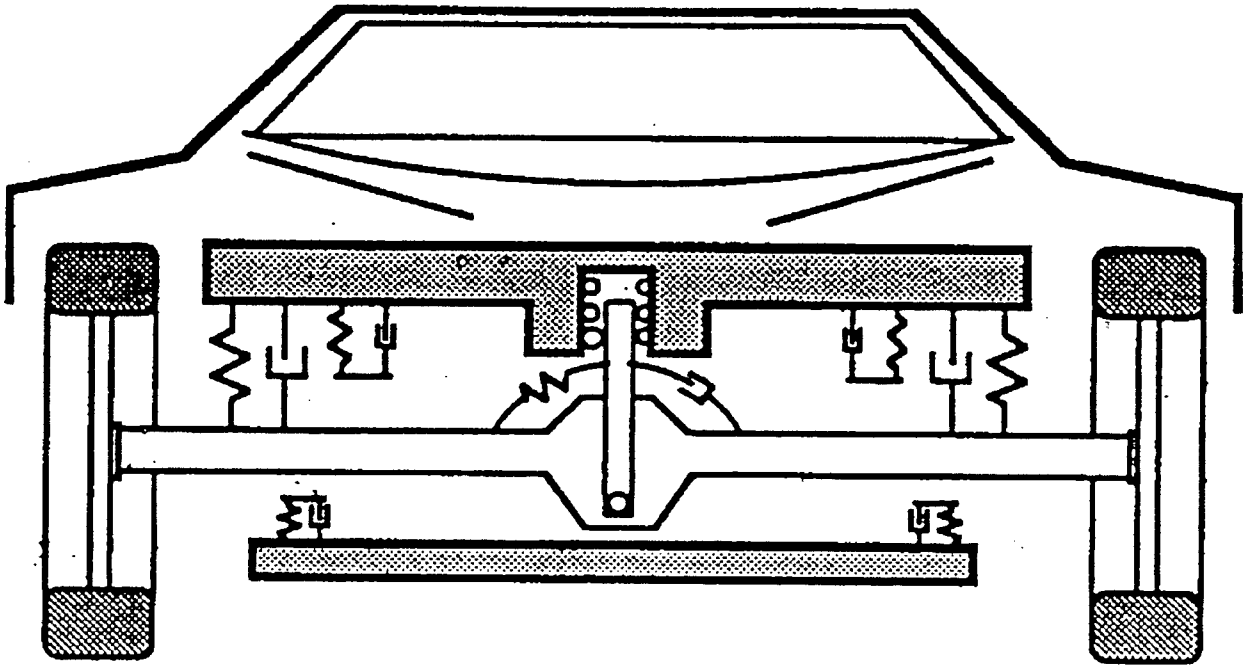

Figure 18 - ADVS Kinematic Suspension Model: Dependent Suspension

Upper and lower bump stops are modeled as acting on each swing arm. The bump stops have nonlinear, rising rate stiffness properties. The bump stop stiffness is modeled to approach infinite stiffness as its length approaches zero. The bump stop dampers are modeled as linear viscous dampers. The position of the upper and lower bump stops are each defined by a bump stop length, their distance from the pivot axis, and the swing arm angular displacement from its static position required to contact each bump stop.

The only road wheel kinematic effect modeled is a fourth-order polynomial used to describe road wheel camber change as a function of swing axle angle. Road wheel steer kinematics as a function of sprung mass bounce or roll are not included in the ADVS model. Past studies [1] have shown axle roll steer characteristics to influence vehicle directional response.

The dependent suspension model, shown schematically in Figure 18, uses a rigid beam to represent the solid axle. A roll center is fixed to a point on the axle and translates in the Z-direction with the unsprung mass.

The springs for the dependent suspension model act vertically between the axle and the sprung mass. The upper and lower vertical locations of the spring ends and the lateral distance from the spring center to the center line of the vehicle are used to define the spring geometry. A second-order polynomial is used to describe the spring stiffness as a function of spring length. Bilinear dampers are modeled as acting along the same line as the springs. An anti-roll bar with constant stiffness and viscous damping characteristics is also included. The bump stops are modeled, like the independent suspension bump stops, as having nonlinear, rising rate stiffness and linear viscous damping properties.

Compliance

No suspension system compliances are modeled by ADVS. Research by the authors and others [11, 12, 13] has demonstrated the importance of suspension system steer and camber compliances to forces and moments generated at the tire contact patch.

4.1.3 Steering System Model

The ADVS does not model the vehicle steering system. Instead, steer angles are applied directly to the front wheels. The model thus ignores the effects of the steering system on vehicle response. The model also assumes that both front wheels steer equal amounts, therefore, ignoring any Ackerman steering affects.

Past research by the authors [1] and others [14] has shown steering system compliance to have first order affects on vehicle steady state and transient response. In a study by Bundorf [12], aligning torque deflection steer was found to contribute over 30 percent of the total vehicle understeer. Bergman, in a similar study [11] found steering compliance to contribute over 20 percent of the total vehicle understeer.

Neglecting the steering system characteristics, and applying a steer angle to the front road wheels is not "incorrect", and can be used to isolate the vehicle response from the influences of the steering system. However, crash avoidance research typically is aimed at studying passenger vehicle response to driver handwheel inputs. ADVS, with no steering system, cannot be used for this. Users of the simulation need to be aware of this limitation and not misinterpret the simulation predictions.

4.1.4 Braking Model

ADVS uses a simple, fixed proportioning, fixed break point braking model. The front to rear brake force distribution,Q, is computed from:

$$Q = Q_0 + Q_1 \cdot (A_x - 0.3) \tag{8}$$

where Q_0 is the front to rear brake force distribution below 0.3 g's, and Q_1 is the rate of increase of front to rear brake force distribution above 0.3 g's.

This model assumes that the break point of the proportioning valve occurs at 0.3 g's, this may not be a valid assumption for many vehicles. The advantage of this brake model is it requires only two parameters. However, adding a variable break point would make the model better able to characterize the brake systems of the vehicle fleet with little added complexity.

The control input for the brake model is desired longitudinal acceleration. Therefore, ADVS cannot be used to predict longitudinal acceleration from brake pedal force or brake line pressure inputs. This makes ADVS unsuitable for studies using driver or driver model control force inputs.

This brake system model has no antilock brake option. Since the number of vehicles equipped with antilock brakes is increasing rapidly, it would be desirable to incorporate an antilock model for studying limit vehicle performance. In addition, load sensing brake proportioning valves are common and should also be modeled.

4.1.5 Drivetrain Model

The ADVS simulation does not contain a drivetrain model. Longitudinal acceleration (positive or negative) can be requested by the user using the brake input menu. The model allows a fixed percentage of the drive torque to be directed to the front axle, therefore allowing front, rear, or four wheel drive. No constant speed governor is provided.

When running pure cornering maneuvers, vehicle speed decreases due to tire friction. Only through a trial and error approach could the user determine a longitudinal acceleration input to cancel the effects

of the tire friction. The longitudinal acceleration required for constant speed operation will be maneuver dependent.

Future NHTSA simulations will require complete drivetrain models. This will include front, rear, and four wheel drive options. For the NADS, this is an area where extensive modeling work will be required. Future IVHS research may also require simulations with extensive drivetrain models.

4.1.6 Tire Model

Quasi-Static:

The ADVS simulation has three different tire models; one for simulating forces generated due to tire deformation from tire/terrain interactions, one for simulating tire friction forces from contact with the terrain, and one for simulating forces due to plowing effects from tire sinkage into soft terrain. For the purposes of simulating handling maneuvers on flat road surfaces, only the tire friction model is of interest. Therefore, only this portion of the tire will be discussed in detail.

Before describing the tire friction model, a few brief comments concerning the other portions of the ADVS tire model are appropriate since they are a significant portion of the ADVS simulation. The tire/terrain interference model has 45 radial "slices" of the lower half of each tire, equally spaced in four degree increments, with 11 springs in each radial "slice". This results in 495 springs per tire, and 1980 springs for the entire vehicle. The simulation monitors the deflection of each spring at each simulation time step. If a spring is deflected from its original length, the resulting forces are computed. This involves a large amount of computer time and slows the simulation considerably, especially when many springs are being deflected, as during a curb strike. The ADVS tire/terrain interference model contains no dampers within the tires. To verify the quality of this tire/terrain interference model, a more detailed study than is provided in this evaluation would be necessary. Experimental tire testing would be required to fully evaluate most aspects of this model, and to determine parameters for the model.

The model used to simulate tire forces caused by plowing into soft soil will also require some verification before it is completely accepted. The forces generated are based on the amount of soil sinkage experienced by the tire. The draft ADVS documentation provides no mention of past experimental research upon which this model was based. If a limited amount of experimental data is available, then additional experimental tire testing would also be required to fully evaluate this model.

The ADVS simulation uses the Calspan (McHenry) tire model, modified to account for severe overload and large camber angles, to represent the quasi-static friction characteristics of the tires. Variations of this tire model, which assume that forces and moments act at a point contact within the tire/road contact area, are widely used in vehicle dynamic simulation tire models. The coordinate system used in the ADVS tire model is the standard SAE recommended coordinate system. This tire model represents the nonlinear characteristics for all of the most important tire relationships; for example, side force versus slip angle, longitudinal force versus slip, etc. Inputs to the tire model include normal load, slip angle, camber angle, and longitudinal slip. Tire model outputs include lateral and longitudinal tire force and tire aligning moment. Overturning moment is not included in the tire model.

The model includes combined braking/driving (slip ratio) effects with simultaneous slip angle effects using a friction ellipse. This requires that the vector sum of the lateral tire force and longitudinal tire force remains on or within an ellipse whose axes are defined by maximum side force and maximum circumferential force values. The use of the friction ellipse concept is fairly widespread among simulation tire models.

Longitudinal force, as a function of longitudinal slip, is determined from empirical equations based on curve fits of Calspan data. This force is limited by the surface coefficient of friction and the friction ellipse. In the ADVS tire model, tire side force is composed of forces arising from the slip angle and from the camber angle. Both slip angle and camber angle effects are determined from empirical equations based on Calspan data. Side force is also limited by the surface coefficient of friction and the friction ellipse. Empirical relationships relating the tire aligning moment to normal force, side force, and camber angle are used in the tire model.

As is common for empirical tire models of this type, some of the coefficients used in the empirical equations for longitudinal and side force are functions of tire normal force. The effects of tire normal load changes which occur during the maneuver are included in the tire model computations. The ADVS tire model includes additional routines to model the tire during severe overload conditions with large slip and camber angles.

In all, the tire model requires 20 parameters based on Calspan measurements, and several other parameters based on assumed or measured tire characteristics. The ADVS tire model is quite similar to tire models used previously at the VRTC. Based on the authors experience, this tire model formulation appears to be adequate for modeling the tire quasi-static forces and moments. A detailed evaluation of

the tire model would require comparison with experimental results. This is beyond the scope of this study. However, a more detailed evaluation of existing tire models is forthcoming at the VRTC. Current plans are to include this (Calspan/McHenry) tire model in the proposed study. Attributes of the ADVS tire model which are unique, such as the modeling of the tire for overloading conditions, warrant additional study as part of the future research project.

Dynamic:

ADVS contains no tire dynamics. All tire forces are generated instantaneously based on the empirical quasi-static tire model. As shown previously by the authors [1, 7], this will limit ADVS's ability to predict transient vehicle responses. Past research has demonstrated that the side force lag present in tires reduces the effective vehicle yaw rate damping.

4.1.7 Driver Model

ADVS contains no driver model. Control inputs to the vehicle are provided by road wheel angle and longitudinal acceleration tables, or generated internally for fixed frequency sinusoidal inputs. The input tables are limited to a 20 point time versus road wheel angle and/or longitudinal acceleration description of the control input.

In the course of past simulation evaluation and metric computation programs, the authors have found it to be important to provide the simulation with realistic driver generated control inputs [1, 7]. When comparing simulation predictions to field test data, simulations are "driven" with measured handwheel and brake pressure data from the field tests. A 20 point input file is only sufficient to accurately characterize the control inputs for simple maneuvers such as pseudo-step inputs and trapezoidal steer lane change maneuvers. Modifying ADVS to allow more points to define steering inputs is not thought to be a difficult task.

ADVS, with no driver model, cannot simulate any closed-loop maneuvers. This is not a problem at present. However, future research for NADS and IVHS may need a driver model.

4.1.8 Aerodynamic Model

ADVS contains a comprehensive aerodynamic model that models the aerodynamic influences on all 6 of the sprung mass degrees of freedom. The equations, which model the effects of wind speed, aerodynamic side slip and pitch angle, are of a standard form used in past automotive studies [15]. The only "non-standard" term is in the yaw moment equation. A term is included that attempts to model the effect of vehicle yaw rate on the vehicle yawing moment, by multiplying an aerodynamic yaw damping coefficient by the vehicle's yaw rate. Typically, aerodynamic parameters are functions of the square of velocity. This term, however, is a linear function of velocity. No references or derivations of this term are given in the report.

4.1.9 Solution Method

For the ADVS simulation, two numerical integration algorithms are used to integrate the differential equations of motion. These methods are a Gear's method, which uses a variable time step, and a fourth-order Runge-Kutta method, which uses a fixed time step. These are common integrators for use in this type of simulation. These integrators are also used successfully for ADVS braking simulation runs. The Gear's method is used as the simulation start-up integrator algorithm, and a switch is made to the Runge-Kutta method, if necessary, when the variable integration step size becomes less than some specified value. This prevents the step size from becoming so small that numerical problems occur.

As mentioned above, the accelerations for the ADVS 14 degree of freedom vehicle model are determined via the matrix inversion and multiplication. All velocity and displacement terms are then computed using the integration algorithms.

Using an integration step size of 0.01 seconds provides reasonable results, however the run times are quite long. Using VRTC's VAX Station 3500, and a step size of 0.01 seconds, a 5 second, steering input only, simulation run requires about 80 to 90 minutes of computer run time (based on benchmarks performed at the VRTC, this would correspond to approximately 110 to 125 minutes on a 25 Mhz IBM Model 80 386 personal computer with a math co-processor). Simulating braking maneuvers does not slow down the simulation run time, since the wheel spin dynamics are coupled with the vehicle dynamics. Using smaller integrator step sizes increases the simulation run time, while larger step sizes reduce integrator accuracy and may result in numerical stability problems. Simulation runs which involve calculating many tire/terrain interference forces, such as during a curb strike, require on the order of 2

hours of computer run time per one second of simulation run time. Short runs require one to two hours, while simulating long runs, such as a slalom run, would require over a day of computer time. Much more powerful computers could ease the compute time burdens. However, some streamlining of the model equations and/or computer code would be beneficial.

4.1.10 Miscellaneous

The ADVS simulation contains several models which are not related to vehicle handling dynamics. The three most significant models are the suspension-wheel crush model, the vehicle-ground impact model and the rollover prevention energy reserve (RPER) computation. The vehicle-ground impact model simulates the vehicle body deformation and forces on impact with the ground after rollover. The RPER criteria is computed to estimate rollover potential for a vehicle. The validity of these models has not been studied as part of this research. However, the predictions made with these models should be compared with experimental results before these models are utilized.

4.2 Parameter Measurement

The vehicle and tire parameters required by ADVS will be described in 5 categories: geometric, inertial, suspension/steering, aerodynamic, and tire.

4.2.1 Required Parameters

Geometric:

The ADVS geometric parameters are used to describe the physical dimensions of the vehicle and its suspension system. Parameters include: wheelbase, front and rear track and wheel center heights, and spring half track width.

Inertial:

Inertial parameters describe the mass and mass moment of inertia magnitudes and locations of the sprung and unsprung masses. The parameters include: mass center position of the sprung and unsprung masses, the mass of the sprung and unsprung masses, the six principal and product mass moment of

inertias of the sprung mass, the principal mass moment of inertias of the unsprung masses for dependent suspensions, and the mass and spin moment of inertia (I_{YY}) of the tire/wheel assemblies.

Suspension:

The parameters used for the ADVS suspension model are used to describe the road wheel kinematics, and the suspension stiffness and damping characteristics. The parameters required for independent suspensions will be described first, followed by the required parameters for dependent suspensions.

Independent suspensions are modeled as equivalent swing arms. The locations of the imaginary pivot points are defined in the YZ plane. The remainder of the parameters are then defined in reference to this imaginary swing arm. A fourth-order polynomial is used to describe the change in road wheel camber angle as a function of swing arm angular displacement. Bump stop locations are defined by acting at a radius from the pivot point, an undeformed length, and the angle at which the swing arm contacts each bump stop.

Independent suspension torsional springs are described by second-order polynomials describing their torsional stiffness as a function of swing arm angle. The anti-roll bar stiffness is a linear function of the difference between the swing arm angles. Bilinear dampers are defined by linear coefficients for extension and rebound for the moment created at the pivot point due to swing arm angular velocity. A linear anti-roll bar damper creates a moment at each pivot point proportional to the difference between the swing axle angular velocities. The upper and lower bump stops each have parameters describing their stiffness and damping.

The computation of the parameters for the independent suspension model is a very difficult and time consuming task. Transforming all of the parameters from the measured data at the wheels to the imaginary swing arm reference system will be very difficult by hand. In addition, by defining all of the independent suspension parameters in reference to the imaginary swing arm rotation, the parameters become dependent on each other. For example, if a change in the suspension geometry is being investigated, if the imaginary swing arm pivot point changes, all of the kinematic, stiffness, and damping parameters will need to be recomputed. This will complicate the analysis. No tools are provided with the simulation to help automate this task.

For dependent suspension systems, a roll center is fixed to the unsprung mass. Springs are defined by a track width, the height of their upper and lower ends, a second-order polynomial defining their stiffness as a function of deflection, and a bilinear damper with extension and compression coefficients. Bump stops are defined by a track width, position above the ground, length, stiffness, and damping coefficients. Anti-roll bars have linear stiffness and damping coefficients.

The final group of suspension parameters define the lateral crush behavior of the suspension system. These parameters are only used in impact type simulation runs. Parameters describe the lateral force required to cause plastic deformation of the suspension system, the amount of constant force plastic deformation, and a secondary stiffness parameters to describe the stiffness of the suspension after the initial plastic deformation has occurred.

Aerodynamic:

Aerodynamic parameters included in the ADVS simulation describe the longitudinal air drag, the effect of side slip angle on the vehicle yaw moment and side force, and the effect of pitch angle on aerodynamic lift and pitch moment. The parameters are: air density, aerodynamic reference angle, aerodynamic reference length, side force coefficient, yaw moment coefficient, yaw damping moment coefficient, drag force coefficient and derivative, zero lift pitch angle and lift force coefficient derivative, and pitch moment coefficient and derivative.

Tire:

The ADVS contains frictional, soil, and impact tire models. The frictional tire model is based on the Calspan model. Twenty "Calspan" curve fit parameters describe the quasi-static tire force and moment properties. Four additional parameters are used to treat high camber angle and tire vertical force overload conditions.

The tire impact model contains 10 parameters to describe the tire/rim geometry. Parameters for tire radial and lateral stiffness, and lateral rim stiffness are also included.

4.2.2 Test Methods

The documentation of the ADVS model gives no information on the procedures or equipment required for the measurement of any of the simulation parameters. This will complicate the task of using the simulation due to the complex nature of the vehicle parameters required by ADVS. With any simulation of this type, there are many subtleties to the definition of the parameters used to describe the vehicle, suspension, etc. The authors of the simulation are best equipped to understand these subtleties and describe them to the simulation users. Without the benefit of this description by the author, the user is forced to make his or her own interpretation of the parameters based on the information provided. This same argument applies to the parameter measurement techniques required.

4.2.3 Compatibility with Existing Test Equipment

Equipment currently available at the VRTC can measure most of the parameters needed for the ADVS simulation. The following are the parameters that can not be measured at the VRTC.

Equivalent swing arm pivot point: Currently, the VRTC does not have equipment (other than tape measures) to accurately measure the suspension pivot coordinates. These are required to graphically compute the swing arm pivot point.

Bump stop stiffness and damping coefficients: These could be estimated based on their shape and known properties of rubber.

Shock absorber damping coefficients: A shock dyno is not available at the VRTC. However, shocks can be sent out to be measured. This is a time consuming and expensive process. If measuring shock absorber characteristics becomes necessary at the VRTC, then better methods of obtaining shock data will need to be investigated.

Suspension crush data: A test device would have to be designed and built if these parameters were needed for a simulation program.

Sprung mass product mass moments of inertia: It is commonly believed that these values are very small compared to the principal mass moments of inertia (approximately 1 percent), and do not have a significant influence on vehicle directional control.

Tire force and moment data: The VRTC does not have a tire test machine. All tire testing needs to be done by outside labs. There are no plans at the present time to develop this capability at the VRTC.

Stiffness data for the tire impact model: The tire stiffnesses may be estimated from the Calspan test data. The rim stiffness will only be important in curb strike simulations and can be set very stiff for handling simulations. Parameters for the curb strike and soil interaction tire models cannot be determined using standard tire test equipment.

Aerodynamic data: Frontal area and characteristic height could be estimated by measuring vehicle dimensions or using photographic techniques. However, the remaining parameters cannot be estimated.

4.3 Road Profile

The road profile can be constructed from up to 19 planes. Each plane is infinitely long in the X direction of the terrain fixed coordinate system and is bounded by two points in the YZ plane. Each plane can be either paved, with its own skid number, or be soft soil.

4.3.1 Flat Road

An infinite length flat road can be constructed using two planes.

4.3.2 Rough Road

No rough road capability is provided.

4.3.3 Roadside (curbs, grades, etc.)

Curbs, grades, etc. can be constructed using multiple planes. Soft shoulders can also be simulated using the soil tire model.

4.4 Comparison with Experimental Data

The ADVS report contains a J-turn and a lane change maneuver for comparison of the simulation predictions to experimental data. The data decks used for the comparisons are not given.

In order to check the performance of the ADVS model, a data deck for a Suzuki Samurai was generated using parameters measured by the VRTC (Table X and Table XI). The model was run and comparisons made to experimental data measured at the VRTC as part of an earlier simulation evaluation program. The comparisons were made in both the time and frequency domains.

Because ADVS does not have a steering system model (Section 4.1.3), direct comparisons with experimental data using a driver supplied control input (hand wheel angle) can not be made. At a given forward speed, if a road wheel steer angle is input to the simulation to match the lateral acceleration level of an experimental run, at steady state, the yaw rate, by definition will be correct because it is a function of forward speed and lateral acceleration ($r = A_Y / U$). Thus, in effect, the user is supplying the simulation with the desired "answer" (yaw rate or lateral acceleration) and using the simulation to predict other unknown vehicle responses (roll angle, side slip angle, etc.).

4.4.1 Steady State

A ramp steer maneuver was run to compare the time domain simulation predictions with the experimental data. The run was made at 50 mph with a nominal lateral acceleration level of 0.4 g's. In order to match the simulated yaw rate with the experimentally measured yaw rate, a slowly increasing steer maneuver (road wheel steer angle increased at 0.25 degrees per second with constant forward speed) was made. The road wheel angle required to give the experimentally measured yaw rate was then determined from the predicted yaw rate versus road wheel angle.

Figure 19 shows the ADVS predictions and the experimental yaw rate time domain response for the 50 mph, 0.4 g J-turn. As can be seen, the simulation transient response predictions are significantly more damped than the actual vehicle. For the J-turn maneuver used for comparison, the experimental data showed approximately 60 percent yaw rate peak overshoot. The ADVS prediction, however, only showed 1.1 percent overshoot. This result is in contrast to the J-turn comparisons given in the ADVS report. In that maneuver, the yaw rate predictions had an overshoot very close to the experimental data. Since both runs were simulating a Suzuki Samurai in a J-turn, it is assumed that changes have been made in the simulation since the time that the comparisons in the report were made.

Table X - ADVS Simulation Vehicle Parameters - Suzuki Samurai Data Deck Generated by VRTC

```
9,'=====================================',+1.111111D+11, 0
9,'= INPUT DATA FOR THE TEST VEHICLE =',+1.111111D+11, 0
9,'=====================================',+1.111111D+11, 0
9,'====== SUZUKI SAMURAI - VRTC ======',+1.111111D+11, 0
9,'=====================================',+1.111111D+11, 0
9,'= CREATION DATE:      MAY 18 1989 =',+1.111111D+11, 0
9,'= LAST UPDATE  :      MAY  9 1991 =',+1.111111D+11, 0
9,'=          BY  : Gary J. Heydinger=',+1.111111D+11, 0
9,'=          BY  : Jeff P. Chrstos  =',+1.111111D+11, 0
9,'=          BY  : TRC of Ohio/VRTC =',+1.111111D+11, 0
9,'=====================================',+1.111111D+11, 0
9,'======= ANALYZED PARAMETERS =======',+1.111111D+11, 0
9,'=====================================',+1.111111D+11, 0
9,'======= PRIMARY GEOMETRICAL =======',+1.111111D+11, 0
9,'========== BASIC DATA ==============',+1.111111D+11, 0
0,'{A}   DISTANCE - CG TO FRONT AXLE  ',+1.074400D+00, 0
0,'{B}   DISTANCE - CG TO REAR  AXLE  ',+0.957600D+00, 0
0,'{HS}  STATIC HEIGHT OF SPRUNG C.G. ',+0.688300D+00, 0
9,'=====================================',+1.111111D+11, 0
9,'======== SUSPENSION  DATA ========',+1.111111D+11, 0
9,'==== DEPENDENT SUSPENSION TYPE ====',+1.111111D+11, 0
9,'=====================================',+1.111111D+11, 0
9,'========== FRONT SUSP. ============',+1.111111D+11, 0
0,'{TRDF} FRONT SUSPENSION TRACK WIDTH',+1.308100D+00, 0
0,'{WCHDF} FRONT WHEEL CENTER HEIGHT  ',+0.322500D+00, 1
0,'{HRC1} STATIC HT. OF RC ABOVE GRND.',+0.264200D+00, 0
0,'{YCUD1} MASS CENTER POSITION,FRONT ',+0.000000D+00, 0
0,'{ZCUD1} MASS CENTER POSITION,FRONT ',-0.058300D+00, 0
0,'{HSUF} UPR.END SPRNG POS    ,FRONT  ',+0.440000D+00, 1
0,'{HSLF} LWR.END SPRNG POS    ,FRONT  ',+0.360000D+00, 1
0,'{TSF} SPRING TRACK          ,FRONT  ',+0.355600D+00, 1
0,'{HBUF} UPR.BUMP STOP POS    ,FRONT  ',+0.420000D+00, 1
0,'{HBLF} LWR.BUMP STOP POS    ,FRONT  ',+0.220000D+00, 1
0,'{HBUF1} UPR CONT SRFS POS   ,FRONT  ',+0.360000D+00, 1
0,'{HBLF2} LWR CONT SRFS POS   ,FRONT  ',+0.300000D+00, 1
0,'{TBUF} UPR BUMP STP TRACK   ,FRONT  ',+0.355600D+00, 1
0,'{TBLF} LWR BUMP STP TRACK   ,FRONT  ',+0.355600D+00, 1
0,'{LBUF} UPR.BUMP STP LENGTH  ,FRONT  ',+0.030000D+00, 1
0,'{LBLF} LWR.BUMP STP LENGTH  ,FRONT  ',+0.030000D+00, 1
9,'========= REAR SUSP. ==============',+1.111111D+11, 0
0,'{TRDR} REAR SUSPENSION TRACK WIDTH ',+1.308100D+00, 0
0,'{WCHDR} REAR WHEEL CENTER HEIGHT   ',+0.322500D+00, 1
0,'{HRC2} STATIC HT. OF RC ABOVE GRND.',+0.269200D+00, 0
0,'{YCUD2} MASS CENTER POSITON,REAR    ',+0.000000D+00, 0
0,'{ZCUD2} MASS CENTER POSITON,REAR    ',-0.053300D+00, 0
0,'{HSUR} UPR.END SPRNG POS    ,REAR   ',+0.440000D+00, 1
0,'{HSLR} LWR END SPRNG POS    ,REAR   ',+0.360000D+00, 1
0,'{TSR} SPRING TRACK          ,REAR   ',+0.476300D+00, 1
0,'{HBUR} UPR.BUMP STOP POS    ,REAR   ',+0.440000D+00, 1
0,'{HBLR} LWR.BUMP STOP POS    ,REAR   ',+0.230000D+00, 1
0,'{HBUR1} UPR CONT SRFS POS   ,REAR   ',+0.360000D+00, 1
0,'{HBLR2} LWR CONT SRFS POS   ,REAR   ',+0.300000D+00, 1
0,'{TBUR} UPR BUMP STP TRACK   ,REAR   ',+0.476300D+00, 1
0,'{TBLR} LWR BUMP STP TRACK   ,REAR   ',+0.476300D+00, 1
0,'{LBUR} UPR.BUMP STP LENGTH  ,REAR   ',+0.030000D+00, 1
0,'{LBLR} LWR.BUMP STP LENGTH  ,REAR   ',+0.030000D+00, 1

9,'=====================================',+1.111111D+11, 0
9,'===== MASS/INERTIA PARAMETERS =====',+1.111111D+11, 0
9,'=====================================',+1.111111D+11, 0
9,'========== SPRUNG MASS ============',+1.111111D+11, 0
0,'{MS}     SPRUNG MASS                ',+892.2100D+00, 0
0,'{IXXS}   SPRUNG ROLL INERTIA        ',+226.5000D+00, 0
0,'{IYYS}   SPRUNG PITCH INERTIA       ',+866.0000D+00, 0
0,'{IZZS}   SPRUNG YAW INERTIA         ',+1039.000D+00, 0
0,'{IXYS}   SPRUNG PDT OF INERTIA      ',+0.000000D+00, 0
0,'{IYZS}   SPRUNG PDT OF INERTIA      ',+0.000000D+00, 0
0,'{IZXS}   SPRUNG PDT OF INERTIA      ',+0.000000D+00, 0
9,'========= UNSPRUNG MASS ===========',+1.111111D+11, 0
9,'==== DEPENDENT SUSPENSION TYPE ====',+1.111111D+11, 0
0,'{MUDF} UNSPRUNG MASS, FRONT         ',+79.80000D+00, 0
0,'{MUDR} UNSPRUNG MASS, REAR          ',+79.80000D+00, 0
0,'{IXXUF} UNSPNG ROLL INERTIA ,FRONT  ',+20.20000D+00, 0
0,'{IXXUR} UNSPNG ROLL INERTIA ,REAR   ',+20.20000D+00, 0
0,'{IYYUF} UNSPNG PITCH INERTIA,FRONT  ',+3.000000D+00, 0
0,'{IYYUR} UNSPNG PITCH INERTIA,REAR   ',+3.000000D+00, 0
0,'{IZZUF} UNSPNG YAW INERTIA  ,FRONT  ',+20.20000D+00, 0
0,'{IZZUR} UNSPNG YAW INERTIA  ,REAR   ',+20.20000D+00, 0
9,'============= TIRE ================',+1.111111D+11, 0
0,'{MW}     TIRE MASS                  ',+18.70000D+00, 3
0,'{IXXW}   MOMENT OF INERTIA          ',+1.060000D+00, 3
9,'=====================================',+1.111111D+11, 0
9,'==== SUSPENSIONS  SPRINGS DATA ====',+1.111111D+11, 0
9,'=== DEPENDENT  SUSPENSION  TYPE ===',+1.111111D+11, 0
0,'{ASDF0} POLY APRX COEF 1,FRONT      ',+44619.00D+00, 1
0,'{ASDF1} POLY APRX COEF 2,FRONT      ',+0.000000D+00, 1
0,'{ASDF2} POLY APRX COEF 3,FRONT      ',+0.000000D+00, 1
0,'{ASDR0} POLY APRX COEF 1,REAR       ',+34671.00D+00, 1
0,'{ASDR1} POLY APRX COEF 2,REAR       ',+0.000000D+00, 1
0,'{ASDR2} POLY APRX COEF 3,REAR       ',+0.000000D+00, 1
0,'{KDARF} ANTI-ROLL BAR SPRNG, FRONT  ',+12201.00d+00, 0
0,'{KDARR} ANTI-ROLL BAR SPRNG, REAR   ',+3490.000d+00, 0
9,'=====================================',+1.111111D+11, 0
9,'==== SUSPENSIONS  DAMPERS DATA ====',+1.111111D+11, 0
9,'===  DEPENDENT SUSPENSION TYPE  ===',+1.111111D+11, 0
0,'{CUDUF} DAMPING CONST.,FRONT COMPR  ',+3637.000D+00, 1
0,'{CUDUR} DAMPING CONST.,REAR  COMPR  ',+3001.000D+00, 1
0,'{CUDLF} DAMPING CONST.,FRONT EXTEN  ',+4846.000D+00, 1
0,'{CUDLR} DAMPING CONST.,REAR  EXTEN  ',+5780.000D+00, 1
0,'{CDARF} A-R BAR DMPNG COEF., FRONT  ',+0.000000D+00, 0
0,'{CDARR} A-R BAR DMPNG COEF., REAR   ',+0.000000D+00, 0
9,'=====================================',+1.111111D+11, 0
9,'=  BUMP STOP STIF. AND DAMP. DATA =',+1.111111D+11, 0
9,'=====================================',+1.111111D+11, 0
0,'{KBUF} UPR B.S. SPRNG C,FRONT       ',+323000.0D+00, 1
0,'{KBUR} UPR B.S. SPRNG C,REAR        ',+140000.0D+00, 1
0,'{KBLF} LWR B.S. SPRNG C,FRONT       ',+137000.0D+00, 1
0,'{KBLR} LWR B.S. SPRNG C,REAR        ',+39000.00D+00, 1
9,'=====================================',+1.111111D+11, 0
0,'{CBUF} UPR B.S. DMPNG C,FRONT       ',+6000.000D+00, 1
0,'{CBUR} UPR B.S. DMPNG C,REAR        ',+6000.000D+00, 1
0,'{CBLF} LWR B.S. DMPNG C,FRONT       ',+6000.000D+00, 1
0,'{CBLR} LWR B.S. DMPNG C,REAR        ',+6000.000D+00, 1
```

Table XI - ADVS Simulation Vehicle Parameters (Continued)

```
9,'=====================================',+1.111111D+11, 0
9,'===== FRICTIONAL  TIRE  DATA ======',+1.111111D+11, 0
9,'=====================================',+1.111111D+11, 0
9,'=== CALSPAN TIRE COEFFICIENTS =====',+1.111111D+11, 0
0,'{A0} CORNERING STIFFNESS COEFF.    ',-261.9100D+00, 3
0,'{A1} CORNERING STIFFNESS COEFF.    ',+23.11000D+00, 3
0,'{A2} CORNERING STIFFNESS COEFF.    ',+2675.990D+00, 3
0,'{A3} CAMBER STIFFNESS COEFF.       ',+1.168000D+00, 3
0,'{A4} CAMBER STIFFNESS COEFF.       ',+2295.690D+00, 3
0,'{P0} PEAK BRAKING FRICTION COEFF.  ',+1.207100D+00, 3
0,'{P1} PEAK BRAKING FRICTION COEFF.  ',-4.194000D-04, 3
0,'{P2} PEAK BRAKING FRICTION COEFF.  ',+2.672000D-07, 3
0,'{B1} PEAK LATERAL FRICTION COEFF.  ',-9.475000D-04, 3
0,'{B2} PEAK LATERAL FRICTION COEFF.  ',+0.000000D+00, 3
0,'{B3} PEAK LATERAL FRICTION COEFF.  ',+1.469000D+00, 3
0,'{B4} PEAK LATERAL FRICTION COEFF.  ',+4.316000D-07, 3
0,'{R0} LONG. SLIP @ PEAK BRAKING     ',-0.192000D+00, 3
0,'{R1} LONG. SLIP @ PEAK BRAKING     ',+4.060000D-05, 3
0,'{S0} SLIDE COEFFICIENT OF FRICTION ',+1.212900D+00, 3
0,'{S1} SLIDE COEFFICIENT OF FRICTION ',-9.347000D-04, 3
0,'{S2} SLIDE COEFFICIENT OF FRICTION ',+4.460000D-07, 3
0,'{K1} ALIGNING MOMENT COEFFICIENT   ',-1.728000D-04, 3
0,'{K2} ALIGNING MOMENT COEFFICIENT   ',+1.551000D-04, 3
0,'{K3} ALIGNING MOMENT COEFFICIENT   ',+0.069000D+00, 3
0,'{CTN} SLOPE OF  MUX  VS. S @ S=0   ',+6.000000D+00, 3
0,'{CA1} CRITICAL CAMBER ANGLE        ',+0.523560D+00, 3
0,'{CR1} FRICTION REDUCTION @ CA1     ',+0.300000D+00, 3
0,'{OMEGT} TIRE OVERLOAD COEFF.       ',+0.900000D+00, 3
0,'{OMEGT2} TIRE OVERLOAD COEFF.      ',+0.500000D+00, 3
0,'{SN} TIRE SKID NUMBER              ',+1.000000D+00, 3
9,'=====================================',+1.111111D+11, 0
9,'========= Terrain Data ============',+1.111111D+11, 0
9,'=====================================',+1.111111D+11, 0
0,'{NTPT} NUMBER OF TERRAIN COORDS    ',+2.000000D+00, 0
0,'{NTPL} NUMBER OF TERRAIN PLANES    ',+1.000000D+00, 0
0,'{Yterr(1)} Y-COORD OF TERR. PT. 1  ',-500.0000D+00, 0
0,'{Zterr(1)} Z-COORD OF TERR. PT. 1  ',+0.000000D+00, 0
0,'{Yterr(2)} Y-COORD OF TERR. PT. 2  ',+500.0000d+00, 0
0,'{Zterr(2)} Z-COORD OF TERR. PT. 2  ',+0.000000D+00, 0
0,'{SNterr(1)} SKID # OF TERR. PL. 1  ',+85.00000D+00, 0
0,'{Jteratb(1)} TERR. ATRB. OF PL. 1  ',+0.000000D+00, 0

9,'=====================================',+1.111111D+11, 0
9,'========= Aerodynamic Data =========',+1.111111D+11, 0
0,'{RO}     Air Density               ',+0.000000D+00, 0
0,'{SAero} Aerod. Reference Area      ',+2.000000D+00, 0
0,'{HAero} Aerod. Reference Length    ',+1.500000D+00, 0
0,'{DCyDBeta_A}   Side Force Coeff.   ',+1.000000D+00, 0
0,'{DCnDBeta_A}   Yaw Moment Coeff.   ',+2.500000D+00, 0
0,'{DNDR}   Yaw Damping Moment Deriv. ',+0.000000D+00, 0
0,'{CD0}    Drag Force Coeff.         ',+0.000000D+00, 0
0,'{DCDDBeta_A} Drag Forc. Coef. Der. ',+0.000000D+00, 0
0,'{Alph0} Zero-Lift Angle            ',+0.000000D+00, 0
0,'{DCLDAlpha_A} Lift Forc. Coef. Der.',+0.000000D+00, 0
0,'{CMy0} Zero-Lift Pitch Mom. Coef.  ',+0.000000D+00, 0
0,'{DCMyDAlpha_A}Pitch Mom. Coef. Der.',+0.000000D+00, 0
0,'{AeroPar}  Reserved For Future Use ',+0.000000D+00, 0
9,'=====================================',+1.111111D+11, 0
9,'========= Wheel Steering Input =====',+0.000000D+00, 0
0,'{NWSTF}  Steering function indic.  ',+1.000000D+00, 0
0,'{NPTW}   Number of point st. data  ',+7.000000D+00, 0
0,'{TMW1}   Time point                ',+0.000000D+00, 0
0,'{TMW2}   Time point                ',+0.100000D+00, 0
0,'{TMW3}   Time point                ',+0.350000D+00, 0
0,'{TMW4}   Time point                ',+4.000000D+00, 0
0,'{TMW5}   Time point                ',+4.250000D+00, 0
0,'{TMW6}   Time point                ',+7.000000D+00, 0
0,'{TMW7}   Time point                ',+7.250000D+00, 0
0,'{DSWM1}  Wheel steer. angle        ',+0.000000D+00, 0
0,'{DSWM2}  Wheel steer. angle        ',+0.000000D+00, 0
0,'{DSWM3}  Wheel steer. angle        ',+3.250000D+00, 0
0,'{DSWM4}  Wheel steer. angle        ',+3.250000D+00, 0
0,'{DSWM5}  Wheel steer. angle        ',+1.550000D+00, 0
0,'{DSWM6}  Wheel steer. angle        ',+1.550000D+00, 0
0,'{DSWM7}  Wheel steer. angle        ',+5.100000D+00, 0
9,'=====================================',+1.111111D+11, 0
9,'====== Braking/Tracting Input =====',+0.000000D+00, 0
0,'{NBTF}   Steering function indic.  ',+0.000000D+00, 0
0,'{NPTBT}  Number of point st. data  ',+0.000000D+00, 0
0,'{TMT1}   Time point                ',+0.000000D+00, 0
0,'{TMT2}   Time point                ',+0.000000D+00, 0
0,'{AXPRIME1}  Desired accel./decel   ',+0.000000D+00, 0
0,'{AXPRIME2}  Desired accel./decel   ',+0.000000D+00, 0
```

4.4.2 Transient

Past research at VRTC has proved frequency response techniques to be quite useful for evaluating dynamic/transient simulation predictions [9, 10]. By generating vehicle output (eg. yaw rate) frequency response to handwheel angle inputs, much can be learned about the characteristics and validity of a simulation model.

Yaw rate frequency responses to road wheel angle inputs have been generated from ADVS simulation runs and to handwheel angle inputs from the experimental data for the Suzuki Samurai. Figure 20 shows the normalized simulated and experimental yaw rate frequency response magnitude curves at 50 mph, and

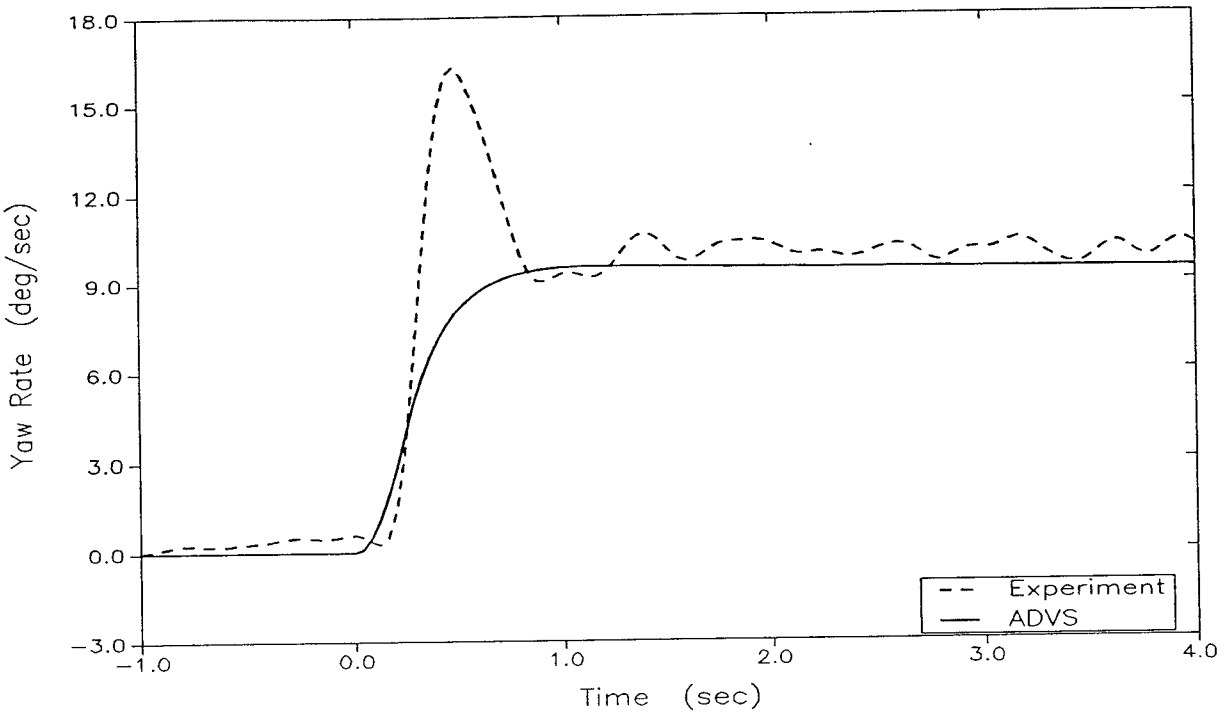

Figure 19 - Samurai Steady State Comparisons

Figure 21 shows the corresponding phase angle curves. These frequency response curves for the simulation have been generated by measuring the amplitude ratio and phase shift of the yaw rate response relative to the road wheel angle input at discrete sinusoidal frequencies.

Research at VRTC has shown that, for the purposes of evaluating a simulation, frequency response comparisons with experimental results can be performed in the vehicle's linear operating range. The experimental and simulated sinusoidal steering inputs used to generate the frequency response curves resulted in lateral acceleration levels which are believed to be in the linear regime for the vehicle. For the simulation runs used to generate the frequency response curves, frequencies of 0.1, 0.2, 0.5, 1.0, 2.0, and 5.0 hertz, and road wheel angle amplitudes of ± 0.825 degrees were used. Experimental data was generated from a sinusoidal sweep steering maneuver with a handwheel angle amplitude of approximately ± 45 degrees.

The experimental yaw rate magnitude has a peak at higher frequencies, as shown on Figure 20. Based on work done at VRTC and elsewhere, many vehicles exhibit this underdamped behavior, and have yaw rate resonance frequencies at approximately 1.0 hertz. The simulated frequency response magnitude does not exhibit this underdamped response. (This is the same result as was shown on Figure 19.) Research performed at VRTC has shown that roll steer, which is not modeled by ADVS has a significant effect

on the Samurai yaw rate damping [16]. In addition, research at the VRTC has shown that modeling tire dynamics in a simulation has a considerable influence on simulated yaw rate transient response. Tire side force lag dynamics have been shown to reduce simulated yaw rate damping [7]. The fact that ADVS does not include tire dynamics accounts for some of the discrepancy seen between the shapes of simulated and experimental magnitude curves.

Experimentally, the Samurai exhibits very little phase lag below 1.0 hertz. The phase lag then drops rapidly to near 135 degrees by 4.0 hertz. The simulation predictions, however, show a near linear increase in phase lag as a function of road wheel frequency. This apparent discrepancy indicates model deficiencies, the main one most likely being lack of tire dynamics.

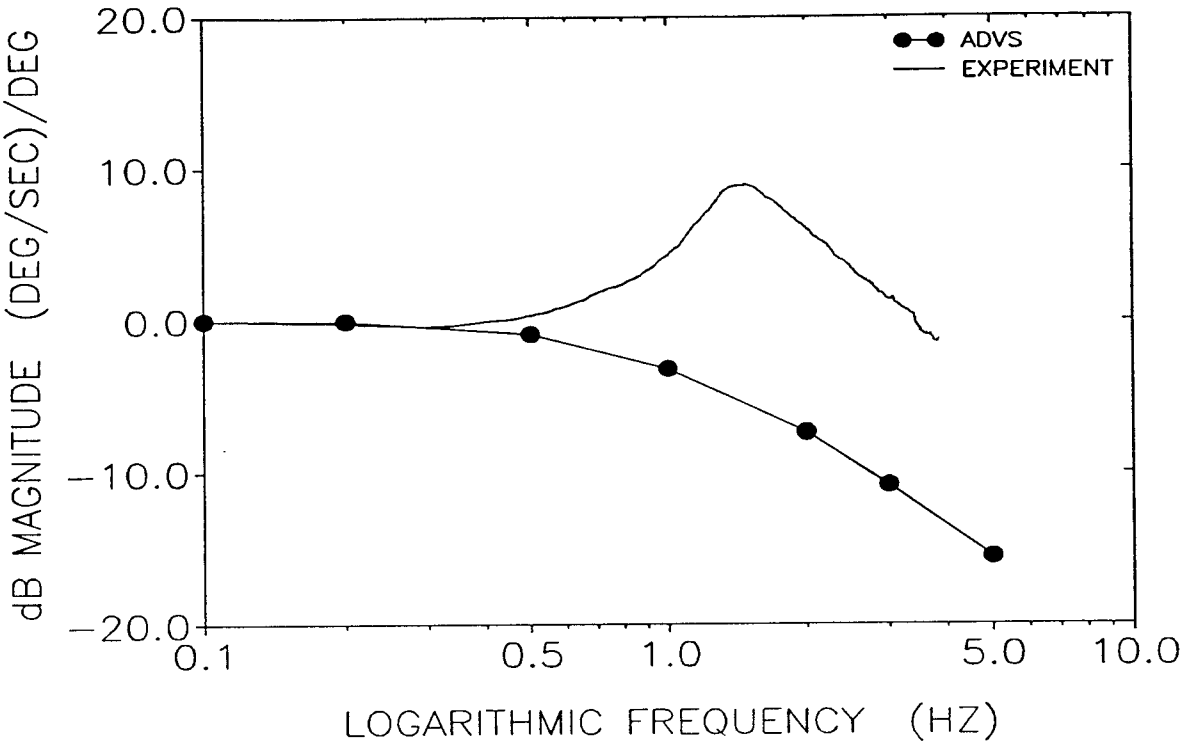

Figure 20 - Yaw Rate to Handwheel Angle Frequency Response Magnitude 50 mph Suzuki Samurai

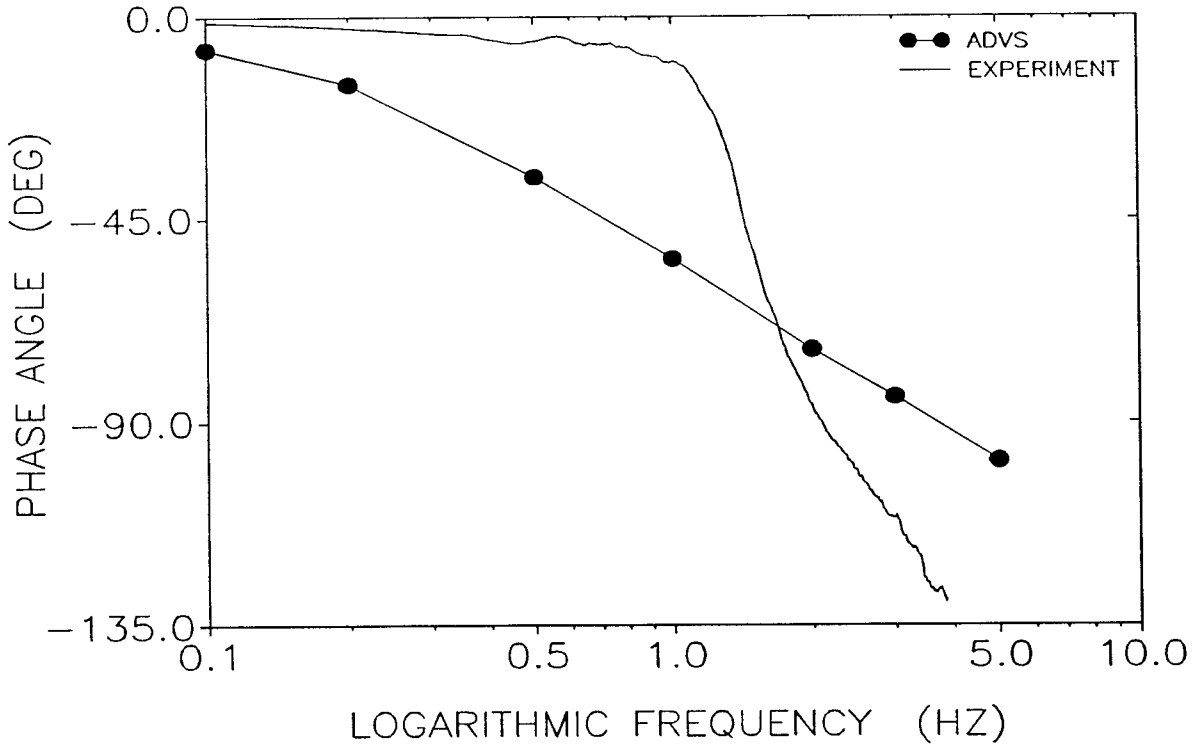

Figure 21 - Yaw Rate to Handwheel Angle Frequency Response Phase Angle 50 mph Suzuki Samurai

5.0 Introduction: VDANL

The "Vehicle Dynamics Analysis, Non-Linear" (VDANL ver. 2.33) simulation evaluated here is the latest version of the VDANL simulation developed by Systems Technology, Inc. (STI) for the NHTSA. The original VDANL simulation was developed in the mid 1980's under NHTSA contract DTNH22-85-C-07151 "Analytical Modeling of Driver Response in Crash Avoidance Maneuvering". Version 2.33 of VDANL, was developed by STI in 1989-1990 under NHTSA contract DTNH22-88-C-07384 "Vehicle Dynamic Stability and Rollover" [5].

The original version of VDANL has been extensively evaluated by the VRTC [1, 9, 10]. The evaluation compared VDANL to the "Improved Digital Simulation, Fully Comprehensive" (IDSFC) [19]. The results of that evaluation showed VDANL to give better predictions, require easier to measure vehicle parameters, and provide a better platform for future expansion than IDSFC.

Version 2.33 of VDANL represents a significant upgrade of the original model and therefore warrants a new evaluation. Several major areas have been improved. The sprung mass is now allowed all six degrees-of-freedom (the original model did not have any pitch or bounce degrees-of-freedom). This has led to a much more complete suspension model with the abandonment of the fixed roll axis concept of the original model. The new suspension model can now differentiate between independent and solid axle suspension systems.

STI has measured the vehicle parameters and conducted experimental handling tests for 12 light vehicles. To demonstrate the validity of the simulation, STI compared the VDANL predictions with the experimental data in both the time and frequency domains. The results of the comparisons, shown in Appendix H of the STI report, showed that VDANL had good correlation with the experimental data.

Figure 22 shows the general design and capabilities of VDANL. The simulation can operate in both open-loop mode, where user specified control inputs are supplied to the vehicle dynamics, or in a closed-loop mode where the driver model attempts to follow a specified path using feed back from the vehicle dynamics. VDANL contains models for vehicle steering and braking systems, an empirical tire model that accounts for tire lateral force lag, wheel spin dynamics, and the basic vehicle dynamics. The vehicle model contains a total of 17-degrees-of-freedom.

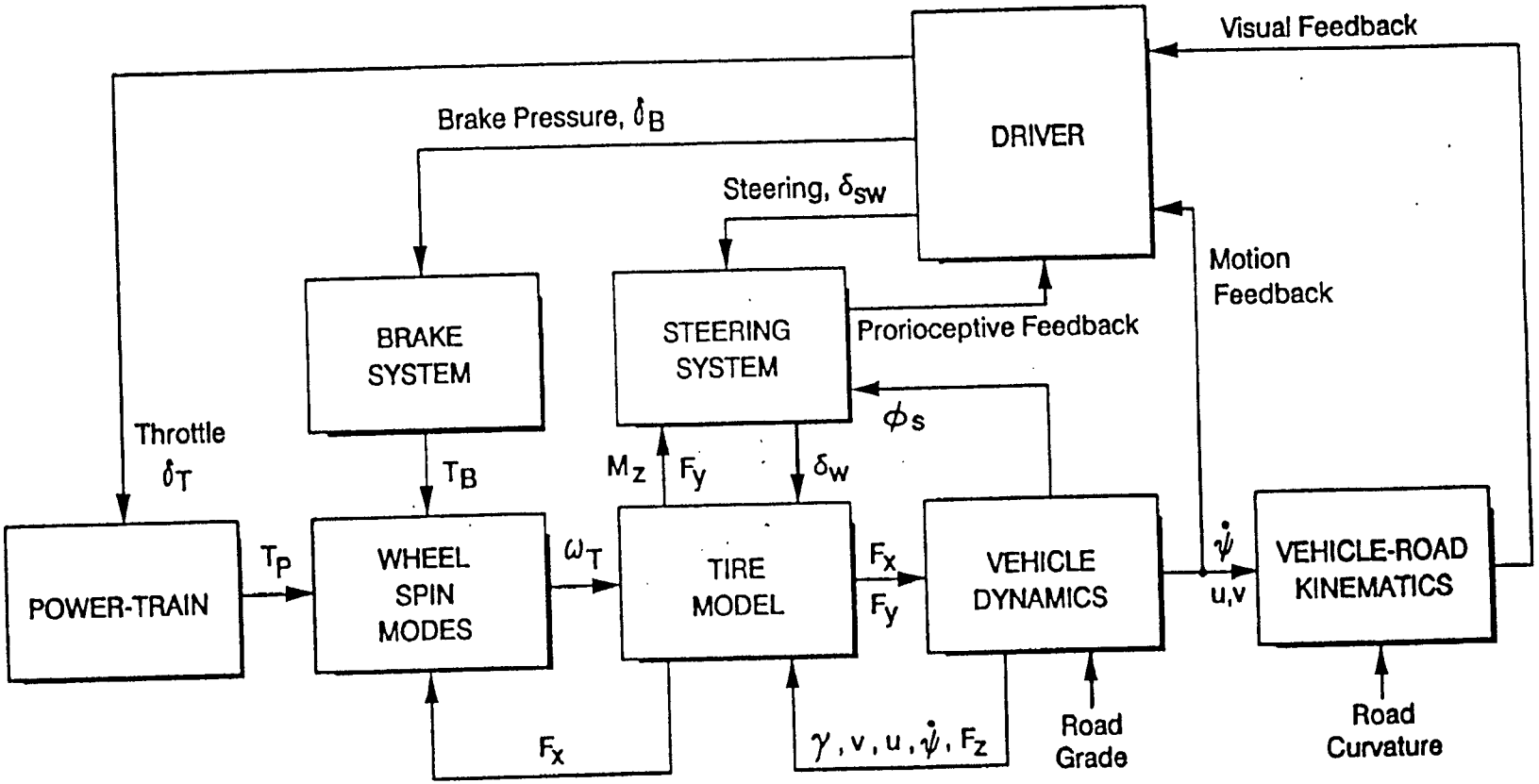

F_x, F_y, F_z = x, y, z forces from or on tire

M_z = Aligning moment from tire

ω_T = Wheel spin velocity

v, u = Vehicle side and forward velocities

δ_{sw}, δ_w = Steering and road wheel angles

ϕ_s, γ = Body roll and wheel camber angles

$\dot{\psi}$ = Vehicle yaw rate

note that tire side slip = $\alpha = f(v, u, \dot{\psi}, \delta_{sw})$

tire longitudinal slip = $S = f(\omega_T, u)$

Figure 22 - VDANL Block Diagram

5.1 Governing Equations

5.1.1 Rigid Body Dynamics

The equations developed for the VDANL simulation are formulated based on a lumped-parameter system model. Three lumped masses are included in the vehicle model. These include the vehicle sprung mass and the front and rear unsprung masses.

The approach used to generate the governing equations for this version of the VDANL is somewhat different than the approach used for previous versions of STI's VDANL simulation. This version of VDANL is not based on a fixed roll axis assumption. Instead, a composite description of wheel/suspension motions is used to determine the instantaneous location of the roll axis at the front and rear axles. Further, this version of the VDANL simulation accounts for the longitudinal pitch mode of the vehicle; thus, all motions in the longitudinal and lateral/directional dynamics are included in the simulation.

The VDANL simulation keeps the sprung and unsprung mass motions separate in the pitch, heave, lateral and roll mode equations (four degrees of freedom); while the yaw and longitudinal motion equations (two degrees of freedom) are for the total vehicle mass. As stated by STI, "This approach was taken in order to provide the simplest set of equations that would adequately account for all longitudinal and lateral/directional motions". Including the total vehicle mass in the yaw and longitudinal motion equations is fairly common for this type of simulation/model.

Figure 23 shows the vehicle axis system used for the VDANL simulation. The axis system used has ψ,y,v,a_y, and z fixed to a "sleeve" over the longitudinal body axis. The "sleeve" carries and defines the unsprung masses in the horizontal roadway plane axis system. The axis system is specified such that ψ,y,v and a_y stay level with the road plane and z remains perpendicular to road plane. The sprung mass, and unsprung masses in rollover motions, can rotate in the roll direction relative to the sleeve. This approach focuses on motions at the road surface, rather than at the sprung mass center of gravity. STI did this because all tire test data and the VDANL tire model define forces and moments acting in the horizontal roadway plane, in response to side slip angle, camber angle, and longitudinal slip relative to this horizontal roadway plane.

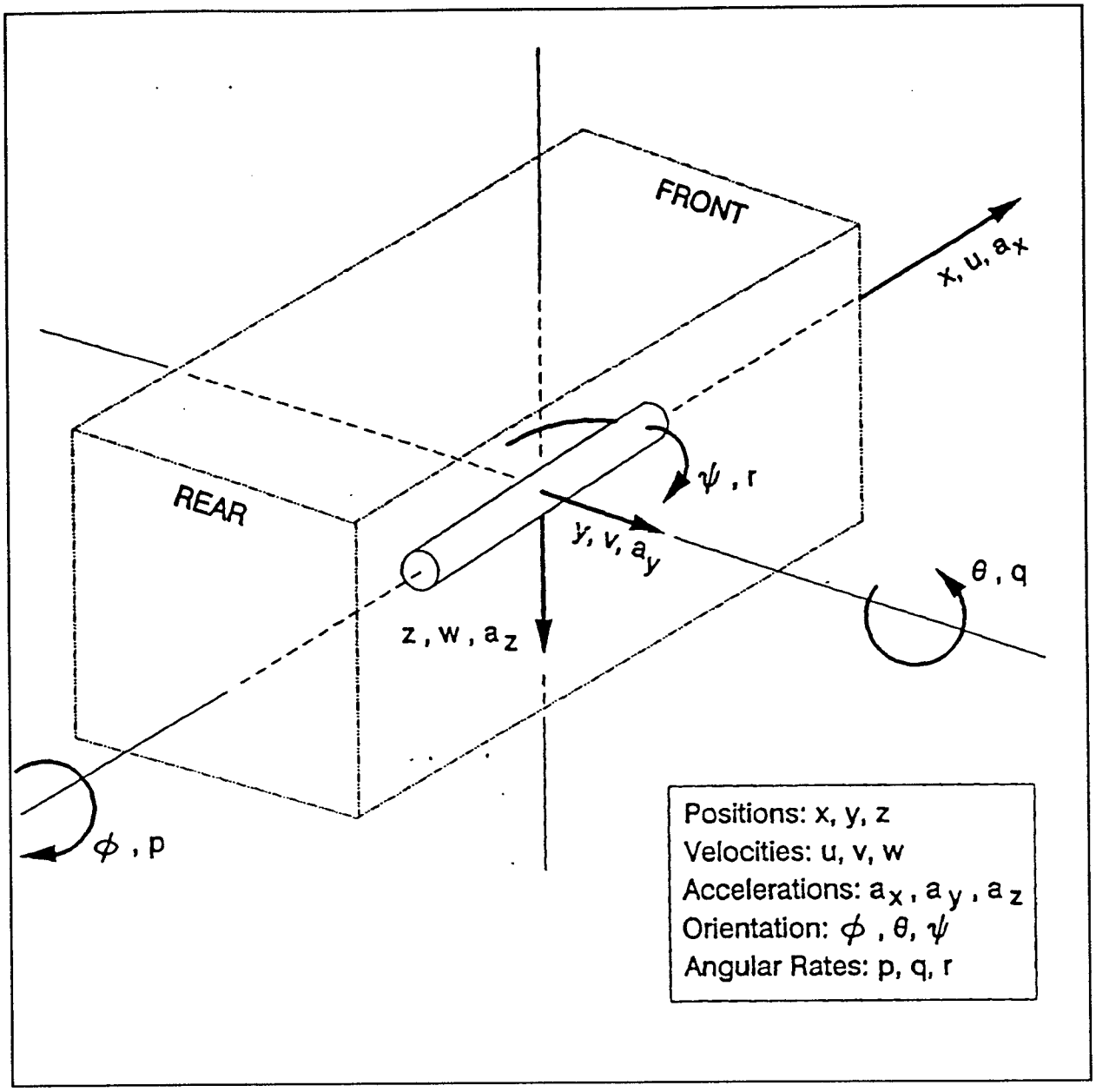

Figure 23 - Vehicle Axis System

The equations of motion for the vehicle are written with respect to the general axis system shown on Figure 23. As mentioned, the yaw and longitudinal motion equations include the entire vehicle mass. Figure 24 shows the major forces acting on the vehicle. Classical Newtonian dynamics are used to generate the equations of motion. The pitch angles are assumed to be very small. This assumption simplifies the equations of motion because classical motion variable cross product terms can be ignored as an insignificant effect.

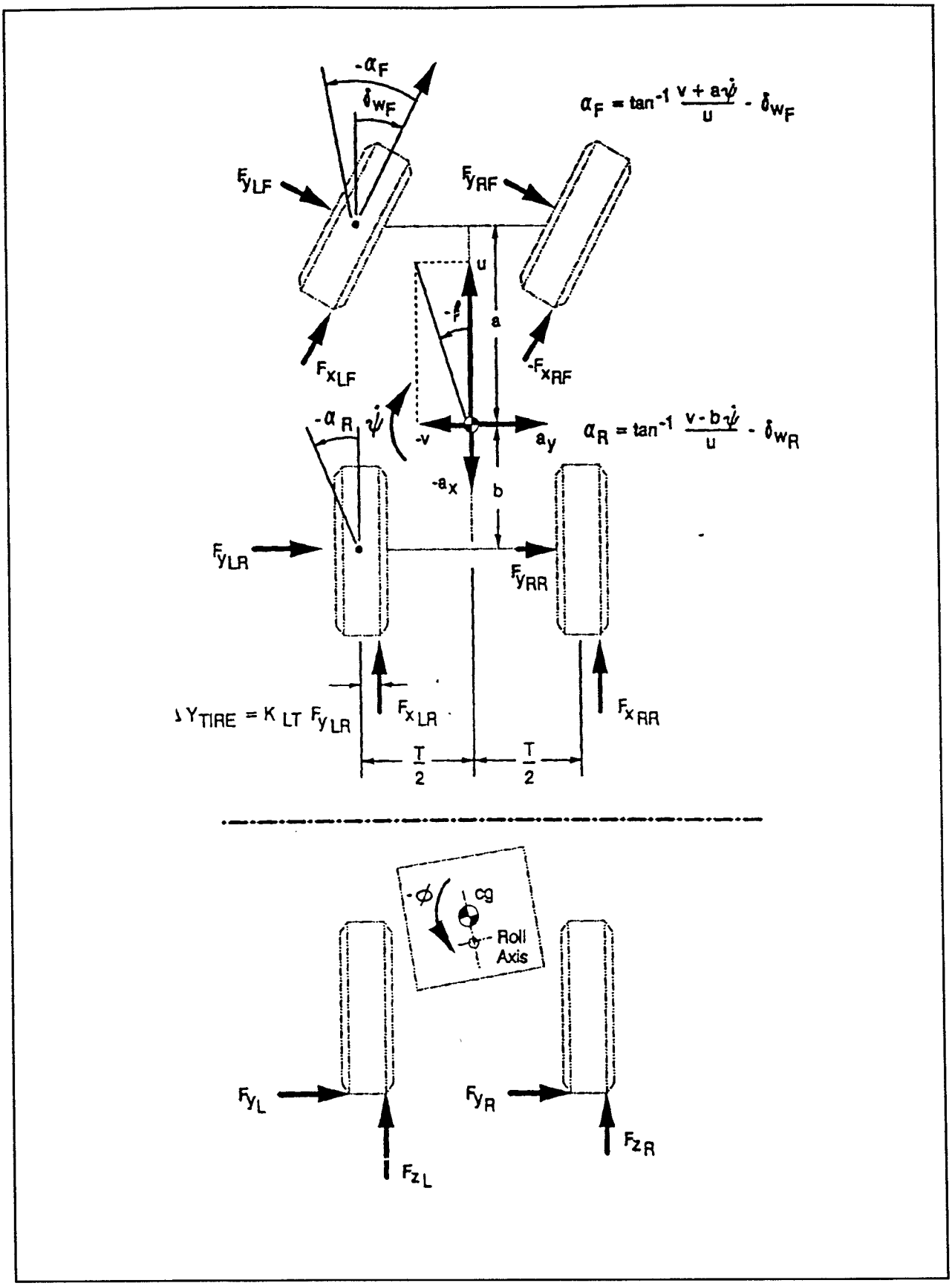

Figure 24 - Major Variables in Transient Model

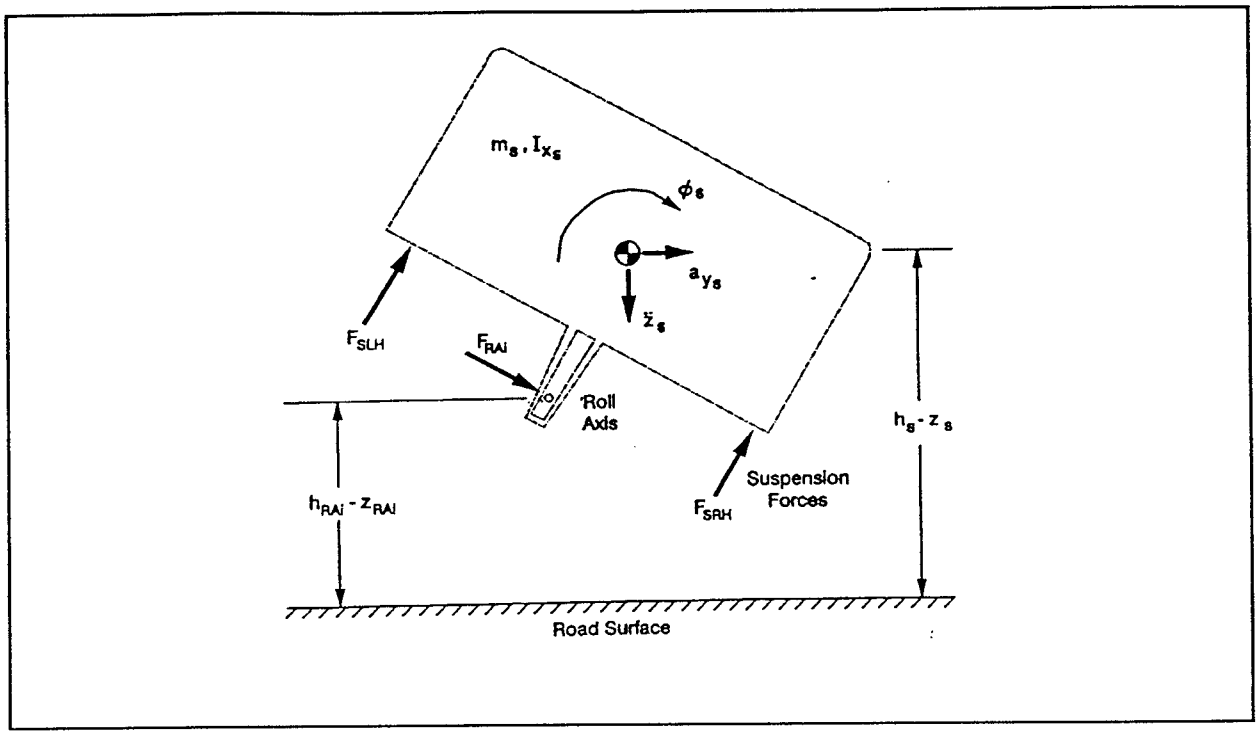

Figure 25 - Sprung Mass Free Body Diagram, End View

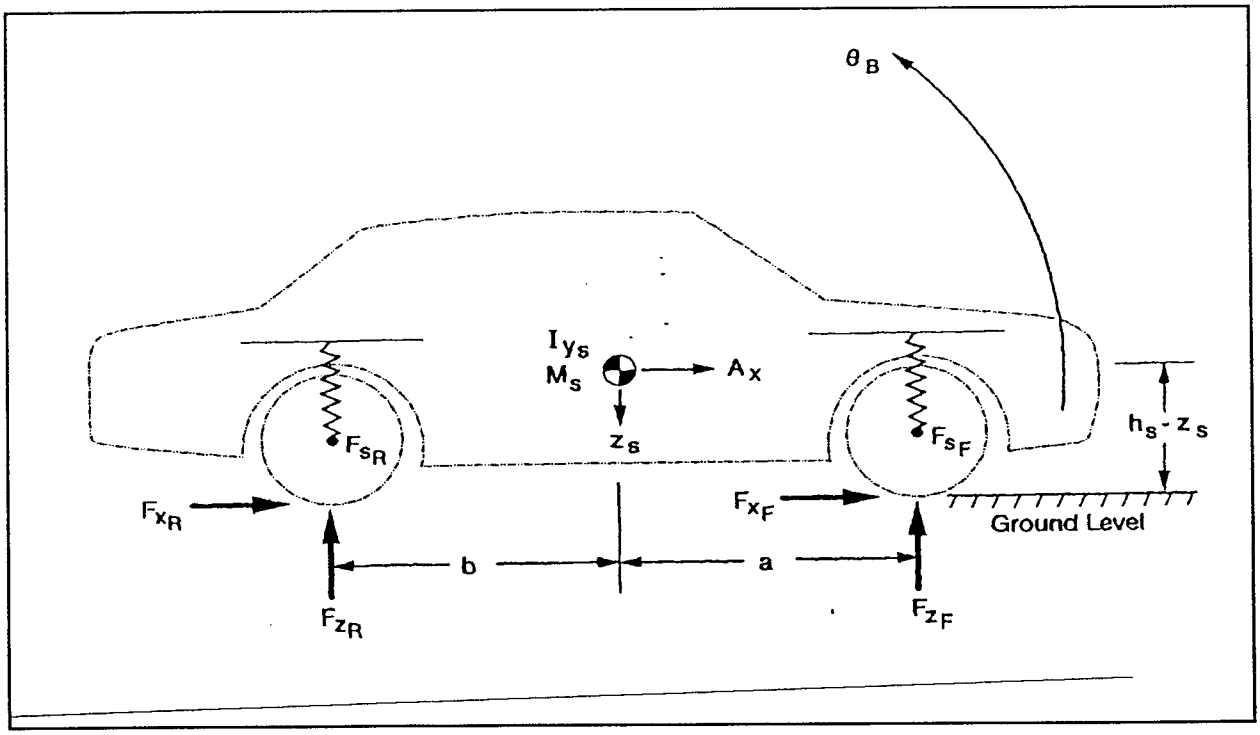

Figure 26 - Sprung Mass Free Body Diagram, Side View

The VDANL free body diagram end view of the sprung mass is shown as Figure 25. The equations for the sprung mass lateral acceleration, sprung mass roll rate, and sprung mass vertical acceleration were

developed based on Figure 25. The sprung mass pitch rate equation was developed based on the sprung mass free body diagram side view shown as Figure 26.

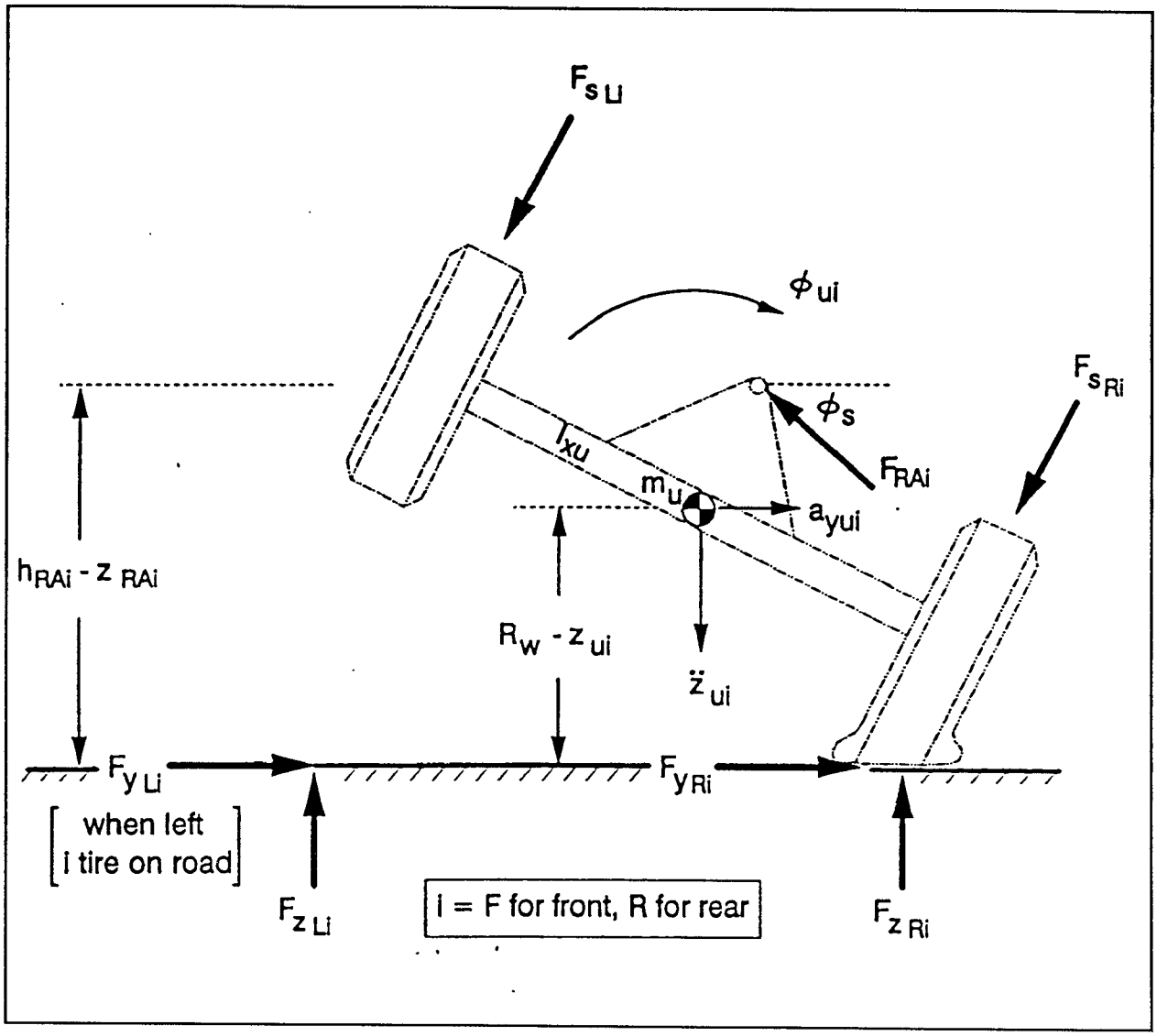

Figure 27 - Unsprung Mass Free Body Diagram

Both the front and rear unsprung masses are provided three degrees of freedom in the VDANL model. Unsprung mass roll, unsprung mass lateral acceleration and unsprung mass vertical acceleration are included in the model. Figure 27 shows the unsprung mass free body diagram used to develop the equations of motion.

The sprung and unsprung masses are acted on by inertial, suspension, and tire forces and moments. The sprung mass is also acted on by aerodynamic forces and moments. The VDANL suspension model includes spring forces, bump stop forces, and damping forces which are characterized by their influences

at the wheel locations. Other existing NHTSA simulations, namely HVOSM and its offshoots, also use this approach. Auxiliary roll stiffness is included in the suspension model. The magnitude of the auxiliary roll stiffness is a function of the roll stiffening members, such as antiroll bars, and a function of the location of the suspension vertical spring members. If the suspension vertical springs are sufficiently inboard of the wheels, then the auxiliary roll stiffness can even be a negative value. Modeling suspension vertical stiffness as being effective at the wheel locations allows for a blackbox type model, thus simplifying the parameters required to specify the suspension stiffness.

The values for damping used at the wheel locations are based on assumed roll damping ratios, and not shock absorber damping characteristics. Typically, for handling maneuvers, much of the suspension roll damping is in the form of coulomb friction. These friction forces are difficult to include into numerical simulations. Specifying an overall roll damping ratio simplifies the parameter requirements as well as the simulation code. Also, based on past work done at VRTC [1], using a specified roll damping ratio to quantify roll damping results in reasonably good roll angle predictions.

The VDANL simulation includes models of compliant pin joints between the sprung mass and unsprung masses. The model has spring and damper elements at the suspension "roll centers" acting in the direction of the sprung mass roll angle. This pin joint connectivity between the sprung and unsprung masses was included in the simulation to avoid computational instabilities as well as represent lateral compliance and damping within the suspension system.

Also included in the VDANL suspension model are suspension squat and lift forces. These forces, developed in independent suspensions systems, cause suspension jacking. Including these forces in the model more accurately represents the behavior of independent suspension than does a fixed roll center model.

This simulation contains all relevant steering/roadwheel kinematic and compliance effects. These include: wheel camber angle and wheel steer angle as a function of suspension deflection, wheel steer as affected by Ackerman steer, steering axis offset, and aligning moment and lateral force compliance steer. The VDANL steering system model also includes a model for steering system lag. Since handwheel angle is the simulation input variable, the steering system provides a single degree of freedom to the total vehicle model. (More will be said about these items in the following sections.)

Lastly, the wheel spin equations, which introduce four degrees of freedom to the simulation model, are typical of this type of simulation.

The VDANL simulation has a total of 17 degrees of freedom. As mentioned, there are six degrees of freedom associated with the sprung/total mass of the vehicle, three degrees of freedom associated with the front unsprung mass, three degrees of freedom associated with the rear unsprung mass, one steering system degree of freedom, and four wheel spin degrees of freedom.

5.1.2 Suspension Model

The VDANL suspension model contains fairly complete descriptions of vehicle kinematic and compliant suspension characteristics. In order to simplify the description of the suspension systems, all suspension motions and forces are related to the tire contact point on the road surface. This allows suspension kinematic and compliance characteristics to be described using composite functions. This type of model defines the suspension input/output relationships, and does not need information about the specific suspension design specifications. Models are included for both independent and solid axle suspension systems at each axle. Appendix A of the STI report gives a detailed derivation of the VDANL model.

Kinematics

VDANL differentiates between independent and solid axle suspensions in its kinematic modeling. Therefore, the models will be described separately starting with the independent suspension model.

VDANL uses an equivalent swing arm model to describe independent suspension systems, shown in Figure 28. Equivalent suspension springs, bump stops, and dampers are modeled as acting vertically over each tire. An auxiliary roll stiffness is also included in the suspension model.

By using the equivalent swing arm model, the classic fixed roll axis concept has been abandoned. The swing arm is defined, in the YZ plane, by the slope of the line connecting the tire contact patch to the swing arm pivot (h_p/ℓ_a in Figure 28). This is the same as the tire patch slope relative to vertical, and is the first order term for suspension jacking. To account for the effect of sprung mass vertical motion on jacking (changes in the slope of h_p/ℓ_a), the suspension vertical deflection is divided by the arc radius of the tire contact patch (L_{SAi} in Figure 29). The resultant slope is multiplied by the lateral force at the tire

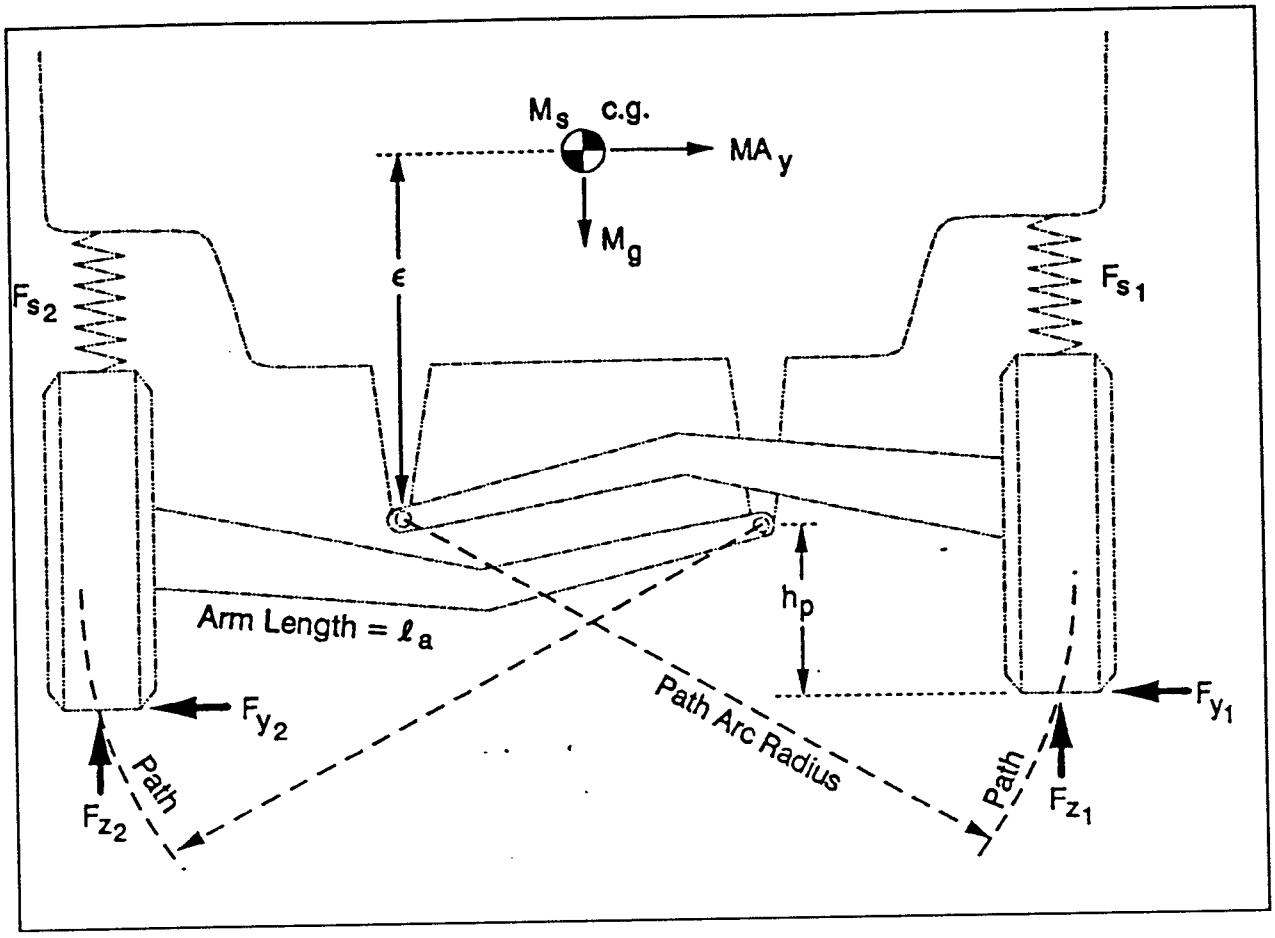

Figure 28 - Equivalent Swing Arm Model for Independent Suspensions

contact patch to give the suspension lift forces (jacking) which bypass the spring and act directly between the sprung and unsprung masses. These forces act vertically at each wheel and contribute to the vertical force acting at each tire contact patch.

Suspension squat/lift due to longitudinal tire forces is modeled in a similar manner to the suspension jacking. The slope of the tire contact patch in the XZ plane is multiplied by the longitudinal tire force to compute the squat/lift force acting at each wheel due to suspension geometry. These forces are commonly referred to as anti-squat and anti-dive forces.

Linear springs are modeled as acting vertically over each wheel. The spring stiffness is the suspension "wheel rate", which is the effective stiffness of the spring acting at the wheel in the vertical direction. Linear viscous dampers also act vertically over each wheel. The damping coefficient is the equivalent damping, in bounce. Bump stops are modeled over each wheel with linear stiffness and a specified compression suspension travel required for contact. A linear auxiliary roll stiffness is modeled to act

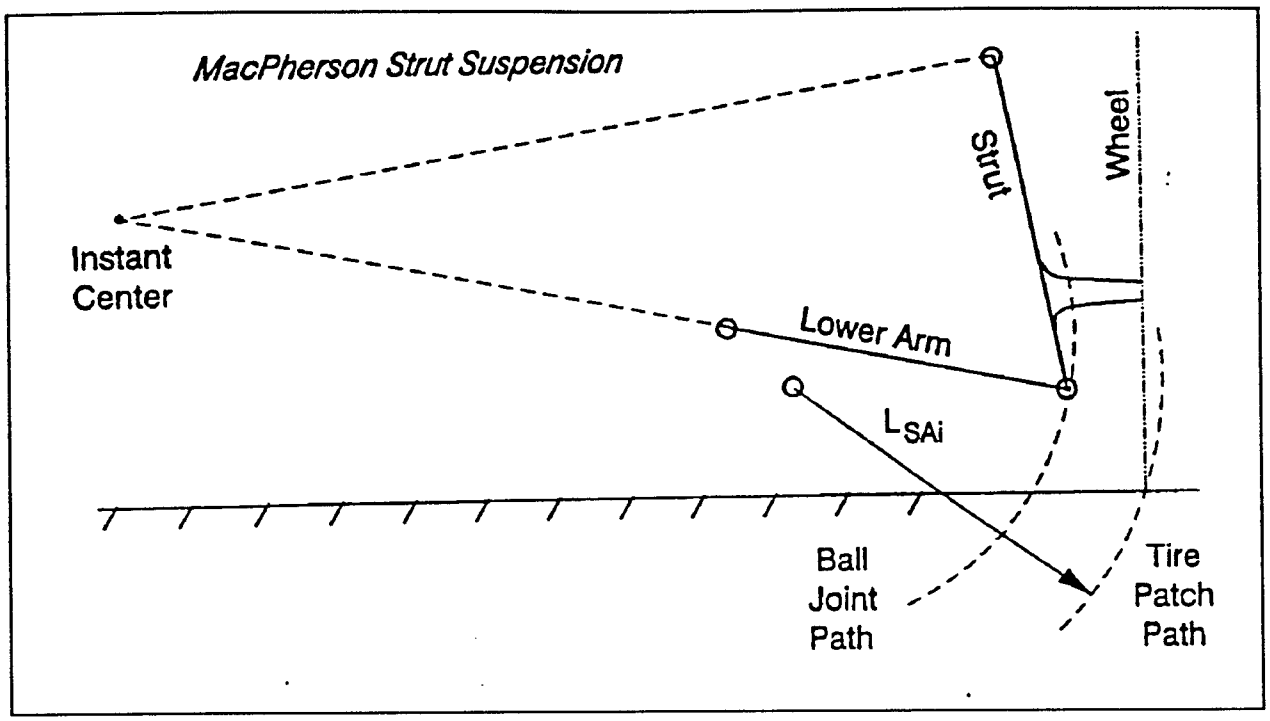

Figure 29 - Determination of Tire Patch Arc Radius

between each wheel. This term accounts for the difference between the measured total axle roll stiffness and the roll stiffness due to the suspension springs in the model.

By using linear models for the springs and dampers, VDANL attempts to account for the first order effects while maintaining simplicity. In order to study vehicle suspension systems in more detail, non-linear spring and damper models could be implemented. It is not thought that this would be a difficult task. VDANL has no model for suspension coulombic friction. In handling maneuvers, this friction force is of the same magnitude as viscous damping forces. It may become necessary to model this effect for detailed examination of vehicle suspensions.

Wheel kinematics are modeled for camber and steer relative to the sprung mass. Second order curve fit parameters of wheel camber and steer as a function of vertical suspension deflection are used to describe the wheel motions. Figure 30 shows the wheel motions used by VDANL to model the wheel kinematics, jacking forces, and squat/lift forces.

Solid axle suspensions are modeled, like the independent suspensions with linear springs, viscous dampers, and bump stops acting vertically over each wheel. An auxiliary roll stiffness produces a linear roll moment proportional to the sprung to unsprung mass roll angle. A roll center is fixed to the

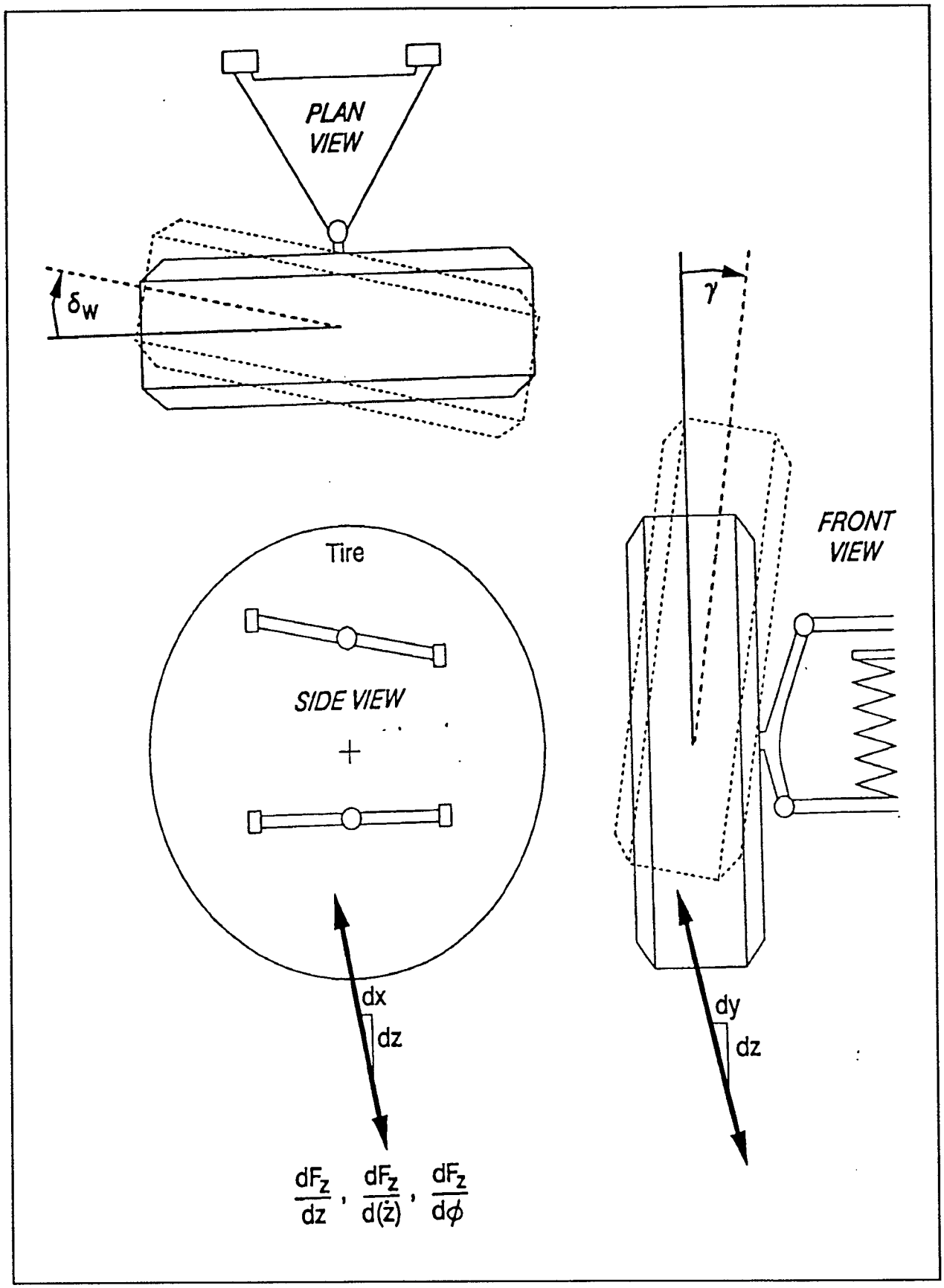

Figure 30 - Wheel Kinematics

unsprung mass that is allowed to move vertically relative to the sprung mass. The unsprung mass inertial and tire forces are transmitted to the sprung mass through a pin joint located at the roll center.

In the kinematic model, the solid axle wheel camber angles are modeled as being equal to the unsprung mass roll angle. Kinematic wheel steer angles are computed based on the angle and length of the axle longitudinal locating links (h/L in Figure 31). This allows for the inclusion of roll steer with no steer due to bounce. This is correct for non-steered axles, however, for steered axles, the wheel bounce and roll steer are influenced by the geometry of the steering linkage. For some vehicles, this can lead to large roll steer effects that will not be accounted for in the VDANL model.

If the actual roll steer is known, there are two ways to partially account for this roll steer in VDANL without modification of the model. The first is to reset h or L (Figure 31) so that roll steer equals h/L. This approach will give the correct roll steer, however, no bounce steer will be included. The second approach is to use the bounce steer curve fit parameters from the independent suspension model. The linear bounce steer coefficient can be set to the roll steer coefficient (deg/deg) divided by the half track width. This will produce the correct roll steer, but also give bounce steer with the wheels steering in opposite directions (both toe in or toe out) due to bounce, which may not be the case for solid axles. For lateral vehicle dynamic studies, the roll mode is much more important than the bounce mode and the steer parameters can be set to give correct predictions in the roll mode with out seriously effecting the model predictions. However, for a complete kinematic description, such as required for simulating a vehicle on a rough road, a more complete model is required.

Compliance

The suspension compliance model uses composite compliances due to road forces and moments at the tire contact patch. The model does not differentiate between independent and solid axles. The compliances modeled are road wheel steer due to tire lateral, longitudinal, and aligning moments, lateral tire deflection due to lateral tire forces, and the lateral deflection of the sprung mass relative to the unsprung mass.

At each road wheel, a compliance is modeled defining the change in road wheel steer angle due to the total moment about the tire's Z-axis. The tire moment is the sum of the tire aligning moment (from the tire model) and the moment caused by the longitudinal tire force acting about the suspension steering axis (kingpin axis). There is also a road wheel steer compliance modeled due to lateral tire forces.

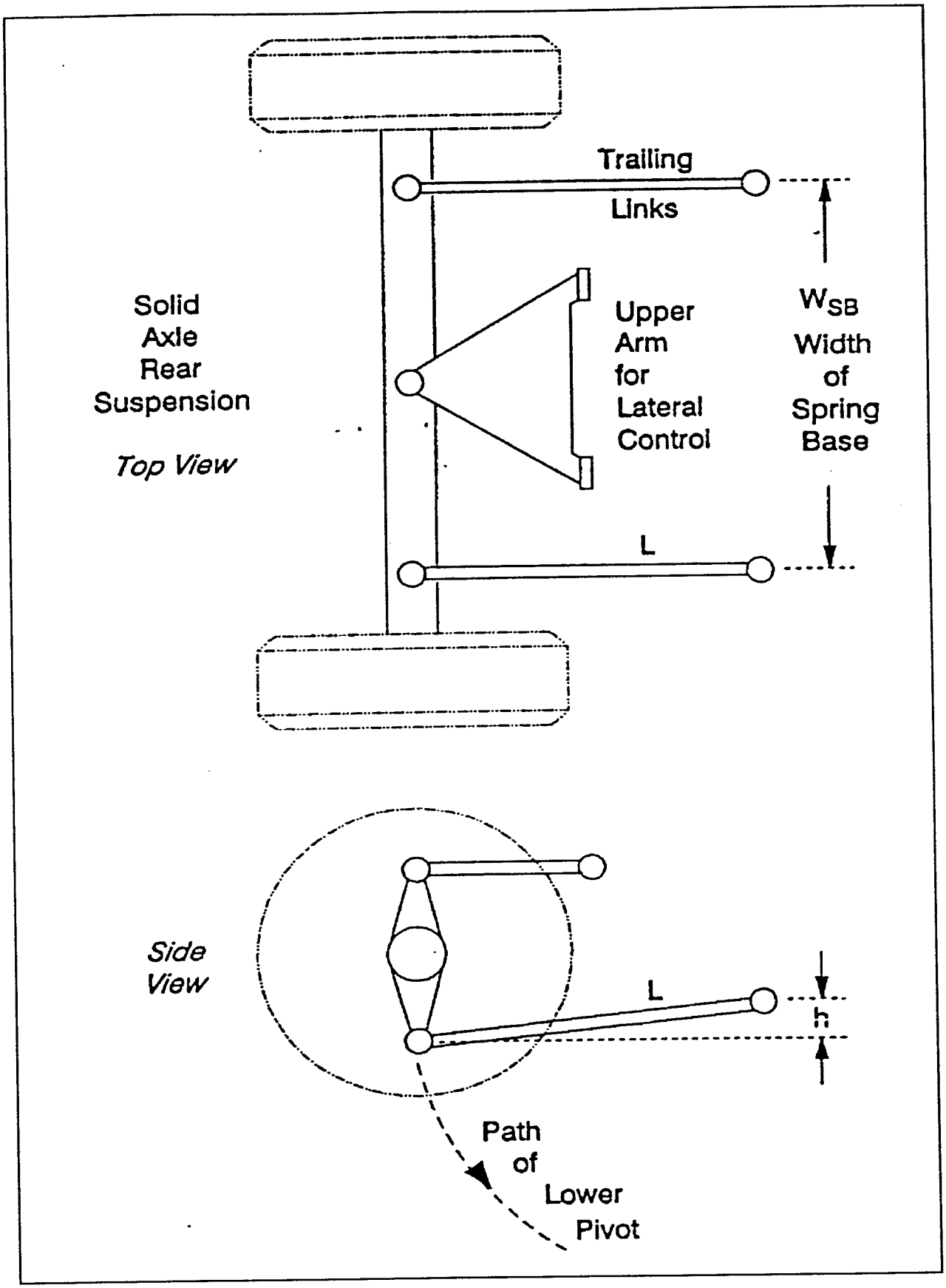

Figure 31 - Solid Axle Kinematics

Tire contact patch lateral compliance is modeled due to lateral tire forces. This parameter defines the total lateral motion of the tire contact point relative to the suspension "roll center" (for independent suspensions, this is set at ground level). This is a composite parameter that includes tire carcass compliance, wheel and suspension bending, and suspension bushing compliance. Lateral deflections of the tire contact patch cause a reduction of the effective vehicle half-track width, and therefore is an important suspension characteristic to model accurately.

The final compliance modeled in VDANL is a spring and viscous damper modeled as acting laterally between the vehicle "roll center" and the sprung mass. The main reason for this parameter is to avoid numerical instabilities in the model solution. However, this can be thought of as an auxiliary compliance, acting in series with the tire contact patch lateral compliance, between the sprung mass and the tire contact patch. When determining the parameters for a vehicle, it is important to take the effect of this compliance into account when computing the value for the tire contact patch lateral compliance.

5.1.3 Steering System Model

The steering system model in VDANL includes steering system gain, compliance, ackerman steering effects, and second order lag dynamics. Handwheel angle is used as its control input.

The steering system gain is modeled as a linear gain between the handwheel and the road wheels. The compliance model assumes a single spring steering model with no interaction between the roadwheels. Research has shown that power steering effects on steering system compliance cannot be accounted for properly using a single spring model [1]. Power steering systems modify the effective steering column compliance as measured at the roadwheels. However, the compliance present in the steering system linkage between the steering box or rack and the roadwheels is unaffected by power steering systems.

Ackerman steering effects are included in the VDANL steering model. This allows each front wheel to steer different amounts due to vehicle steering system geometry. Many vehicles are designed to have the inside wheel steer more than the outside wheel in a corner. This is done primarily for low speed operation when the steer angles and path curvatures are high.

VDANL uses a second order lag in the steering system to model the inertial effects of the wheel inertia about its steer axis acting on the steering system compliances. The natural frequency and damping ratio are defined by Equation (9).

$$\omega_n = \frac{1}{\sqrt{2 \cdot I_W \cdot K_{SCF}}} \qquad \zeta = C_V \sqrt{\frac{K_{SCF}}{8 \cdot I_W}} \tag{9}$$

where:
ω_n = *steering system natural frequency*
ζ = *steering system damping ratio*
I_W = *road wheel inertia*
K_{SCF} = *steering system compliance*
C_V = *steering system damping*

STI uses natural frequencies in the range of 6 to 15 hertz with typical damping ratios of 0.5. This will give the steering system a fairly flat frequency response in the range of handwheel frequencies seen during handling maneuvers. Therefore, only a small influence should be seen on the vehicle's transient response predictions.

A steering system characteristic not included in VDANL is steering system freeplay. Some light vehicles, especially pickup trucks and utility vehicles, can have a large amount of steering system freeplay (up to ± 8 degrees at the handwheel). Research has shown that freeplay has a large influence on vehicle steady state and transient behavior [1].

5.1.4 Braking Model

The VDANL braking system uses a fixed brake point proportioning valve, front brake effectiveness, vacuum brake boost with limiting, and a simple anti-lock module. Brake pedal force is used as the command input. The model uses a brake pedal gain, along with the vacuum booster, to convert brake pedal force to front brake line pressure. This front brake line pressure is multiplied by the front brake effectiveness to compute the brake torque at each front wheel. The rear brake torque is computed the same way except the pressure is first reduced by the proportioning valve. The proportioning valve coefficients are based on the ratio of the front to rear braking forces at the contact patch to give the system composite proportioning.

A simple antilock module is included to prevent wheel lockup. This module can be applied to the front, rear, or both axles. The algorithm controls brake torque to each wheel to keep the slip ratio below a user defined limit. A gain term is included to control the response of the system.

No model is included to account for load sensing proportioning valves. These are common and could be modeled. The anti-lock module acts independently at each wheel and therefore can only simulate 4 channel systems. Extensions of the model to include other common control strategies (3 channel, select low, etc.) would be a useful addition.

5.1.5 Drivetrain Model

The drivetrain model in VDANL allows front, rear, or four wheel drive vehicles to be run in either free rolling or speed control modes. In the speed control mode, the simulation reads the desired speed from an input file, then set the vehicle longitudinal velocity to this value.

STI has developed a fairly complete drivetrain model (2 and 4 wheel drive, automatic and manual transmissions, various types of differentials). While incorporated into version 2.33 of the VDANL simulation, this module was not developed as part of the NHTSA contract. Drive train models will be required in the future to support research for the NADS and IVHS. The model developed by STI may provide a good bases on which to develop future NHTSA drivetrain models.

5.1.6 Tire Model

Quasi-Static

The VDANL simulation tire model is an empirical model which uses some Calspan based empirical relationships to define tire parameter variations with load. This tire model represents the nonlinear characteristics for all of the most important tire relationships; for example, longitudinal force versus slip, side force versus slip angle, etc. For this tire model, equations for longitudinal, lateral, and vertical force, and aligning torque are given in terms of various computed coefficients which are functions of tire vertical load, slip angle, longitudinal slip ratio, and camber angle.

The VDANL tire model, instead of using a friction ellipse to handle combined braking and cornering, computes a composite slip variable from the longitudinal slip ratio and the lateral slip angle. This is input

into a force saturation function, which gives the rolloff of lateral tire force with increasing longitudinal force. The composite slip and force saturation functions were developed based on models of tire contact patch pressure distribution and integrated composite forces. Tire width, tire pressure, tire design load, and tire/road coefficient of friction are used in the model to determine tire contact area and scaling factors for the composite slip function. Based on preliminary research done at VRTC, this composite slip function model represents measured tire characteristics, both initial slopes and overall curve shapes, slightly better than the standard Calspan model.

STI has made other modifications to the standard Calspan tire model in attempts to improve the performance of the model. In particular, the VDANL tire model for tire slip to slide transition is better than the Calspan model. A separate tire model module was supplied with the previous version of the VDANL simulation. This computer program contains only the VDANL tire model and can be used to study tire characteristics and improve tire model performance by adjusting coefficients to make the model better match measured tire responses.

In all, the tire model requires 16 parameters, 10 based on Calspan measurements. The VDANL tire model differs in several ways from a standard Calspan tire model. Based on the authors experience, the VDANL tire model appears to offer several improvements over other tire models for modeling tire quasi-static forces and moments. A detailed evaluation of the tire model would require comparison with experimental results. This is beyond the scope of this study. However, a more detailed evaluation of existing tire models is forthcoming at the VRTC. Current plans are to include this tire model in the proposed study. Several attributes of the VDANL tire model are unique and may warrant inclusion in an improved tire model.

Dynamic

VDANL models tire transient characteristics by applying a second order lag to the tire side force. The lag is implemented to be a function of the tire characteristic rolling distance. Including tire side force dynamics has been shown [1, 7] to be critical for accurately simulating vehicle transient responses.

The second order lag is applied to the tire side force output from the quasi-static tire model. The model requires a constant (K_{TL}), which is related to the natural path frequency (ω_{path}) of the tire as follows:

$$\omega_{path} = \frac{U}{(K_{TL} \cdot R_R)} \qquad (rad / ft)$$

where: (10)

U = *vehicle speed*
R_R = *tire rolling radius*

The lagged tire side force is then given by:

$$F_{TyL} = \frac{F_{Ty}}{(T_L \cdot S + 1)^2}$$

where: (11)
F_{Ty} = *quasi-static tire side force*
F_{TyL} = *lagged tire side force*
$T_L = \frac{1}{\omega_{path}}$

This equation models the tire side force lag as a critically damped second order system. Research has shown that passenger car tires exhibit under damped responses at high speeds, above approximately 40 mph (20). A more accurate representation of the tire lag can therefore be made by allowing the damping ratio of the lag to be specified.

The fact that the VDANL tire lag damping characteristics are not vehicle speed dependent, and the fact that the tire lag is applied to the tire output (side force), and not the tire model input (slip angle), are two areas where the VDANL tire dynamics model differ from the model currently used at VRTC. These differences, for the most part, represent subtle differences in predicted transient vehicle response. However, further research planned by VRTC, which includes experimental measurements of dynamic tire response characteristics, should prove useful in developing better models for tire dynamics. Additionally, side force is the only tire characteristic for which the dynamic response has been modeled in VDANL; and it has been shown that tire aligning moment also exhibits dynamic characteristics [21]. This is an area where future expansion of the model is warranted.

The VDANL tire dynamics model does include a low speed term in the second-order system representation. Details of this low speed correction are provided in the VDANL documentation [5]. This modification prevents the modeled tire natural frequency from going to zero as vehicle speed goes to zero. This modification will be incorporated into the tire dynamics model used at VRTC.

5.1.7 Driver Model

Both open and closed-loop driver models are incorporated in VDANL. The open-loop model will be described first, followed by the closed-loop model.

The open-loop drive mode allows user supplied script files to be read containing any combination front and rear steer inputs, brake pedal force, road curvature, throttle position, and desired forward velocity. Each file is an ASCII file containing time/input pairs. VDANL performs a linear interpolation between the script file time increments to map the control input. The length of the input files is only limited by the length of the simulation run. The point spacing can be as small as the integration time step, or as long as the entire run. This type of input file structure makes it convenient to compare the simulation predictions to experimental data, by writing the experimental handwheel angle and brake pedal force to script files and using these files as the control input for the simulation run.

VDANL also contains a closed-loop driver model. This model is capable of supplying steering inputs to keep the vehicle on a desired path, throttle inputs to control the vehicle's longitudinal velocity, and brake pedal force input to achieve a desired longitudinal deceleration. The control laws used in this driver model are described in detail in [22].

5.1.8 Aerodynamic Model

The aerodynamic model in VDANL computes the aerodynamic longitudinal and lateral forces, and the aerodynamic roll and yaw moments acting on the sprung mass due to longitudinal and lateral vehicle velocity and lateral wind gusts. The model uses simple linear coefficients taken at a reference aerodynamic velocity to compute the aerodynamic forces. No affects of changes in vehicle attitude are included in the model.

The lateral aerodynamic force and the aerodynamic moments are computed using the general Equation:
Longitudinal aerodynamic drag is computed by:

$$AERO_{DRAG} = 0.5 \cdot \rho \cdot U^2 \cdot A_{REF} \cdot CDX$$

where:
ρ = *air density*
U = *longitudinal vehicle velocity*
A_{REF} = *aerodynamic reference area*
CDX = *coefficient of drag*

(13)

$$AERO_{FORCE/MOMENT} = \frac{U}{U_{REF}} \cdot AERO_{COEFF} \cdot (V + V_{AERO}) \quad (12)$$

where:
U = *longitudinal vehicle velocity*
U_{REF} = *reference aerodynamic velocity*
$AERO_{COEFF}$ = *aerodynamic coefficient*
V = *lateral vehicle velocity*
V_{AERO} = *lateral wind velocity*

5.1.9 Solution Method

The sprung mass, unsprung mass, and steering system motions are described by a total of thirteen second-order nonlinear differential equations; six for the sprung mass, three each for the front and rear unsprung masses, and one for the steering system. As is usual for this type of simulation, with the accelerations specified, numerical integration is used to solve for the velocity and displacement components of each of the degrees-of-freedom. The VDANL simulation uses Euler method of numerical integration. This method is self-starting and produces quite stable results for physically realistic simulation inputs.

The VDANL simulation differential equations are not independent of one another. Unlike many of the simulations of this type, the VDANL numerical solution method does not involve inverting a coupled system mass matrix, formed from the system equations of motion, in order to determine an acceleration vector. Instead, the VDANL simulation numerically integrates each equation of motion separately. That is, the velocity and displacement associated with each degree of freedom acceleration are computed at each time step using the Euler integration method. Since the coupled equations are solved separately, the order of solution is important. STI has studied solving the system equations in various sequences, and determined a suitable order in which to solve the equations. In general, the overall VDANL solution technique works well.

Integrating the wheel spin equations is a problem from a numerical integration stability perspective. Methods have been devised to cope with the highly nonlinear longitudinal tire force characteristics which arise during the simulation of braking maneuvers. VDANL uses a method similar to that discussed by Bernard [23]. This method involves using a Taylor series expansion of terms in the tire longitudinal force equation, to generate a perturbation equation to describe the wheel spin moment equations in a numerically solvable form. This process, along with some additional logic, allows for the wheel spin

equations to be solved using the Euler integration method. The performance of this method has been found to be quite good. Also, for severe braking, where the wheel slip is in the highly nonlinear region, the VDANL simulation has a provision that allows the spin mode to be iterated several times within a simulation time step. For heavy braking, four iterations of the wheel spin equations per simulation time step have been found to be satisfactory for a simulation time step of 0.005 seconds.

The simulation integration time step used for the VDANL simulation was 0.005 seconds. Larger time steps, up to 0.01 seconds, were used without any noticeable changes in simulation performance. Using an integration step size of 0.005 seconds, and a 25 Mhz IBM Model 80 386 personal computer with a math co-processor, a 5 second simulation run requires about 22 seconds of computer run time. For braking runs, where the additional iterations of the wheel spin equations are required, a 5 second simulation run requires about 60 seconds of computer run time. Using smaller integrator step sizes increases the simulation run time, while larger step sizes reduce integrator accuracy and may result in numerical stability problems.

5.1.10 Miscellaneous

In order to avoid simulation startup transients, VDANL simulation provides a routine to determine initial load conditions on the tires and suspension. This routine finds the initial tire and suspension loads based on the vehicle static weight conditions.

5.2 Parameter Measurement

The vehicle and suspension parameters required by VDANL are described in the 1991 STI report [5]. The tire parameters are described in the original STI report on VDANL [22]. Appendices B, C, and D of the 1991 STI report contain a fairly complete description of the parameter measurement and estimation procedures used by STI for VDANL. This section of the report will describe the parameters, review the test methods needed, and assess the effort required for the VRTC to measure/obtain them.

5.2.1 Required Parameters

The vehicle and suspension parameters required by VDANL are listed in Table XII, Table XIII, and Table XIV. The tire parameters are shown in Table XV.

Table XII - VDANL Parameter List

PARAMETERS

i = F, or R ij = LF, RF, LR, RR

PARAMETERS	SOURCE CODE MNEMONIC	UNITS	DEFINITION
a	LENA	ft	X distance from M_s c.g. to front axle
A	REFAREA	ft^2	Frontal area of vehicle, used for longitudinal drag
b	LENB	ft	X distance from M_s c.g. to rear axle
B_i	BF, BR	1/ft	First order coefficient for change in wheel steer angle with suspension deflection
C_i	CF, CR	$1/ft^2$	Second order coefficient for wheel steer with suspension deflection
Cd	CDX		Longitudinal drag coefficient
D_i	DF, DR	1/ft	First order coefficient for change in wheel camber angle, with suspension deflection
E_i	EF, ER	$1/ft^2$	Second order coefficient for wheel camber angle with suspension deflection
F_{sijo}		lbs	Static load on suspension spring at each wheel (computed in program)
F_{zio}		lbs	Static load on each tire (computed in program).
g		ft/sec^2	Gravity = 32.16 ft./sec.^{2}
h_{BS}	HBS	ft	Equivalent suspension clearance to bump stop at each wheel
h_i	HF, HR	ft	L_i times slope of trailing link in trailing arm suspension
h_{cg}	HCG	ft	c.g. height of total mass
h_{RAi}	HRAF, HRAR	ft	Height of roll axis above ground
h_s	HS	ft	M_s c.g. height above ground
I_{ϕ_s}	IXS	lb ft sec^2	Moment of inertia for sprung mass in roll
I_{xz_s}	IXZ	lb ft sec^2	Cross product of inertia for sprung mass about X-Z axis
I_{ui}	IXUF, IXUR	lb ft sec^2	M. of I. for unsprung mass about X axis

Table XIII - VDANL Parameter List

PARAMETERS (CONTINUED)

i = F, or R ij = LF, RF, LR, RR

PARAMETERS	SOURCE CODE MNEMONIC	UNITS	DEFINITION
I_{y_s}	IYS	lb ft sec^2	M. of I. for sprung mass about y axis
I_{y_w}	IYW	lb ft sec^2	Wheel inertia about spin axis
I_z	IZZ	lb ft sec^2	M. of I. for entire mass about Z axis
K_{ack}	KACK	ft/ft	Ackerman steer coefficient
K_{BS}	KBS	$\frac{lbs}{ft}$	Bump stop spring rate equivalent at each wheel
K_{ci}	KCF	$\frac{rad}{lb}$	Lateral force steering compliance for suspension and steer linkage
K_{LAGV}	KLAGV	rad/sec	Tire side force lag modifier for low speed operation
K_{LT}	KLT	ft/lb	Lateral compliance rate, of tire, wheel, and suspension, per tire
K_{RAD}	KRADP	$\frac{lb/sec}{ft}$	Damping rate at compliant pin joint between M_s and M_u
K_{RAS}	KRAS	lbs/ft	Lateral spring rate at compliant pin joint between M_s and M_u
K_{SAi}	KSAF, KSAR		= 1.0 for solid axle, = 0.0 for independent suspension
K_{SADi}	KSADF, KSADR	ft/ft	Anti dive coefficient, or slope in side view of an equivalent single suspension arm
K_{SAD2i}	KSAD2F, KSAD2R	ft/ft	Special case for K_{SADi} when there is positive F_x with independent suspension
K_{Si}	KSF, KSR	$\frac{lbs}{ft}$	suspension spring rate equivalent at each wheel
K_{SCi}	KSCF, KSCB	$\frac{rad}{ft\ lb}$	Steering compliance for steering gear
K_{SDi}	KSDF, KSDR	$\frac{lb\ sec}{ft}$	Suspension damping rate equivalent at each wheel

Table XIV - VDANL Parameter List

PARAMETERS (CONCLUDED)

i - F, or R ij - LF, RF, LR, RR

PARAMETERS	SOURCE CODE MNEMONIC	UNITS	DEFINITION
K_{SLi}	KSLF, KSLR	ft/ft	Lateral slope of an equivalent single suspension arm, at curb load
K_{STR}	KSTR	rad/rad	Overall steering ratio
K_{TL}	KTL	ft	Tire lag, expressed in rolling distance
K_{ZT}	TSPRINGR	$\frac{lbs}{ft}$	Vertical spring rate of tire
K_{TSi}	KTSF, KTSR	$\frac{ft\ lb}{radian}$	Auxiliary torsional roll stiffness per axle, (normally negative)
ℓ		ft	Wheelbase = a + b
L_i	LF, LR	ft	Length of trailing link, in a trailing arm suspension
L_{SAi}	LSAF, LSAR	ft	Length of the K_{SLi} arm
L_{so}	LSO	ft	Lateral steering axis offset from king pin to tire patch center
m	MASS	$\frac{lb\ sec^2}{ft}$	Total vehicle mass
m_s	SMASS	$\frac{lb\ sec^2}{ft}$	Sprung mass
m_{ui}	UMASSF, UMASSR	$\frac{lb\ sec^2}{ft}$	Front, or rear, unsprung mass
R_W		ft	Effective wheel/tire radius, and same as c.g. height of M_{ui}
T_i	TRWF, TRWB	ft	Track width
ω_{n_s}	SWW	rad/sec	Natural frequency for second order steering system lag
ζ_s	SWZ		Damping ratio for steering system lag
z_{sio}		ft	Initial static deflection of suspension spring at each wheel (computed in program)
z_{uio}		ft	Initial static deflection of each tire (and m_{ui}), (computed in program)

Table XV - VDANL Tire Parameters

TABLE B-1. TIRE PARAMETER FILE INPUT VARIABLES

MATHEMATICAL SYMBOLS	PROGRAM VARIABLE INPUT NAME	DEFINITION
T_w	TWIDTH	Width of the tire tread; inches
K_{A0} K_{A1} K_{A2}	KA0 KA1 KA2	Calspan coefficients for defining Y_{∞} vs. F_z
K_{A3} K_{A4}	KA3 KA4	Calspan coefficients for defining $Y_{\gamma o}$ vs. F_z
K_a	KA	Coefficient of elongation of the tire patch length due to braking or accceleration
$K\mu$	KMU	Coefficient of decay in μ with increasing tire slip
T_p	TPRES	Cold pressure in the tire; lbs/in^2
K_{B1} K_{B3} K_{B4}	KB1 KB3 KB4	Calspan coefficients for defining the peak lateral force coefficient
K_{RAD}	KRAD	No longer used; see TIRE$ below
$\frac{CS}{F_z}$	CSFZ	Calspan coefficient for defining $\left.\frac{\partial F_x}{\partial s}\right\|_{s=0}$ (Normalized with F_z)
μ_{nom}	MUNOM	Surface coefficient of friction
F_{ZT}	FZTRL	100% design load for tire at given TPRES
K_1	KK1	Calspan coefficient for aligning torque
TIRE$	TIRE$	Tire type (i.e., Radial, Bias Ply) calls the "radial" or "bias ply" saturation functions discussed in Volumes I and II.

Geometric:

The geometric parameters required by VDANL are the longitudinal distance from the sprung mass center of gravity to the front and rear axles, and the front and rear track widths.

Inertial:

The inertial parameters required by VDANL are used to describe the center of gravity location of the sprung and unsprung masses, and their mass moments of inertia. In addition, the mass of the sprung mass and each of the unsprung masses are also required.

The center of gravity height of both the sprung mass and the total vehicle are required, while the center of gravity height of the unsprung masses are assumed to be at the wheel center heights. The pitch, roll and X-Z (cross product) mass moments of inertia of the sprung mass, along with the total vehicle yaw mass moment of inertia are required. The roll mass moment of inertia of each unsprung mass, along with the spin inertia of each wheel/tire assembly are also required.

Suspension/Steering:

The parameters used to describe the vehicle suspension system include: 2^{nd} order polynomial coefficients for wheel steer and camber as a function of suspension deflection, bump stop stiffness and clearance, roll axis height for solid axles, anti-pitch and anti-roll coefficients, equivalent spring stiffnesses and damping coefficients at each wheel, auxiliary roll stiffnesses, wheel steer compliances due to lateral tire force and aligning moments, and lateral suspension compliance due to lateral tire force. The steering system model requires the overall steering ratio, ackerman steer coefficient, steering system natural frequency and damping ratio.

Aerodynamic:

The required aerodynamic parameters are: frontal area, longitudinal drag coefficient, reference aerodynamic velocity, and coefficients for the lateral force and roll and yaw moments caused by lateral air velocity (side winds).

Tire:

The VDANL tire model uses 10 Calspan coefficients to describe the tire lateral and longitudinal force and aligning moment generating properties. In addition to the Calspan coefficients, tire tread width, a coefficient describing the elongation of the contact patch due to longitudinal force, the decay of friction at high tire slip, the cold inflation pressure, the surface coefficient of friction, the 100% design load of the tire, the vertical tire spring rate, and the tire lag coefficients are required.

5.2.2 Test Methods

STI gives detailed procedures for the measurement and/or estimation of the vehicle and suspension parameters required by VDANL in Appendices B, C, and D of their report [5]. The procedures described by STI are geared toward a laboratory without an extensive amount of dedicated test equipment for vehicle parameter measurement. These techniques require minimal lab facilities and instrumentation. STI used these techniques for the 12 vehicles in their report, and the validation section of their report showed that VDANL predictions had very good agreement with STI's experimentally measured field test data.

5.2.3 Compatibility with Existing Measurement Equipment

VRTC has the facilities to perform all of the vehicle and suspension measurement procedures described by STI in their report. In many of the cases where STI gives estimation procedures (mainly for mass moment of inertia), however, VRTC has facilities to measure these parameters directly. The following are simulation parameters that can not be measured at the VRTC.

Suspension damping rate: A shock dyno is not available at the VRTC. However, shocks can be sent out to be measured. This is a time consuming and expensive process. If measuring shock absorber characteristics becomes necessary at the VRTC, then better methods of obtaining shock data will need to be investigated. STI lumps all suspension damping (viscous and coulomb) into a single axle damping coefficient. This coefficient is set based on an estimated or measured vehicle roll damping ratio. Techniques to experimentally measure the vehicle roll damping ratio need to be developed at the VRTC.

Tire force and moment data: The VRTC does not have a tire test machine. All tire testing needs to be done by outside labs. There are no plans at the present time to develop this capability at the VRTC.

Aerodynamic data: Frontal area and coefficient of drag can be estimated from vehicle dimensional data and coast down tests. However, the side force and roll and yaw moment coefficients can not be measured. There are no plans at the present time to develop this aerodynamic measurement capability at the VRTC.

Suspension anti-roll and anti-dive/squat characteristics: These characteristics can either be measured using a very high accuracy suspension test device (beyond the current state of development of the CPMD at the VRTC) or computed based on suspension geometric data. To compute these values, the 3-dimensional coordinates of all suspension pivots need to be measured. This can be done in an adhoc fashion using a steel tape, etc. However, it will be very difficult to achieve a high level of accuracy (it is estimated that the accuracy of this type of measurement will be ± 0.25 inches at best). In addition, this will be a fairly time consuming process. To perform this type of measurement accurately and efficiently, the purchase and/or development of a high accuracy 3-dimensional suspension measurement facility should be investigated. In addition, software to post-process the geometric data should be developed.

5.3 Road Profile

VDANL version 2.33, as developed for the NHTSA, was only to consider flat roads with constant coefficients of friction. However, the program has been extended by STI, as part of other contracts, to allow many different types of road profiles to be simulated. Some of these extensions are present in the source code for version 2.33. This section will discuss these extensions, where appropriate, since they may offer capabilities needed for future NHTSA research.

5.3.1 Flat Road

The default mode of VDANL is for an infinite flat road with a constant coefficient of friction specified by the user. This is the mode used for all of the runs made by the VRTC.

5.3.2 Roadside (curbs, grades, etc.)

The NHTSA version of VDANL allows sloped roads, and changes in road surface friction properties.

5.4 Comparison with Experimental Data

As part of the simulation development, STI compared the simulation predictions for both steady state and transient conditions to experimentally measured responses for 12 test vehicles. The results of these comparisons are contained in Appendix H of the STI report. Two of the vehicles that STI used for the comparisons, the Suzuki Samurai and the Ford Thunderbird, were loaned to STI by the VRTC. Both of these vehicles were used by the VRTC as part of a previous simulation evaluation program [9, 10], and therefore the VRTC has both vehicle parameter data and experimentally measured vehicle responses.

In the following sections of the report, the VDANL predictions will be compared to VRTC measured vehicle responses. The comparisons will be made in both the time and frequency domain using both the STI and VRTC vehicle parameter data decks. It should be noted that the VRTC and STI data decks were not generated for exactly the same vehicle test conditions. The VRTC data deck is for the "as field tested" condition, and therefore its mass and inertial values are somewhat higher than STI's. A more complete description and comparison of the VRTC/STI vehicle data decks can be found in [24].

5.4.1 Steady State

A ramp steer maneuver was run to compare the time domain simulation predictions. The run for both vehicles was made at 50 mph with a nominal lateral acceleration level of 0.4 g's. Figure 32 and Figure 33 show the VDANL predictions and the experimental yaw rate response for the Samurai and Thunderbird respectively.

For the Samurai, the predictions using the VRTC data deck had an approximately 45 percent higher steady state gain than the experimental measurements. The predictions using the STI data deck, however, showed very good steady state predictions. There are a few factors that contribute to the differences in the predictions using the two data decks. As stated earlier, VDANL does not model steering system freeplay. However, measurements at the VRTC show that the Samurai has considerable freeplay in its steering system ($\pm$8 degrees at the handwheel). The handwheel input for this maneuver was approximately 67 degrees, therefore, the freeplay present in the Samurai steering system will reduce the effective handwheel angle input 12 percent (8/67). At 0.4 g's, the Samurai is still in its linear operating regime and this freeplay will reduce its steady state gain approximately 12 percent.

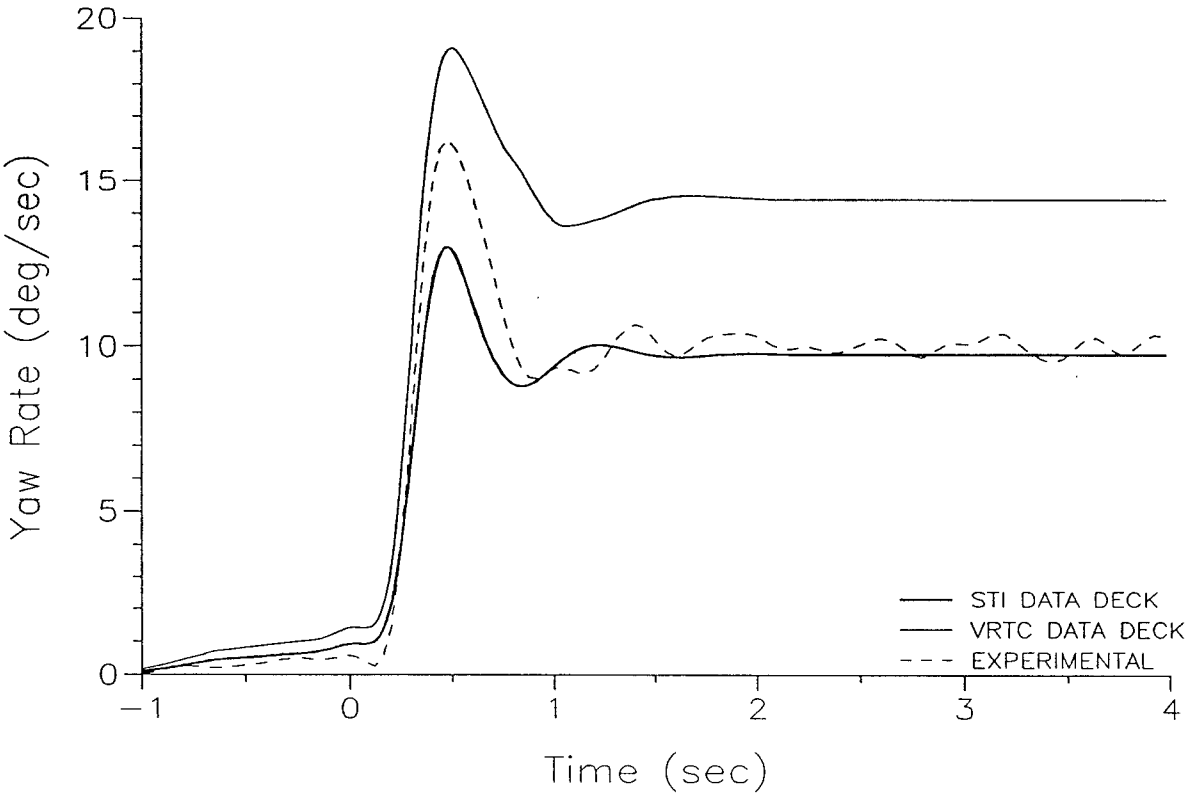

Figure 32 - Samurai Steady State Comparison

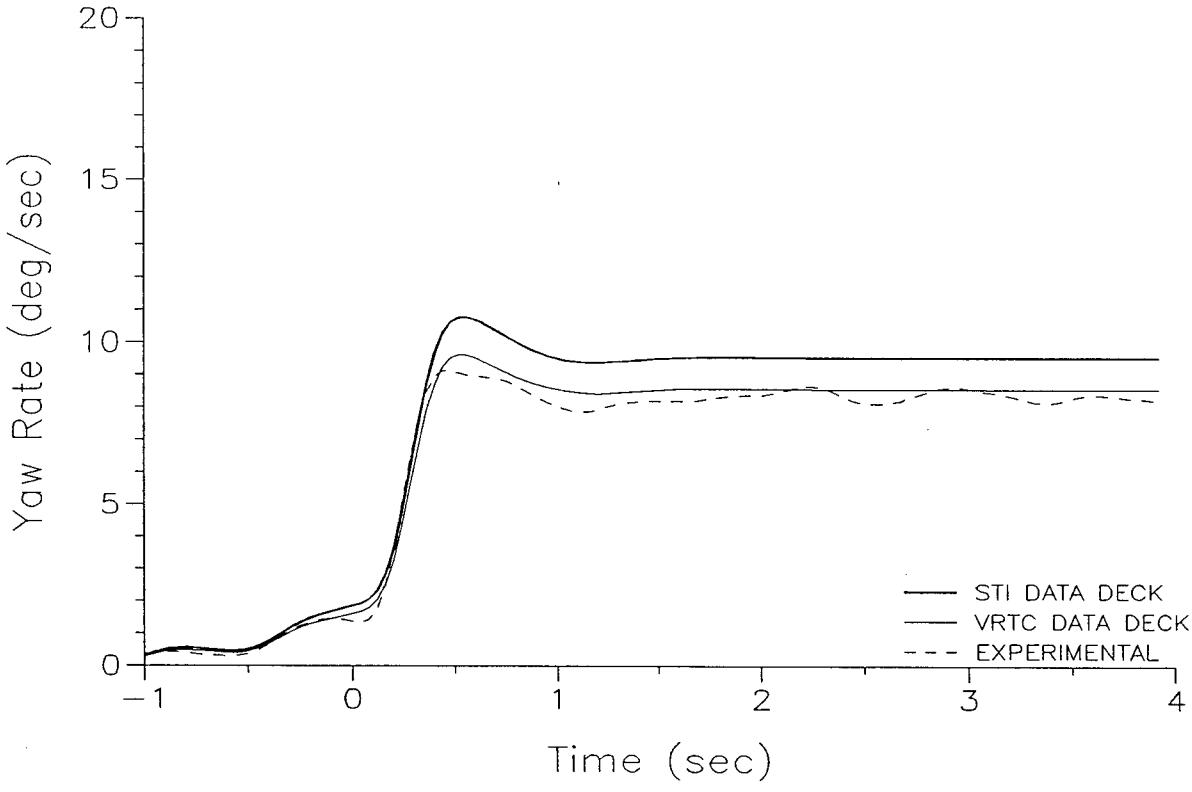

Figure 33 - Thunderbird Steady State Comparison

A second difference between the data decks is the steering column compliance. The VRTC measurements show the steering column to be approximately 5 times stiffer than the STI parameter. Measurements at the VRTC [1] have shown that only approximately 50 percent of the Samurai's steering compliance comes from the steering column, with the other 50 percent coming from the steering linkage. A final difference between the data decks is that the VRTC data deck includes the front axle roll steer effects, while STI's data deck does not. Modifying the VRTC data deck to account for this additional compliance and taking the effects of freeplay into account, the VDANL predictions then match the experimental steady state measurements very well.

Discussions with STI revealed that the steering column compliance parameter used in their data deck was used to "tune" the simulation predictions to match the experimental data. This tuning was done because of the Samurai's unusually high steering freeplay, and additional compliances in the steering system not modeled in VDANL. Past modeling work at the VRTC using the earlier version of VDANL has addressed both of these issues. The resulting model enhancements could be easily incorporated into the current version of VDANL. These additions would significantly improve the simulation's predictions, especially for vehicles like the Samurai.

The Thunderbird comparisons (Figure 33) show the VDANL predictions using the VRTC data deck to match the experimental data very well. The predictions using the STI data deck have a steady state gain approximately 15 percent higher than the experimental data.

An additional area of interest in Figure 32 and Figure 33 is the prediction of the yaw rate overshoot. For the Samurai, the experimental data showed approximately 60 percent overshoot, while the VDANL predictions had approximately 30 percent overshoot. For the Thunderbird, the experimental data showed approximately 9 percent overshoot, while the VDANL predictions had approximately 13 percent overshoot. More insight in the VDANL predictions of vehicle transient response is contained in the next section of the report. However, it can be seen that in both cases the VDANL predictions match the general shape of the experimentally measured yaw rate response.

5.4.2 Transient

Past research at the VRTC has demonstrated that frequency response techniques are quite useful for evaluating dynamic/transient simulation predictions [9, 10]. By generating vehicle output (eg. yaw rate)

frequency response to handwheel angle inputs, much can be learned about the characteristics and validity of a simulation model.

Yaw rate frequency responses to handwheel angle inputs have been generated for both the Samurai and the Thunderbird. Figure 34 and Figure 35 show the frequency response magnitude and phase angle curves for the Samurai at 50 mph. The 3 curves show the experimentally measured frequency response, and the VDANL predicted frequency response using both the STI and the VRTC data decks. Figure 36 and Figure 37 show the same frequency response curves for the Thunderbird at 50 mph.

At low frequencies, the Samurai frequency response magnitude curve (Figure 34) shows the same basic characteristics as the steady state maneuver (Figure 32). Namely, that VDANL using the STI data deck does a very good job of predicting steady state gain, while using the VRTC data deck, the steady state gain predictions are much too high. At higher frequencies (greater than 0.5 hertz), the VDANL predictions show the same basic underdamped response as the experimental data. However, the simulation predictions have a much lower peak amplitude ratio (the magnitude at the peak divided by the magnitude at steady state) than the experimental measurements. The peak amplitude ratio of VDANL is approximately 1.7 compared to 2.8 for the experimental data. Research at the VRTC has shown that this high peak amplitude ratio for the Samurai is strongly influenced by its high front axle roll steer. It is possible that with a better roll steer model for steered solid axles (see the description of suspension Kinematics under the Suspension Model section of this report), the VDANL predictions could be improved.

A second area of interest in the frequency response magnitude curves is the prediction of the frequency at which the peak amplitude occurs. Figure 34 shows that using the STI data deck, VDANL predicted this frequency very well, however, using the VRTC data deck, the predicted frequency was lower than the experimentally measured data. This low predicted peak frequency, using VDANL, was also seen in the earlier VRTC evaluation of VDANL. The cause of this is thought to be lumping the sprung and unsprung yaw inertias together, further research, however, is needed.

Figure 35 shows the frequency response phase angle curves for the Samurai. VDANL, using both data decks, is doing a good job here, showing only slightly more phase lag at higher frequencies than the experimental data.

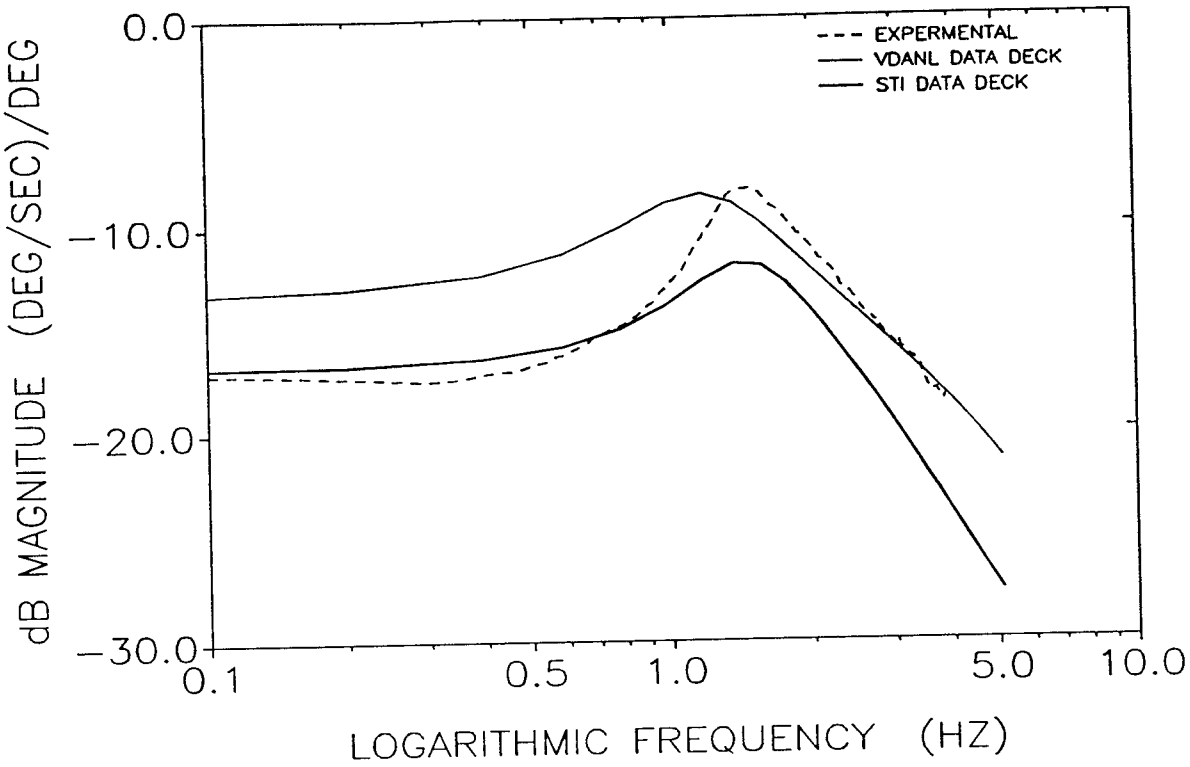

Figure 34 - Yaw Rate to Handwheel Angle Frequency Response Magnitude 50 mph Samurai

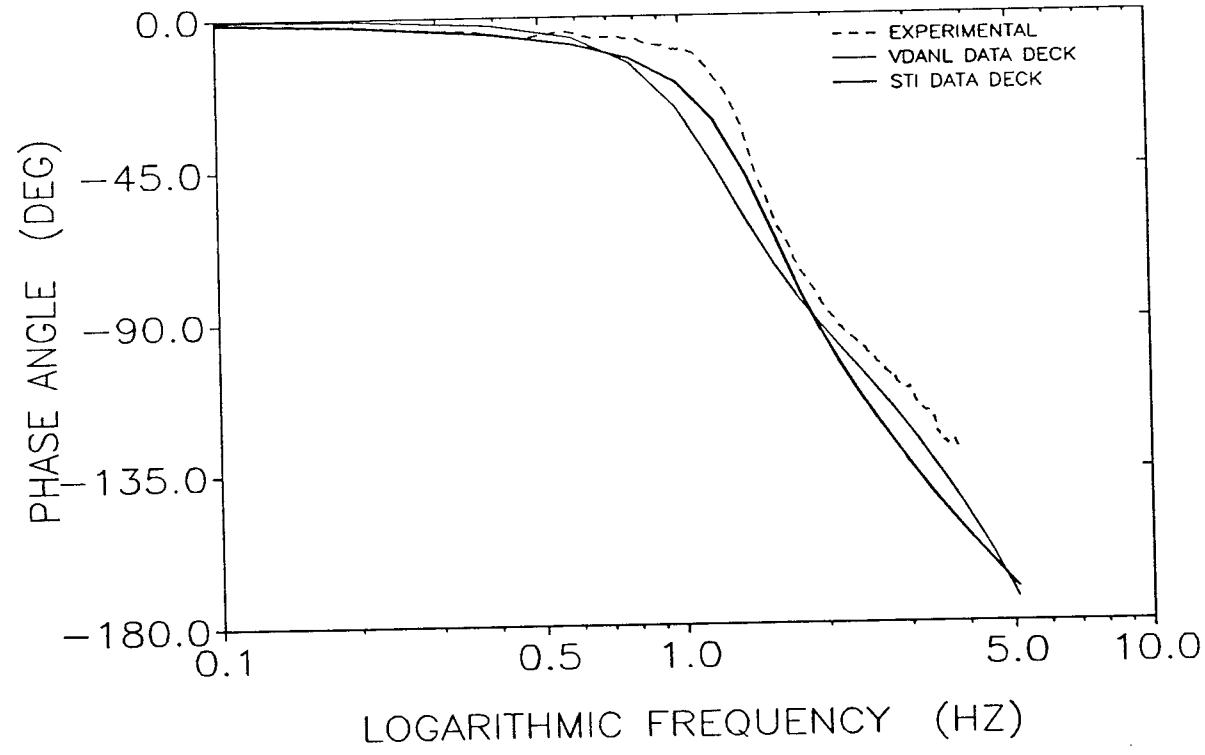

Figure 35 - Yaw Rate to Handwheel Angle Frequency Response Phase Angle 50 mph Samurai

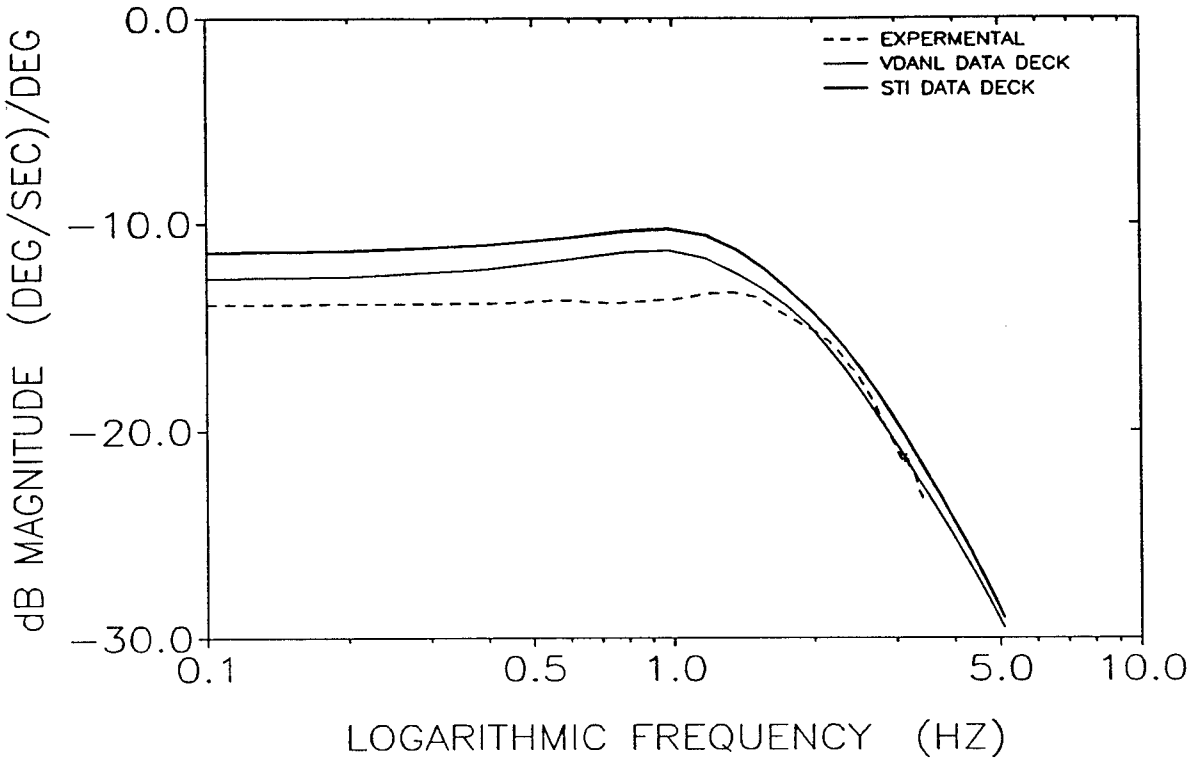

Figure 36 - Yaw Rate to Handwheel Angle Frequency Response Magnitude 50 mph Tbird

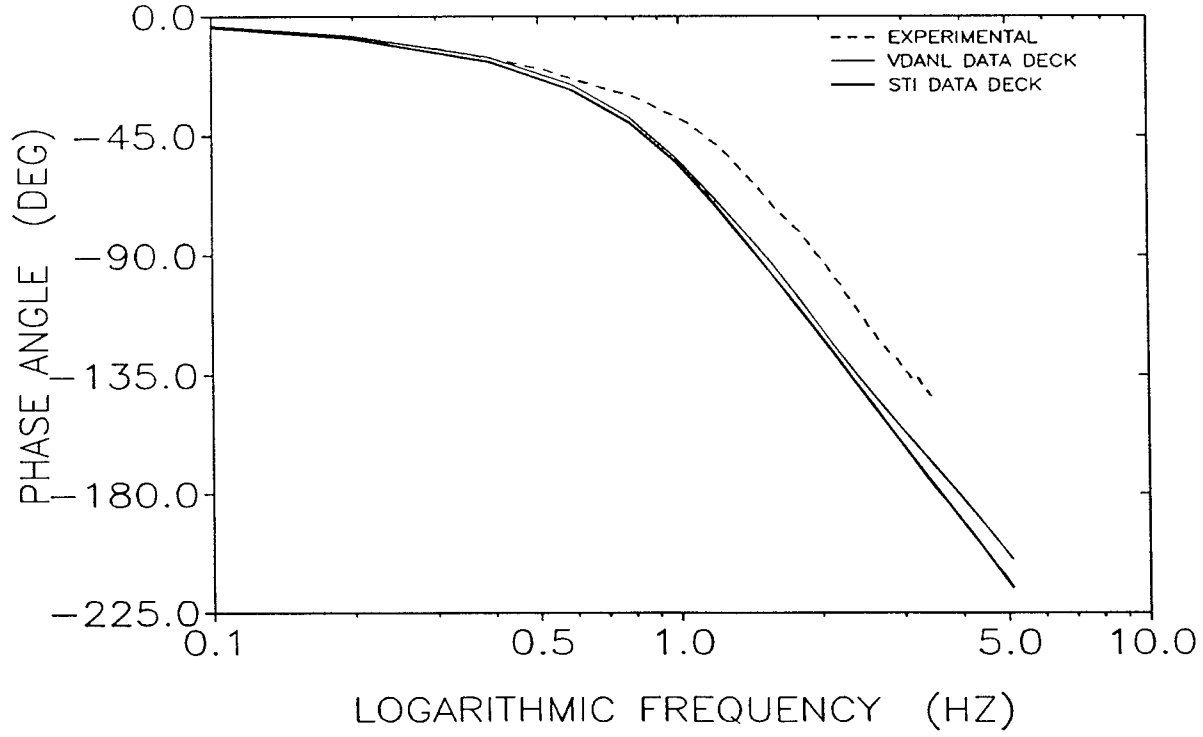

Figure 37 - Yaw Rate to Handwheel Angle Frequency Response Phase Angle 50 mph Tbird

The Thunderbird frequency response curves (Figure 36), like the Samurai curves, show that VDANL is predicting the basic shape to the vehicle response curve fairly well. The VDANL predictions have a peak overshoot ratio of approximately 1.15, while the experimental measurements show only approximately 1.07. Again, like the Samurai, the VDANL predictions of peak frequency are lower than the experimental data. The Thunderbird phase angle curves (Figure 37) show that the VDANL predicts slightly more phase lag at higher frequencies than the experimental data.

6.0 Summary and Conclusions

This report contains evaluations of four light vehicle stability and control simulations developed for the NHTSA: FOROL developed by Dynamic Research Inc. [2], the "Intermediate Maneuver Induced Rollover Simulation" (IMIRS) [3] and the "Advanced Dynamic Vehicle Simulation" (ADVS) [4], both developed by the University of Missouri, and the most recent version of "Vehicle Dynamics Analysis, Non-Linear" (VDANL) [5] developed by System Technology, Inc. The report contains an analytical review that describes and evaluates the modeling techniques and capabilities of each simulation. Each simulation's ability to predict low to moderate g flat road vehicle responses has been examined by comparing simulation predictions to experimentally measured vehicle responses.

Table XVI summarizes some of the capabilities of the four simulations. Also included are the pertinent vehicle characteristics modeled, and other miscellaneous aspects of the simulations. Table XVI does not, however, compare the simulations' ability to predict vehicle directional responses.

The FOROL simulation models light vehicles in open-loop, flat ground handling maneuvers up to vehicle rollover. FOROL is an 18 degree-of-freedom lumped parameter model using composite parameters to describe the suspension system and empirical curve fit parameters for its tire model. The significant non-linearities present in the vehicle and tire systems are included in the model. Open-loop handwheel angle and brake pedal force are the maneuver control inputs allowed. Speed control is accomplished by either a fixed drive torque at the rear wheels or a speed governor allowing constant speed operation. The vehicle parameters required by FOROL are fairly standard and can be measured in the laboratory at the VRTC. Calspan tire parameters are used in the quasi-static tire model.

The IMIRS simulation models light vehicles in open-loop, flat ground handling maneuvers up to vehicle rollover. IMIRS contains a 3 degree of freedom handling model coupled to a 5 degree of freedom rollover model. An empirical, steady state tire model using Calspan curve fit parameters is used. The significant non-linearities present in the vehicle and tire systems are included in the model. Open-loop roadwheel angle and longitudinal acceleration are the maneuver control inputs allowed.

IMIRS contains a fixed roll axis vehicle model comprised of a simple kinematic suspension model with no suspension compliances included. All wheel kinematics associated with vehicle bounce are neglected. No steering system is modeled, therefore neglecting the effects of steering system compliance and freeplay. The braking model is limited to a user specified longitudinal acceleration profile.

Table XVI - Comparison of Simulation Features

	FOROL	IMIRS	ADVS	VDANL
Number of Degrees-of-Freedom	18	8	14	17
Independent Suspension (Y/N)	Y	Y	Y	Y
Solid Axle Suspension (Y/N)	Y	Y	Y	Y
Suspension Compliance (Y/N)	Y	N	N	Y
Anti-Lock Brakes (Y/N)	N	N	N	Y
Steering System Model (Y/N)	Y	N	N	Y
Lateral Control Input (HandWheel, RoadWheel, Ay)	HW	RW	RW	HW,Ay
Braking Control Input (Brake Pressure, Ax)	BP	Ax	Ax	BP,Ax
Speed Control (Drive Torque, Speed Governor)	DT,SG	DT	DT	DT,SG
Tire Dynamics (Y/N)	N	N	N	Y
Aerodynamic Model (Y/N)	N	Y	Y	Y
Computer Hardware (PC, VAX, Work Station)	PC,WS	PC	VAX	PC
Number of Vehicle Parameters (approximate)	93	70	+170	115
Road Profile (Flat, Slope, Rough)	F	F	F,S	F,S
Road Side Features (Curb, Soil, Δ Friction)	–	–	C,S,F	F
Description of Required Parameters Contained in Documentation (Y/N)	Y	N	N	Y
Description of Parameter Measurement Techniques Contained in Documentation (Y/N)	Y	N	N	Y

The ADVS simulation models light vehicles in open-loop, handling maneuvers up to and including vehicle rollover. ADVS contains a 14 degree of freedom vehicle handling/rollover model. An empirical, steady state tire model based principally on Calspan curve fit parameters is used. The significant non-linearities present in the vehicle and tire systems are included in the model. Open-loop roadwheel angle and longitudinal acceleration are the maneuver control inputs allowed.

The ADVS model is a complex Lagrangian formulation of the dynamic equations describing vehicle motions. An equivalent swing axle suspension model is used for independent suspension systems. For solid axle type suspensions, a fixed roll axis model is used. Only road wheel camber change is included in the kinematic suspension model with no axle roll steer effects included. No modeling of suspension system lateral compliance is included. No steering system is modeled, therefore neglecting the effects

of steering system compliance and freeplay. The braking model is limited to a user specified longitudinal acceleration profile.

The VDANL simulation models light vehicles in open-loop flat ground handling maneuvers. VDANL also allows modeling closed-loop vehicle response and sloped roadways. The VDANL simulation contains 17 degrees of freedom and can simulate vehicle response up to and including vehicle rollover. An empirical, steady state tire model using Calspan curve fit parameters is used, with lateral tire force dynamics included. The significant non-linearities present in the vehicle and tire systems are included in the model. Open-loop hand wheel angle, throttle position or desired speed, and brake pedal force are the maneuver control inputs allowed.

VDANL contains a 6-degree-of-freedom model of the vehicle sprung mass coupled to the unsprung masses. The vehicle suspension systems are described using fairly complete models for wheel kinematics and compliances. For independent suspensions, the classic fixed roll axis model has been abandoned, in favor of functions describing the kinematic relationships of the tire contact patch relative to the sprung mass. A fixed roll axis model is used, however, for solid axle suspension systems.

This evaluation has found VDANL to be the most highly developed and tested vehicle handling simulation developed for NHTSA. Its ability to predict vehicle directional responses in moderate g, open-loop flat road handling maneuvers was found to be better than the other simulations evaluated (previously, an earlier version of VDANL was found to be superior to the "Improved Dynamic Simulation, Fully Non-Linear" (IDSFC) [1]). Of the simulations evaluated, VDANL most correctly characterized vehicle transient behavior.

7.0 References

1. Heydinger, G. J., *Improved Simulation and Validation of Road Vehicle Handling Dynamics*, PHD Dissertation, The Ohio State University, 1990.

2. Kebschull, B.K., Weir, D.H., and Zellner, J.W., "Rollover, Braking, and Dynamic Stability - Modified Suspension Vehicles, Final Report, Volume II. Appendices A-D," Report DOT HS 807 663, August, 1990.

3. Nalecz, A. G., "Intermediate Maneuver Induced Rollover Simulation (IMIRS) and Sensitivity Analysis," DOT-HS-807-672, Feb. 1991.

4. Nalecz, A. G., Lu, Z. Y., and D'Entremont, K., "Advanced Dynamic Vehicle Simulation (ADVS) To Investigate Rollover Behavior, Part I: User's Manual", U.S. DOT - NHTSA, Document in Progress, April, 1991.

5. Allen, R. W., Szostak, H. T., Rosenthal, T. J., Klyde, D. H., and Owens, K. J., "Vehicle Dynamic Stability and Rollover," NHTSA Final Report No. DTNH22-88-C-07384, Jan. 1991.

6. Kebschull, B.K., Weir, D.H., and Zellner, J.W., "Rollover, Braking, and Dynamic Stability - Modified Suspension Vehicles, Final Report, Volume I. Technical Report," Report DOT HS 807 662, August, 1990.

7. Heydinger, G. J., Garrott, W. R., and Chrstos, J. P., "The Importance of Tire Lag on Simulated Vehicle Transient Response," *SAE Transactions*, SAE Paper 910235, Feb. 1991.

8. Chrstos, J. P.,"An Evaluation of Static rollover Propensity Measures," NHTSA Final Report, DOT-HS-807-747, May 1991.

9. Heydinger, G.J., Garrott, W.R., Chrstos, J.P., and Guenther, D.A., "Validation of Vehicle Stability and Control Simulations," *Transportation Research Record No. 1270*, 1990.

10. Heydinger, G.J., Garrott, W.R., Chrstos, J.P., and Guenther, D.A., "A Methodology for Validating Vehicle Dynamics Simulations," *SAE Transactions*, SAE Paper No. 900128, 1990.

11. Bergman, W., "Effects of Compliance on Vehicle Handling Properties," SAE Paper No. 700369, 1970.

12. Bundorf, R. T., "The Influence of Vehicle Design Parameters on Characteristic Speed and Understeer," SAE Paper No. 670078, Jan. 1967.

13. Nedley, A. L. and Wilson, W. J., "A New Laboratory Facility for Measuring Vehicle Parameters Affecting Understeer and Brake Steer," SAE Paper No. 720473, May. 1972.

14. Segel, L., "On the Lateral Stability and Control of the Automobile as Influenced by the Dynamics of the Steering System," Transactions of the ASME, Vol. 8, No. 3, page 283-295, 1965.

15. Sayers, M. W., MacAdam, C. C., and Guy, Y., "Chrysler/UMTRI Wind-Steer Vehicle Simulation," University of Michigan Transportation Institute Report No. UMTRI-89-8/1, User's Manual, Version 1.0, February 1989.

16. Garrott, W. R., "Rollover Research Activities at the Vehicle Research and Test Center - Frequency Response Testing," NHTSA Final Report Draft, 1991.

17. Nalecz, A. G., Lu, Z. Y., and D'Entremont, K., "Advanced Dynamic Vehicle Simulation (ADVS) To Investigate Rollover Behavior, Part II: Technical Report", U.S. DOT - NHTSA, Document in Progress, April, 1991.

18. Nalecz, A. G., Lu, Z. Y., and D'Entremont, K., "Advanced Dynamic Vehicle Simulation (ADVS) To Investigate Rollover Behavior, Part III: Applications", U.S. DOT - NHTSA, Document in Progress, April, 1991.

19. Garrott, W. R., and Scott, R. A., "Improvement of Mathematical Models for Simulation of Vehicle Handling - Volume 7: Technical Manual for the General Simulation," DOT-HS-805-370, The University of Michigan College of Engineering, March 1980.

20. Collins, R. L., "Frequency Response of Tires Using the Point Contact Theory," Journal of Aircraft, Vol. 9, No. 6, June 1972.

21. Rogers, L. C. and Brewer, H. K., "Synthesis of Tire Equations for Use in Shimmy and Other Dynamic Studies," Journal of Aircraft, Vol. 8, No. 9, Sept. 1971.

22. Allen, R. W., Rosenthal, T. J., and Szostak, H. T., "Analytical Modeling of Driver Response in Crash Avoidance Maneuvering, Volume I: Technical Background", NHTSA Final Report No. DOT-HS-807-270, April, 1988.

23. Bernard, J. E., "Some Time-Saving Methods for the Digital Simulation of Highway Vehicles," *Simulation*, Vol. 21, No. 6, Dec. 1973, pp. 161-165.

24. Heydinger, G. J., "Vehicle Dynamic Simulation and Metric Computation for Comparison With Accident Data," NHTSA Final Report, DOT-HS-807-828, March, 1991.